

Fire Regimes in National Parks of the Pacific Northwest:
Implications for Climate Change

Karen E. Kopper

A dissertation
submitted in partial fulfillment of the
requirements for the degree of

Doctor of Philosophy

University of Washington

2022

Reading Committee:

Donald McKenzie, Chair

David L. Peterson

Regina M. Rochefort

Program Authorized to Offer Degree:

School of Environmental and Forest Sciences

© Copyright 2022

Karen E. Kopper

University of Washington

Abstract

Fire Regimes in National Parks of the Pacific Northwest:
Implications for Climate Change

Karen E. Kopper

Chair of the Supervisory Committee:

Donald McKenzie

School of Environmental and Forest Sciences

There has been a significant increase in fire activity in the western United States over the past two decades, attributed to climate change, but much of the data that support this attribution are from fires in frequent, low-severity fire regimes. Recent increases in fires with mixed- and high-severity fire regimes of the Pacific Northwest have highlighted the importance of collecting baseline data and understanding fire-climate interactions in forests with less frequent fire to inform research and guide management. My dissertation focuses on these objectives in three chapters. In the first chapter, I characterized historical fire frequency and severity over 400 years in a dry, mixed conifer forest in Stehekin, Lake Chelan National Recreation Area in Washington state, and used ANOVA and GLM to identify the bottom-up controls on fire in this mountainous terrain. I found that fire frequency was high before the fire suppression era (31-year mean fire-

interval), increased significantly during the non-Indigenous settlement period, and was impacted by fire suppression (51-year mean fire interval following suppression). Both fire frequency and severity are controlled by a complex interaction among topography, site, and environmental variables, which could increase resilience to climate change. In the second chapter, I classified and mapped fuel characteristics (fuelbeds) and fire potentials across a low-frequency, high-severity fire regime (Mount Rainier National Park, (the Park)) using a combination of field data, LiDAR, and climate data. Using this examination at high-resolution, I identified higher fuel loadings and fire potentials on the west side of the Park that could eventually indicate greater impacts and changes there, although the effects of climate change are more certain and will come sooner on the east side. In the last chapter, I reviewed bottom-up controls (topography and fuels) on fire frequency across the continuum of moist, high-severity fire regimes to dry, low-severity fire regimes from the west side of the Olympic Mountains to the east side of the north and central Cascades. Using this examination, I identify and describe a corresponding “fuel management continuum” to inform wildfire and forest management strategies.

TABLE OF CONTENTS

Introduction.....	1
Chapter 1. A checkered past: the history of a mixed-severity fire regime on a mountain landscape in the Cascade Range, Stehekin, Washington, USA.....	3
1.1 Abstract.....	3
1.2 Introduction.....	4
1.3 Literature Review.....	5
1.4 Research Questions.....	7
1.5 Methods.....	8
1.5.1 Study Area	8
1.5.2 Fire History Plots	10
1.5.3 Increment Cores.....	13
1.5.4 Identifying High-severity Fires.....	13
1.5.5 Wedge Samples.....	14
1.5.6 Derivation of Environmental Predictors	15
1.5.7 Statistical Analysis of Fire Frequency	16
1.5.8 Analysis of Predictors	18
1.6 Results.....	19
1.6.1 Historical Fire Frequency	19
1.6.2 Mean Composite Fire Intervals.....	22
1.6.3 Establishment Dates.....	24
1.6.4 Effects of Settlement and Fire Suppression	25
1.6.5 Historical Fire Severity	26
1.6.6 Fire Frequency Predictors	28
1.6.7 Fire Severity Predictors.....	30
1.6.8 Fire Frequency and Severity per Plot.....	32
1.7 Discussion.....	33
1.8 References.....	37

Chapter 2. Fuel characteristics of Mount Rainier National Park, Washington, USA: Mapping with a combination of field, environmental, and LiDAR data	42
2.1 Abstract.....	42
2.2 Introduction.....	43
2.3 Research Questions	46
2.4 Methods.....	47
2.4.1 Summary	47
2.4.2 Study Area	48
2.4.3 Field Data Collection	50
2.4.4 Climate Metrics.....	52
2.4.5 Airborne LiDAR Data and DTMs	53
2.4.6 Forest Structure Metrics.....	54
2.4.7 Topographic Variables.....	54
2.4.8 Defining and Mapping Forest Structure Classes	56
2.4.9 Surface Fuel Modeling and Mapping	58
2.4.10 Definition and Mapping of Fuelbeds	59
2.4.11 Assigning Values to Fuelbeds.....	60
2.4.12 Integration with the Fuel Characteristic Classification System.....	61
2.4.13 FCCS Fire Potentials.....	61
2.5 Results.....	62
2.5.1 Structure Classes and Map.....	62
2.5.2 Surface Fuel Models and Map	64
2.5.3 Fuelbed Map	67
2.5.4 Fire Potentials	70
2.6 Discussion	72
2.6.1 Distributions of the Fuelbeds and Fire Potentials	72
2.6.2 Benefit of LiDAR	74
2.6.3 Management Implications.....	75
2.6.4 Using the Map.....	79
2.7 References.....	79

Chapter 3. Fire-climate interactions: local controls and management implications for moist and dry conifer forests of the Pacific Northwest	86
3.1 Abstract.....	86
3.2 Introduction.....	87
3.3 Fire Regimes of the Pacific Northwest	88
3.3.1 Moist and Dry Forests.....	88
3.3.2 High-Severity Fire Regimes	90
3.3.3 Mixed- and Low-Severity Fire Regimes.....	92
3.4 Top-down and Bottom-up Controls.....	94
3.4.1 Top-down Control: Climate in the Pacific Northwest	95
3.4.2 Bottom-up Controls: Fuels and Topography	96
3.4.3 Bottom-up Control: Fuel Moisture in High-Severity Fire Regimes	96
3.4.4 Bottom-up Control: Fuel loading in Low-Severity Fire Regimes	98
3.4.5 Bottom-up (but Multi-scale) Control: Topography	98
3.5 Effects of Climate Change in Moist and Dry Forests.....	99
3.6 Management Implications.....	100
3.7 Conclusions.....	104
3.8 References.....	105
Conclusions.....	110
Appendix A:.....	111

LIST OF FIGURES

Figure 1 - 1. Map of the study area in Lake Chelan National Recreation Area.	8
Figure 1 - 2. Diagram of circular fire-history plot.....	11
Figure 1 - 3. The Stehekin fire chart.....	20
Figure 1 - 4. Stehekin composite fire chart.....	21
Figure 1 - 5. Fire index plot for Stehekin.....	22
Figure 1 - 6. Boxplots of the mean composite intervals	24
Figure 1 - 7. Dates of tree establishment in 30 fire history plots.....	25
Figure 1 - 8. Scatterplot of the proxy for fire severity.....	27
Figure 1 - 9. Fire severity per plot	27
Figure 1 - 10. Scatterplot of CFI by aspect.....	30
Figure 1 - 11. Scatterplot of the proxy for fire severity.....	31
Figure 1 - 12. Fire severity ranks and mean CFI	32
Figure 2 - 1. Flowchart illustrating the parallel processing of four datasets.....	47
Figure 2 - 2. Map of study area showing field plot locations by dominant tree species..	51
Figure 2 - 3. Final structural classes.	57
Figure 2 - 4. Box plots of structural class characteristics	63
Figure 2 - 5. Map of nine distinct structure classes	64
Figure 2 - 6. Relative importance of predictors to classification of surface fuels.	66
Figure 2 - 7. Map of surface fuel classes across Mount Rainier National Park.....	67
Figure 2 - 8. Map of fuelbeds for Mount Rainier National Park	68
Figure 2 - 9. Fire and fuel potentials across Mount Rainier National Park	71
Figure 2 - 10. Fuelbeds in subalpine fir / whitebark pine vegetation map class.....	78
Figure 3 - 1. Map of fire regimes of the Olympic and Cascade Mountains.....	89
Figure 3 - 2. Fire frequency across Mount Rainier National Park, 2000–2019.....	92
Figure 3 - 3. 32-year fire history in North Cascades National Park Service Complex....	93
Figure 3 - 4. Diagram of the fuels management continuum	101

LIST OF TABLES

Table 1 - 1. Characteristics of trees that had wedges removed.....	12
Table 1 - 2. Sources and ranges of environmental predictors.....	16
Table 1 - 3. Composite fire intervals	23
Table 1 - 4. Analysis of settlement and fire suppression	26
Table 1 - 5. Summary of structural and environmental characteristics per unit.....	29
Table 1 - 6. ANOVA of fire frequency predictors.....	29
Table 1 - 7. GLM of fire severity predictors.....	31
Table 2 - 1. Input variables to classify surface fuel loads and canopy structure classes...	55
Table 2 - 2. Results of regressions and classifications for surface fuels.....	65
Table 2 - 3. Twenty-nine fuelbeds from structure and surface fuel combinations	69
Table 2 - 4. Median values for surface fuel classes.	70

ACKNOWLEDGEMENTS

My Fabulous Committee: Thank you first and foremost to my Committee Chair, Don McKenzie, for your wisdom, depth, and unwavering support from those early visits to Stehekin, all the way through to these final words. You have been such an excellent teacher and advisor to me, allowing me the room to explore and find my way through my research, and yet also being there to point the way towards deeper meanings and novel concepts. Thank you for your time and patience throughout my long journey, and for helping me to uncover the gems in my research.

Dave Peterson, thank you for your support, encouragement, and guidance over all these years; from chairing my master's study, inviting me to practice my chainsaw skills on your land, to your attention to details as well as to the big picture on my final dissertation.

Regina Rochefort, thank you for being my mentor at the national park service for so many years, and for your time, guidance, and support of my research at the university. Your commitment to science-based management serves as my guidepost. Thank you for leading the way so adeptly.

Ernesto Alvarado, thank you for your encouragement and interest throughout this long journey. Your suggestions have always been helpful and added value to my research.

Van Kane, thank you for being a collaborator and a committee member. Thank you for taking on the challenge of mapping surface fuels with LiDAR and hence, for your substantial collaboration on chapter two. Thank you also for being such an encouraging and supportive committee member.

Mark Scheuerell, thank you for joining my committee as GSR towards the end of my research, upholding the standards of the university, and seeing me through to the finish-line.

The North Cascades National Park Fire Management Team: Enormous thanks to Scott Ebel, Cedar Drake, Tonya Neider, Lesha Zitkovich, Aaron Anderson, and all the fire staff over the years for your support, help, encouragement and patience. Special thanks to Loretta Duke for letting me stay at your wonderful home in Stehekin for several summers and encouraging me to take on this research. Tod Johnson, thank you for supporting me and allowing me to take on this project. Special thanks to the fire crew for help collecting the wedges: Ryan Bayes, Winter West, Peter Young, Ellen Bivona, and Michael Koenen. Special thanks also to Carolyn Schroeder for all the long hours measuring rings and cross-dating!

The Fire and Mountain Ecology Lab and Pacific Wildland Fire Sciences Lab: Thanks for your friendship, encouragement, and collaboration: Alina Cansler, Crystal Raymond, Christina Restaino, Ella Elman, Susan Prichard, Maureen Kennedy, Rich Gwozdz, Paige Eagle, Diana Olson, Morris Johnson, Rob Norheim, Jeremy Littell, Summer Kemp-Jennings, and Michael Tjoekler. I hope to keep up with each of you throughout our careers. Immeasurable thanks to Dave and Don for leading the FaME lab.

The fire effects monitors, fuel mappers, fire ecology interns, and associates: Dallas Anderson, Avery Marciano, Elizabeth Hook, Katie Heard, Kara Schwanger, Abby Neff, Nick Casey, Jason Webster, Julia Bartley, Andy Cockle, Katie Roloson, Allie Lalor, Tom Brussel, and Matt Hughes. Hearty thanks to each of you for your hard work and rugged determination to meet the many challenges of working in a remote wilderness area.

National Park Service: Immense gratitude to the NPS for the in-kind support to perform this research. Special thanks to Catharine Copass of Olympic National Park for your collaboration on chapter two. You got this project started and helped keep it going through many iterations. Robin Wills, thanks for your guidance and encouragement on the Stehekin fire history study. Vicki Gempko, thanks for your help on the post-sampling surveys. Samantha Richert, thank you for your work and energy to archive the fire history samples at North Cascades National Park.

My family and friends: Thanks for your love, patience, and encouragement throughout this long process. Dad, thanks for cheering me on towards the finish line, and helping me feel Mom there with me. Scott Bunk, thanks for being a true friend, excellent father to our girl, and supporting my research in so many ways. Extra special thanks to my kind, thoughtful and generous daughter Maggie, for motivating and celebrating this accomplishment with me.

DEDICATION

I dedicate this dissertation to the trees, and to my daughter Maggie.

Trees, thank you for the samples, and for your peaceful nature.

Maggie, thank you for your love and wisdom beyond your years.

May you, and many future generations to come,

have wilderness areas with plenty of wise old trees.

Introduction

The size and frequency of wildfires are increasing throughout the Pacific Northwest in response to climate change. Land managers are facing the difficult challenge of managing fires in areas where vegetation is not fire adapted and fires were uncommon, historically. Researchers are also facing new challenges to predict and project the effects of climate change in a rapidly changing environment with little empirical data and uncertain and complex climate-fire interactions. This dissertation is intended to provide base-line data on fire frequency and fuels in areas where this information is lacking, to improve fire projections, explore innovative research techniques, and guide and inspire new strategies for managing fire with climate change.

The first chapter is a fire history study of a conifer forest with a mixed-severity fire regime on the eastern slopes of the northern Cascades, where vegetation assemblages and fire effects are on a gradient between moist and dry climate, no analogous community exists, and proactive fire management is imperative to protect visitors and ecosystem services in a national park. I used a combination of fire scar data and stand ages to quantify fire frequency and severity, and I identified the drivers of fire regime characteristics to aid in adapting fire management strategies for climate change.

The second chapter is focused on characterizing fuels in a high-severity fire regime on the west side of the Cascade range, where until recently, there was little need to quantify fuel loads beyond a coarse resolution since large fires only occurred every 400+ years. I used a combination of field, LiDAR and environmental data to map surface and canopy fuels (fuelbeds) and their fire potentials at high resolution across Mount Rainier National Park. This analysis enabled me to identify fuelbeds and areas of the Park most vulnerable to climate change and to provide strategies for fire management.

The third chapter merges the information gained in chapters one and two on bottom-up controls on fire frequency and severity, and fuel load properties across east and west side forests, to propose a strategy for managing fuels and fire potential across the old-growth forests of the Olympic and Cascade Mountains. This chapter takes a broader view across the Pacific Northwest emphasizing the important differences between fire regimes and their drivers.

Although these three chapters are different and stand alone in their contribution to fire ecology in the Pacific Northwest, they all share the common theme of providing information and assistance to forest managers as they navigate the challenges of fire management with respect to climate change. As a fire ecologist in the national park service, and as a researcher, the importance of providing accessible and applicable research is critical to me. I hope that in reading my dissertation, you will be encouraged and empowered to bridge the gap between research and management as I strive to do.

Chapter 1. A checkered past: the history of a mixed-severity fire regime on a mountain landscape in the Cascade Range, Stehekin, Washington, USA

1.1 Abstract

I used a combination of fire scars, forest structure, and stand age to characterize the historical fire frequency and range of fire severity for a complex and variable mixed-conifer forest in Stehekin, Lake Chelan National Recreation Area. I collected and cross-dated a total of 264 fire scars in twenty-eight 5-hectare fire history plots throughout the Stehekin watershed. I identified 109 different fire years over the 462-year sampling period (1558 – 2020), comprising a mean historical composite fire interval (CFI) of 31 years, and found a significant increase in fire frequency during the settlement period, and lengthening of CFI during the fire suppression era. No significant environmental predictors of the historical CFI were identified through linear regression, however ANOVA revealed that CFI varied in response to a complex interaction among location, presence of ponderosa pine, and SW/NE-facing slopes. Using a proxy for fire severity based on the proportion of fire-scarred trees to total trees per hectare, I found a wide range of fire severities over various stand densities (11% to 0.6% of trees scarred on plots with lowest and highest fire severities, respectively). Slopes ranged from 21% to 65%, with lowest fire severities on steeper slopes, and on NE-facing aspects in interaction with slope. The significant interactions between topographic variables and other local factors with respect to CFI and fire severity verify the influence of bottom-up controls in this rugged mountainous terrain. I determined a baseline range of fire frequencies and severities dependent upon complex interactions between environmental predictors. The variability and complexity inherent to mixed-severity fire regimes may provide greater resiliency to climate change by increasing the

diversity of post-fire effects.

1.2 **Introduction**

Conifer forests on the east slopes of the northern Cascades are spatially complex, consisting of a mosaic of stand ages and fire scars typical of the mixed-severity regime (Agee 2005, Hessburg et al 2007, Halofsky et al 2011). The remote town of Stehekin in Lake Chelan National Recreation Area, of the North Cascades National Park Service Complex, is in a mixed-conifer forest, a popular summer tourist destination subject to a mixed-severity fire regime that has experienced 117 natural ignitions that have burned over 4,250 hectares within the past three decades (USDI BLM 2020). Forest managers and researchers need quantifiable baseline fire frequency and severity information to project and prepare for climate-altered fire regimes before current stand histories are erased by the next stand-replacing fires.

The Douglas-fir (*Psuedotsuga menziesii* var. *menziesii*) / ponderosa pine (*Pinus ponderosa* var. *ponderosa*) forests of Stehekin are dominated by more mesic vegetation and soil moistures than stands farther south along Lake Chelan, though drier than Douglas-fir dominated stands to the north. Although the vegetation in this area is unique due to its location in the ecotone between more mesic and drier sites, this examination is applicable to mixed-severity forests throughout the Pacific Northwest, as well as to studies of fire frequency and severity in mountainous terrain. Not only will it provide an in-depth study on historical fire frequency and severity where information was lacking, but in so doing, it increases our knowledge of another location along the continuum from moist to dry forests across the Cascade Range.

My study is the first empirically based examination of fire history for this area, quantifying fire history for the past 400+ years with fire dates ranging from 1596 to 2015. I used

fire scar data, stand ages, and forest structure data to identify fire intervals before and after non-Indigenous settlement and fire suppression, characterized the range of fire severities, and examined the environmental factors associated with different fire frequencies and severities.

1.3 Literature Review

There have been several fire-history studies in the northern Cascades, but none is transferable to the mixed-severity fire regime associated with the Douglas-fir / ponderosa pine forests of Stehekin. Most existing studies focus on low-severity fire frequency as derived from fire-scar data (e.g. Everett et al. 2000, Hessl et al. 2004, Wright and Agee 2004), or higher-severity fires using stand reconstructions (Harrod et al. 1999) or lake-sediment cores (Prichard 2003). A fire history at Desolation Peak (Agee et al. 1986) does examine both low- and high-severity fires using fire-scar data and stand reconstructions, but the moister environment and different forest composition (western hemlock / Douglas-fir at low elevations to Pacific silver fir / subalpine fir at high elevations) of the Desolation Peak study limit its relevance to fire frequency in Stehekin.

The differences between the Desolation Peak study and my own exemplify the broad scope encompassed by mixed-severity fire regimes. Fire scientists recognize the need to characterize more precisely the ratios of high- and low-severity fire within the mixed-severity regime, where every fire that is neither stand-replacing nor low-severity is lumped into one category (Agee 2005, Hessburg et al. 2007). I assumed that the Douglas-fir / ponderosa pine forests of Stehekin have always burned with mixed severity, given the ecology of the area (Agee, personal communication, 2005), but did not know if fire suppression had altered fuels enough to

increase the severity of current fires, or if moderate- and high-severity fires were more common historically than previously thought (Hessburg et al. 2007).

There is a resurgence of interest in defining historical fire regimes, especially within the mixed-severity regime. Stand reconstructions of Douglas-fir forests on both sides of the Cascade Range of Oregon (Weisberg 2004, Poage et al. 2009) acknowledge the importance and prevalence of mixed-severity fire in Douglas-fir forests. Poage et al. (2009) identified four distinct age structures of Douglas-fir in 250 old forest sites in western Oregon, each defined moderately well by regional climate and fire history, including mixed-severity fire. Weisberg (2004) also identified non-stand-replacing fire as an important factor in western Oregon.

Other researchers have used fire-scar data to quantify historical fire frequencies, and interpreted fire severities from timber records and early aerial photographs (Beaty and Taylor 2001, Klenner et al. 2008) or stand reconstructions (Fulé et al. 2003, Taylor and Skinner 2003, Beaty and Taylor 2008) in mixed-severity fire regimes. Heyerdahl et al. (2012) combined fire-scar data and stand reconstructions to identify the historical fire frequency of low-, moderate-, and high-severity fires in southern interior British Columbia, Canada. This approach may be most appropriate for identifying fires in mixed-severity regimes given that they experience low-severity fire recorded by fire scars, and higher-severity fire that kills recorder trees (Hessburg et al. 2007).

Heyerdahl et al. (2012) defined their study area as a mixed-severity regime dominated by frequent low-severity fires and interspersed with less common, small high-severity disturbances. They did not find aspect to be an important predictor of fire severity along an east-west gradient, nor between plots, which they attributed to their small (1,105 hectare) study area.

Topography has been shown to exert bottom-up control on fire frequency in low-severity fire regimes, whereby fires are smaller and more irregularly shaped (Kellogg et al. 2008, McKenzie and Kennedy 2012), likely due to topographic barriers and patchy spatial patterns of fuels (McKenzie et al. 2006). Longer fire-free intervals were also associated with steep terrain (Heyerdahl et al. 2001, Iniguez et al. 2008) and north aspects (Beaty and Taylor 2001, Taylor and Skinner 2003) in mixed-severity fire regimes. However, the influence of aspect on fire frequency may be scale-dependent, since Iniguez et al. (2008) did not find significant differences between aspects at the stand level, even on steep terrain. They surmised that topographic facets were not separated by barriers to fire spread, a requirement Heyerdahl et al. (2001) identified for aspects to influence fire frequency.

The goal of my research is to characterize the historical fire frequency and severity of Stehekin using quantifiable measures that can be used as a baseline from which to assess the effects of climate change. My objective is to identify the drivers of fire frequency and severity and understand the effects of settlement and fire suppression on the current stand structure and composition and how they have affected the baseline historical condition. These topics have been identified as research needs (Agee 2005, Perry et al. 2011, Heyerdahl et al. 2012), and will characterize mixed-severity regimes at a finer level of detail than currently exists for Pacific Northwest forests.

1.4 Research Questions

- 1) What are the mean fire frequencies for the Douglas-fir / ponderosa pine forests of Stehekin?
- 2) What are the proportions of low-, moderate-, and high-severity fires?
- 3) Have fire frequency and severity varied by topographic or other environmental factors?

A further goal is to generate data that inform management activities that increase resilience of these forests, and their fire regimes, to climate change.

1.5 Methods

1.5.1 Study Area

The study area comprises 4,108 hectares within the Douglas-fir / ponderosa pine forest (which ranges from 365 to 1800 meters elevation) surrounding the town of Stehekin in the southeastern portion of the North Cascades National Park Service Complex in Lake Chelan National Recreation Area. Fire-history plots were located in areas that were accessible via Park trails, game trails, or the lakeshore, and outside areas that have been thinned (Figure 1-1). In most cases, it was not possible to safely traverse beyond a 0.5 km distance of trails due to steep, unstable terrain and cliffs.

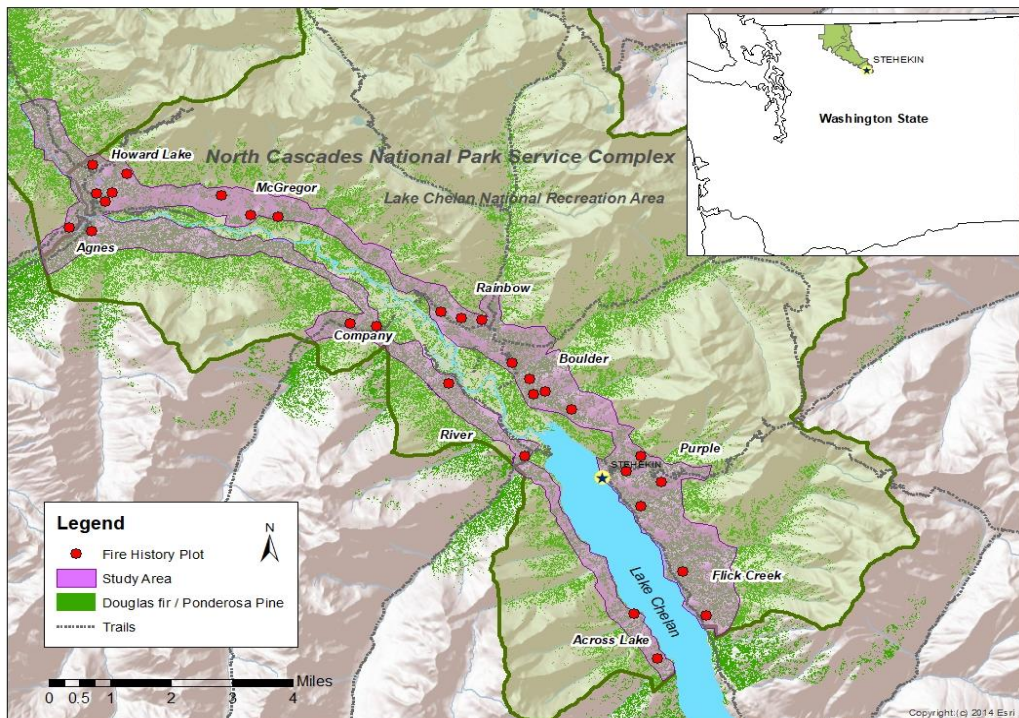


Figure 1-1. Map of the study area in Lake Chelan National Recreation Area. Thirty 5-hectare plots were installed in 10 units (labeled in italics) based on topographic features.

The town of Stehekin has a long history of human occupation and disturbance. Indigenous people lived in this area for thousands of years and regularly burned the forest for hunting, gathering, and clearing the land. The name “Stehekin” originates from a Salishan phrase with one of several interpretations being “the way through,” because this area provided the best route over the Cascades (*personal communication* K. Dicenzo, NPS Archeologist). The Chelan tribe had a village at the south end of Lake Chelan and regularly traveled over the Cascades to trade with the Skagit tribes. Chief Moses and the Chelan tribe were able to delay non-Indigenous settlement by negotiating with President Rutherford Hayes to establish the “Moses Reservation” in 1879, from the south end of Lake Chelan to the Canadian border, including Stehekin. Only seven years later though, in 1886, the reservation was confiscated, and the “Settlement Period” began (e.g., logging, mining, and homesteading) (Caldick 2012).

Several accounts from early explorers describe the surrounding mountains alight with fire, and oral history provides an account of an especially large fire in 1889 that swept through the Stehekin valley (Oliver and Larson 1981, Stone 1983). The “fire suppression period” began in 1908 when the Chelan National Forest was established and remained in effect through 1968 (Stone 1983, Van Wagendonk 2007). Wildfire is still prevalent in the Stehekin watershed, as is evident from the North Cascades National Park Service Complex fire atlas, which includes perimeters and ignition points for all recorded fires between 1954 and present.

Fires in the Douglas-fir / ponderosa pine forests of the Stehekin watershed are mixed severity, with a complex mosaic of low-, moderate-, and high-severity patches of variable size and grain. The forest mirrors this complexity in variable-sized, even- and mixed-aged stands, and scattered fire-scarred trees. The variability in patch size and fire size may be due to the high spatial complexity of both the terrain and vegetation of the northern Cascades, where fire

severity and fire spread are influenced by variable fuel moisture patterns (e.g., avalanche chutes, talus fields, etc.) (Cansler 2011, McKenzie 2020).

1.5.2 *Fire History Plots*

Thirty 5-hectare, circular plots were randomly located within the study area using a fire interval sampling approach (Johnson and Gutsell 1994), each within one kilometer from a trail or other access point. The individual plots were grouped by location into 10 “units”. I did not stratify the plots by topographic position because this would have further constrained the sampling area, which was already confined to areas that were not northern spotted owl (*Strix occidentalis caurina*) habitat, and that were proximal to trails. In a field reconnaissance in 2007, the 5-hectare plot size was determined to yield a sufficient sampling of fire-scarred trees and yet be homogeneous enough in structure to represent a single fire severity.

The fire-history plots serve several purposes: 1) to collect fire-scarred tree samples (wedges) to identify low- and mixed-severity fires, 2) to collect tree cores to identify cohorts of trees that established after high-severity fires, and 3) to conduct stand surveys to determine the ratio of fire-scarred trees to total tree density as a proxy for fire severity. The locations of the sampling areas for each of these activities are shown in Figure 1-2.

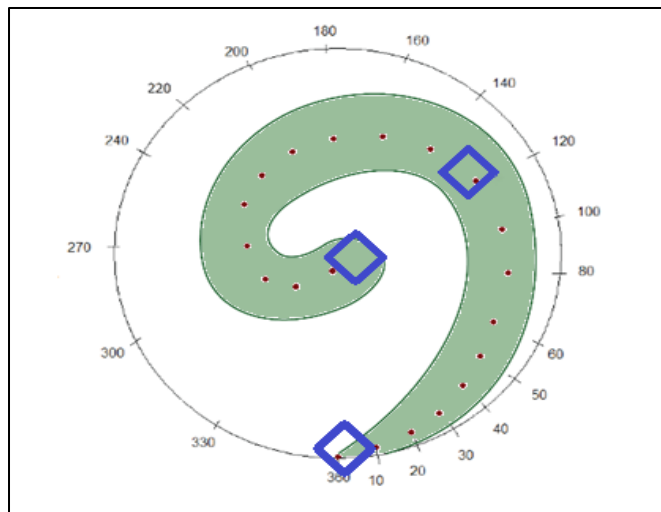


Figure 1-2. Diagram of circular fire-history plot. Each contains 20 sampling points (brown dots) for tree ages. Three 100-m² plots (blue squares) located at the first, last, and middle points are sampled for structural characteristics. An inventory of all fire-scarred trees is performed in the 20-meter band of the sampling spiral (green), comprising 0.94 hectares of each 5-hectare plot. Figure not drawn to scale.

Twenty-eight of the 5-hectare plots were surveyed for fire-scarred trees, 98 of which were chosen as wedge trees, and had sections cut from their boles to examine for internal scars indicative of low- to moderate-severity fires (Arno and Sneck 1977) (Table 1-1). Wedges could not be cut in two of the 30 plots because it was determined that they were in northern spotted owl habitat after the plots were inventoried. Therefore, these plots were included in only the fire severity assessment. All accessible areas within each plot were surveyed for potential wedge trees with the goal of collecting up to two samples from live trees, out of a total of four (to six) samples per plot. Each potential wedge tree was examined and photographed, and data were collected on both tree characteristics (diameter at breast height (DBH, 1.37 meters height), species, position in canopy (emergent, dominant, canopy, subcanopy)) and the local environment (slope, aspect, elevation). The wedge trees were selected after a thorough examination of all candidate trees. Recently dead trees were favored over live trees, and less vigorous live trees

were preferred over healthy individuals. These preferences were determined through discussion with the North Cascades National Park Service Complex wilderness committee.

Table 1-1. Characteristics of trees that had wedges removed: species, numbers of live and dead, and their average diameters (DBH).

Species	Number Live	DBH (cm) Live	Number Dead	DBH (cm) Dead	Total Number
Ponderosa pine	19	83.6	45	80.4	64
Douglas-fir	12	69.4	22	77.6	34
Total	31	78.1	67	79.5	98

Twenty trees were selected systematically along the transect (spiral) that began at a random point along the perimeter of the 5-hectare plot and spiraled in towards plot center. Tree cores from the 20 trees (with minimum DBH of 10-cm) were collected at DBH height and converted to base-height per species to derive establishment dates, and the same individual tree characteristics and local environmental data as collected for wedge trees were collected at these points. Eight plots had topographic barriers (cliffs, steep slopes) or environmental hazards (bees, hazard trees) which prevented sampling all 20 points.

I inventoried all fire-scarred trees along the 20-meter-wide (0.94 hectare) sampling spiral in 25 of the 30 plots to derive the proportion of fire-scarred trees to total trees as a proxy for fire severity. This proxy is based on my assumption that there are higher proportions of fire-scarred trees to total trees in plots with the lowest fire severity, given that more trees survived burning. Additional data were collected to aid in determining this ratio; species and diameter of all live and dead trees, including those without fire scars, were recorded on seven of the 20-meter bands, and tree density by species was recorded at three 100-m² subplots along each spiral. Two different scar types were recorded: 1) “cat-face” was used to describe charred, triangular

openings at the bases of trees, and 2) “zipper” was used to describe prominent longitudinal ridges on charred trees (usually Douglas-fir).

1.5.3 *Increment Cores*

Twenty increment cores per spiral were collected, mounted, and sanded as described in Stokes and Smiley (1968). After sample processing, in which some cores were omitted due to decay or missing rings, there were 552 cores in total. Dates of tree establishment were derived from the increment cores through ring counts. All samples were cross-dated using the tree-ring width analysis program COFECHA (Holmes 1983) and methods described by Stokes and Smiley (1968). Individual chronologies were developed for each unit using the oldest non-fire-scarred trees per plot and cross-dated to a master chronology for Stehekin (Littell et al. 2008) from Littell (2015 personal communication). The cores used to develop each unit chronology had COFECHA correlations of 0.30 or greater for each sample. All cores were taken at DBH height and adjusted from breast height age (BHA) to true age (Nigh 1995). I used an age correction of 14 years for Douglas-fir and 10 years for ponderosa pine based on comparisons of ages at base and breast height, and other local studies (Agee et al. 1986, Wong and Lertzman 2001).

1.5.4 *Identifying High-severity Fires*

The establishment dates of trees on the spirals were examined to identify cohorts of similar-aged trees that regenerated following high-severity fires that would not have been recorded by surviving fire-scarred trees. I inspected each spiral for the presence of even-aged cohorts of six or more trees whose establishment dates occur within 40-year periods without fire scars, my criteria for high-severity fire. This criterion was based on Heyerdahl et al. (2012) who

assigned high-severity fire to even-aged cohorts where five or more trees established in a plot within a 20-year period, proceeded by at least 30 years during which no trees established. I lengthened the establishment period to 40 years based on Oliver and Larson (1981) who identified peaks in establishment (pulses) of Douglas-fir in Stehekin that occurred 35 to 40 years after fires.

1.5.5 *Wedge Samples*

Wedge samples were sanded and analyzed under a microscope to identify and date each fire scar. Ring widths were measured, and dates for fires were derived through cross-dating as described for the increment core samples and visual matching of fire-scar sequences between samples in the same plots. Scars were considered to have been caused by fire if they originated from a charred cat-face or other scar that contained apparent charcoal, or if they were duplicated on another wedge or core in the plot with evidence of fire. Scars that could not be linked to direct fire evidence were still considered to be potential fire scars if they corresponded to a prominent cohort, and other fire-scarred trees were in the vicinity.

Twenty-eight of the 98 wedge samples were omitted from the fire-history analysis due to the presence of extensive rot or inability to cross-date visually or with COFECHA. The most problematic samples were from dead and decaying trees, which often did not contain large enough areas of solid wood to identify clear marker rings. This problem was exacerbated on samples with multiple fire scars where ring-width patterns were distorted by the fire scars and often included false or missing rings.

Many of the samples were cross-dated in a three-step process whereby tentative dates were derived from COFECHA, these scar dates were re-examined by matching intervals between

scars to the most reliable samples, and then re-running any revised sample dates through COFECHA again. The final COFECHA correlation values and methods used to cross-date the fire scars are documented and preserved in the sample database, and all samples are preserved in the North Cascades National Park curatorial building in Marblemount, Washington. Despite extensive effort to cross-date, some of the wedge samples have less than 0.30 correlation, a commonly used minimum value for dendrochronology (Cook and Kairiukstis 1992). Samples from Howard Lake were especially difficult due to the presence of multiple scars on each sample that did not match up visually or in COFECHA. This issue was anticipated given that COFECHA yields low correlation values in decades with fire scars on samples (Holmes 1983).

1.5.6 *Derivation of Environmental Predictors*

I used the Spatial Analyst tool in ArcGIS to derive mean values for slope, aspect, and elevation of each plot from Digital Elevation Models (DEMs) for North Cascades National Park Service Complex (Table 1-2). The mean values for aspect were manually rescaled from zero in the northeast (coolest aspect) to one in the southwest (warmest aspect) using a calculation from McCune and Keon (2002) to derive the “cosine-aspect” (COS-Asp) for each plot. Mean values for direct incident radiation (DIR) and heat load were also calculated on a spreadsheet using equations from McCune and Keon (2002). The calculation of DIR combines slope, latitude, and aspect, whereas heat load uses COS-Asp in place of aspect.

Table 1-2. Sources and ranges of environmental predictors used in regression models for historical fire frequency and severity.

Variable	Label	Source	Plot Range
Slope (percent)	Slope	DEM	21 – 82
Aspect Adjusted	COS-Asp	Aspect from DEM, adjusted using $(1-\cos(\theta-45))/2$, where θ = aspect	0 – 1
Elevation (meters)	Elev	DEM	403 – 885
Direct Incident Radiation	DIR	Equation using slope, latitude, and aspect (McCune & Keon 2002)	0.1 – 1.0
Heat Load	Heatload	Same equation as DIR except COS-Asp replaces aspect (McCune & Keon 2002)	0.1 – 1.0

1.5.7 Statistical Analysis of Fire Frequency

Point fire-return interval (point FRI) estimates, which are calculated by averaging the interval lengths between fires on individual tree samples, are likely to over-inflate the fire interval because not every fire will scar every tree, and some scars are burned off by more recent fires (Agee 1993). Composite fire intervals (CFI), in which the average interval length is based on the combined fire dates from multiple samples within an area (5-hectares in this study), reduces the likelihood of missing fires; however, it overestimates the number of individual fires if fire dates for the same fire differ among samples. To prevent overestimation of the number of individual fires in plots with low correlation values in COFECHA, fires that were within three years of each other within the same plot were assigned the fire date from the sample with the highest correlation value for the fire. Given the high probability of individual point samples not recording all fires due to rot, and the conservative approach taken to assign fire dates, I am confident in my assumption that the CFI is the most accurate and complete estimate of fire frequency per plot.

The fire history samples were entered into Fire History Analysis and Exploration System (FHAES) (Brewer et al. 2016) to build a master fire history chronology for Stehekin. The mean point FRI, and composite intervals for the full sampling period (CFI) and for the time-period before non-indigenous settlement in 1886 (historical CFI) were calculated for each plot in FHAES. The Weibull mean probability interval (WMPI), a composite fire interval following a negative exponential curve (Agee 1993, Scheiner and Gurevitch 2001), was also calculated for each plot. The point FRI and CFIs were also hand-calculated in excel to examine which plots had the greatest effect on the resulting intervals. Plot 23 in the Rainbow unit was identified as an outlier due to lack of sufficient samples and excluded from all the interval calculations. I computed the grand mean CFI for the area with the remaining 27 plots, and the mean historical CFI with 23 plots that contained samples with intervals before non-indigenous Settlement. I also calculated CFIs and historical CFIs for each unit.

I used paired t-tests to analyze the effects of settlement and fire suppression on fire frequency (number of fires) and compared fire interval lengths before and after fire suppression. The samples were evaluated to confirm that they met the assumptions of t-tests (Ramsey and Schafer 2002): 1) quantile plots followed a normal distribution, 2) the dates of each fire were identified independently of other fires, 3) the fire samples were collected randomly, and 4) the variances were approximately equal before and after settlement and fire suppression. I maintained equal sampling periods on either side of each fire frequency analysis, comparing the number of fires for 21 years before and after settlement in 1886, and 59 years before and after fire suppression from 1908 to 1968. For the analysis of fire suppression on fire interval lengths, it was not necessary to maintain equal sampling periods because I was interested in the average length of the intervals before and after suppression rather than the number of intervals. I counted

the time from the most recent fire within the suppression era to the most recent fire after 1968 as the suppression interval. If there were no fires after 1968, then I used the end of the sampling period (2020) as the end of the interval, knowing that the true interval is at least as long. I could not accurately analyze the effects of settlement on interval length because the settlement period is shorter than the mean interval length for the plots.

1.5.8 *Analysis of Predictors*

I began each analysis of fire frequency and severity by using graphical methods for data exploration and model testing appropriate for ecological data (e.g., Ramsey and Schafer 2002, Scheiner and Gurevitch 2001). I used R statistical software (R Core Team 2021) to construct a matrix of scatterplots, rescale the data, and add log-transformed variables to fit the preliminary models and meet the assumptions of linear models (Harrell 2015). I examined the distribution of the log-transformed response and predictor variables and confirmed that they were normally distributed. Plot 23 in the Rainbow unit was identified as an outlier and removed from the fire frequency analysis due to low sample size and the presence of additional fires that could not be definitively verified. Similarly, Plot 13 in the Agnes unit was identified as an outlier and eliminated from the fire severity analysis due to questionable “zipper” scars reported on Douglas-firs that may not have been fire-caused, since no other fire evidence was present.

I used Ordinary Least Squares (OLS) linear regression to identify potential environmental predictors of historical (before non-indigenous settlement) fire frequency with the model:

$$Historical\ CFI = \beta(Slope) + \beta(Aspect) + \beta(Elevation) + \beta(DIR) + \beta(Heat\ load)$$

A secondary analysis to test the influence of categorical predictors (presence/absence of ponderosa pine, NE/SW-facing plot locations, plots grouped by unit) on fire frequency was performed using ANOVA to test the model:

$$CFI = \beta(PIPO) + \beta(SW-face) + \beta(Unit) + \epsilon$$

I used a General Linear Model (GLM) “quasi-binomial”, which is appropriate for proportional response variables, to determine the influence of environmental factors on fire severity. In GLMs, the goodness of fit of the model is assessed using the proportional reduction in deviance (PRD) rather than R-squared. I tested the model:

$$\text{Scarred / Total Trees} = \beta(\text{Slope}) + \beta(\text{Aspect}) + \beta(\text{Elevation}) + \beta(\text{DIR}) + \beta(\text{Heat load})$$

1.6 Results

1.6.1 *Historical Fire Frequency*

I collected and cross-dated a total of 264 fire scars from 78 trees in 28 fire-history plots throughout the Stehekin watershed (Figure 1-3). I identified 109 different fire years over the 462-year sampling period (1558 – 2020), which is just under one fire every four years. The Stehekin fire chart has an average of 4 scars per sample (tree or core), whereas the Stehekin composite fire history chart (Figure 1-4) consolidates all the fires within each plot into one record, with an average of 7 fire scars on each.

I added three recent wildfires (2006 Flick Creek, 2010 Rainbow and 2015 Wolverine fires) that burned through eight of the plots, extending the interval calculation period from 2009 to 2015, and the sampling-interval period to 2020. The 2837-hectare Flick Creek fire scarred trees in five of the six plots in which it burned (confirming that my sampling schema was

effective at capturing large fires) and was added to the one plot in which it was known to have burned but was not recorded.

Stehkin Fire Chart

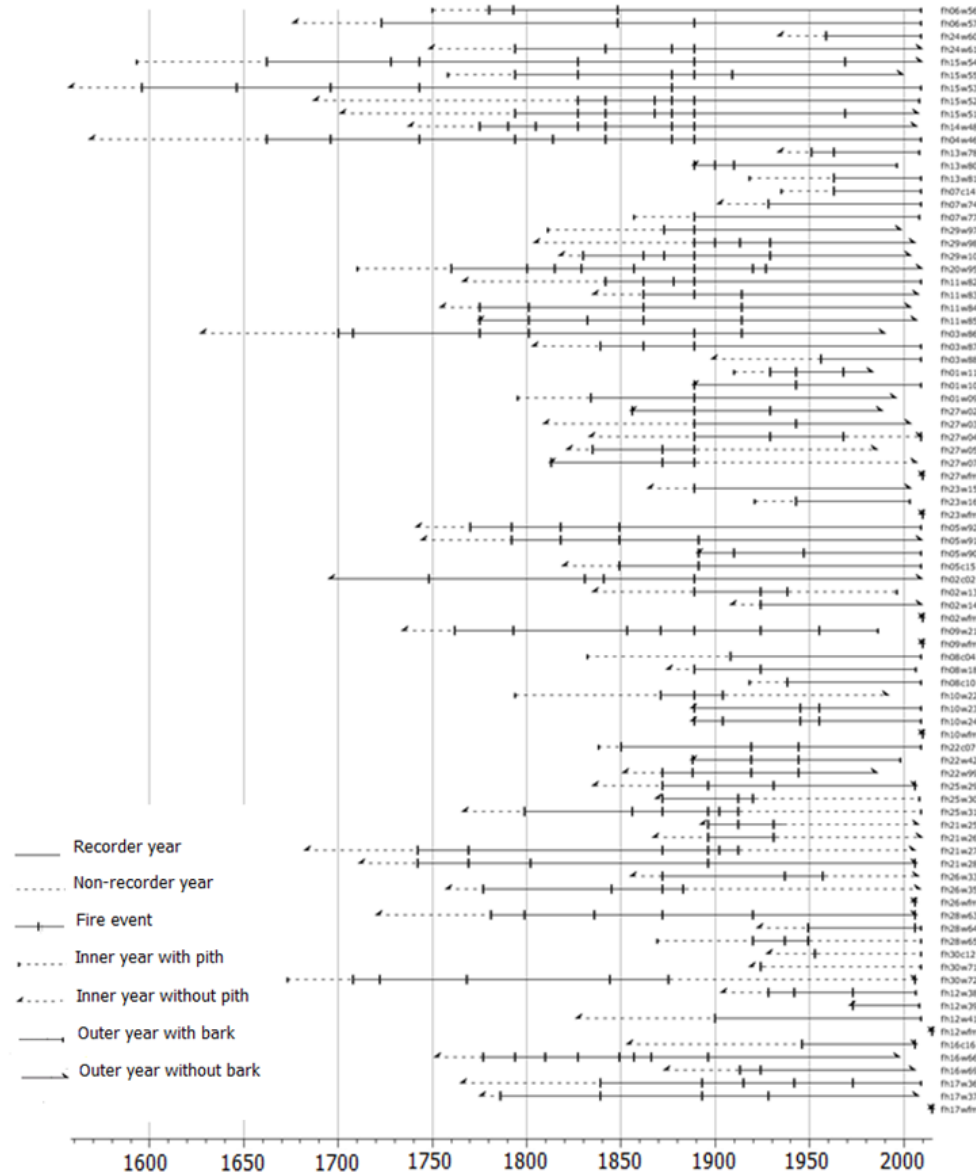


Figure 1-3. The Stehkin fire chart contains 78 individual tree samples with a total of 264 fire scars recording 109 different fire dates during the sampling period between 1558 and 2020. Three recent fires (2006, 2010, and 2015) that burned through eight plots are represented by rows with the fire dates only. Samples are ordered from north to south. Each horizontal line shows the fire scars identified on a single tree sample (point).

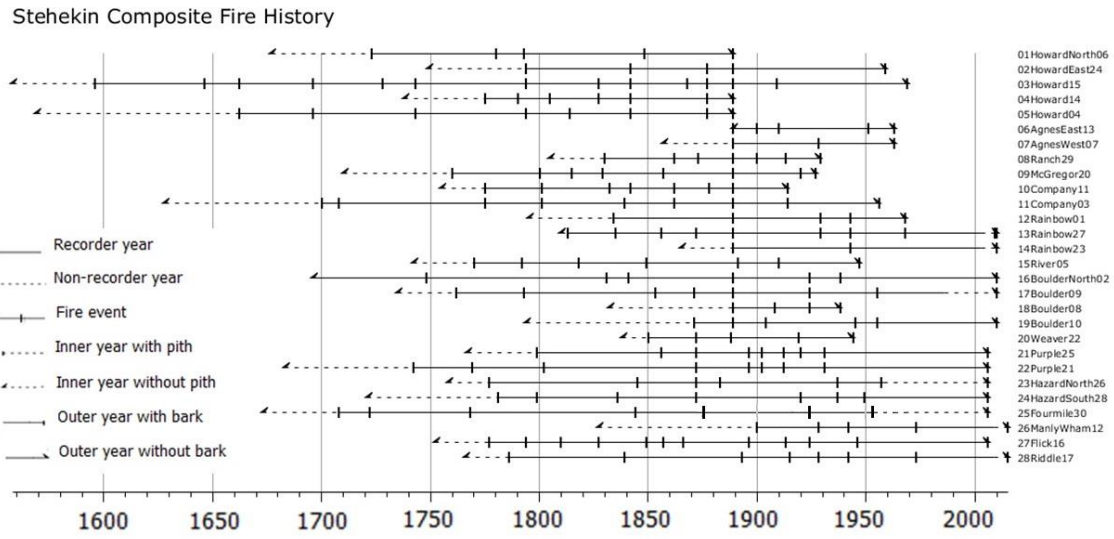


Figure 1-4. Stehkin composite fire chart using all 28 fire-history plots. Each horizontal line represents a composite of the fires recorded on trees within a 5-hectare plot. A total of 109 individual fire dates were recorded on 192 fire scars in the sampling period of 1558 through 2009. Three recent fires (2006, 2010, 2015) were added to eight plots, extending the sampling period to 2020.

The 1889 fire was recorded in 42% (33 of 78) of the samples and thus served as a reference fire for cross-dating (Figure 1-5). My plots show that this fire, documented by early settlers as a “major fire that swept through the (Stehkin) valley” (Stone 1983), burned through all the northeastern units (Howard Lake, McGregor, Rainbow, and Boulder). Prominent fire scars cross-date to 1889 in the Agnes and Company units on the west side of the Stehkin River. Given that winds and fire spread predominantly eastward and northward from the Company and Agnes units (NPS 2010), it is likely that the 1889 fire started on the west side of the Stehkin River and spotted across to the northeastern units. The year 1872, with 10 scars recording fire, and the years 1877 and 1896 with seven scars each, were also big fire years. Most fires, however, were recorded by one scar (49 fires), or two scars (30 fires), indicating that they were relatively small or were high severity and recorded by only a few legacy trees.

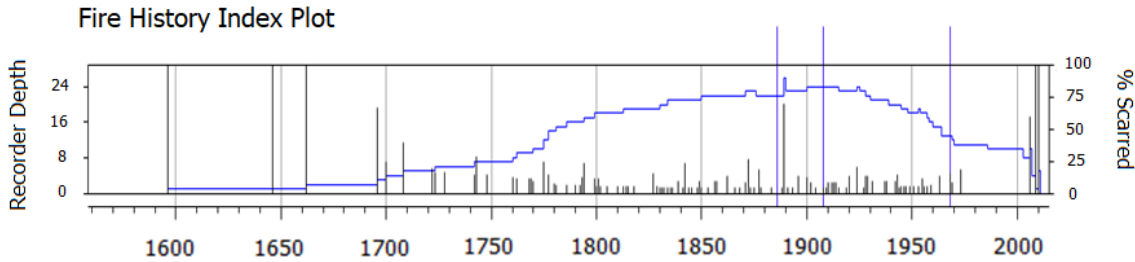


Figure 1-5. Fire index plot for Stehekin. Blue line shows how many samples are in recording status each year (recorder depth), and bars show the percent of scars recorded each year. The year of the 1889 fire is recorded by 33 trees. 1872 (10 scars), 1877 and 1896 (7 scars each) are also big fire years. Purple lines extending beyond graph mark non-Indigenous settlement (1886), fire suppression (1908), and post-suppression (1967) eras.

1.6.2 *Mean Composite Fire Intervals*

The grand mean CFI for Stehekin is 30 years ($SD = 8$, 27 plots) (outlier plot 23 omitted from computation), and the mean historical CFI is 31 years ($SD = 11$, 23 plots) (Table 1-3). The WMPI is equivalent to the CFI, whereas the point FRI is six years longer (Mean = 36 years, $SD = 13$). This was partly due to several samples with trees that did not have the minimum two scars to define an interval, and therefore could not be included in the calculation. There were also too few intervals per sample to accurately report the historical point FRI for the unit.

The CFIs per plot ranged from 16 to 44 years, and the historical CFIs had an even wider range of variability at the plot level (17 to 55 years). Mean CFIs at the unit level ranged from 20 years in the McGregor unit to 33 years at Howard Lake. Boxplots of the unit CFIs illustrate that although the unit CFIs are all within 12 years of each other, they vary widely within that narrow timeframe (Figure 1-6). For example, the range of the CFI for the McGregor plots is completely outside of the range of the CFI for the Purple plots.

Table 1-3. Composite fire intervals for all years (CFI) and before non-Indigenous settlement (Historical CFI) with means and standard deviations (SD) for 10 individual units, and all units combined (All-Unit) in the Stehekin watershed. Number of plots for CFI (C) and Historical (H). Plot 23 in Rainbow unit not included due to low sample size. Number of trees and scars listed for CFI. Weibull median probability interval (WMPI) and the point FRI are comparable to the all-unit composite interval. Not enough intervals (NA) for some Historical CFIs. Last scars with * are from fire records.

Unit	Plots			CFI		Historical CFI		Fire Scars		Analysis Years	
	C/H	Trees	Scars	Mean	SD	Mean	SD	First	Last	Begin	End
Howard Lk.	5/5	11	54	33	9	30	8	1596	1969	1558	2020
Agnes	2/0	6	9	28	13	NA	NA	1857	1963	1857	2020
McGregor	2/2	4	19	20	5	23	4	1760	1929	1710	2020
Company	2/2	7	26	26	9	25	9	1700	1956	1628	2020
Rainbow	2/2	7	22	28	8	37	26	1813	2010*	1795	2020
Boulder	4/3	10	32	31	12	32	15	1748	2010*	1696	2020
River	2/2	7	23	27	4	25	8	1770	1947	1742	2020
Purple	4/4	12	48	32	5	34	4	1742	2006	1683	2020
Flick Ck.	2/2	6	20	32	15	29	18	1708	2006	1673	2020
Across Lk.	2/1	5	16	31	3	54	NA	1786	2015*	1766	2020
All-Unit								1596	2015	1558	2020
Composite	27	75	269	30	8	31	11				
WMPI	27	75	269	30	8	32	11				
Point FRI	NA	66	260	36	13	NA	NA				

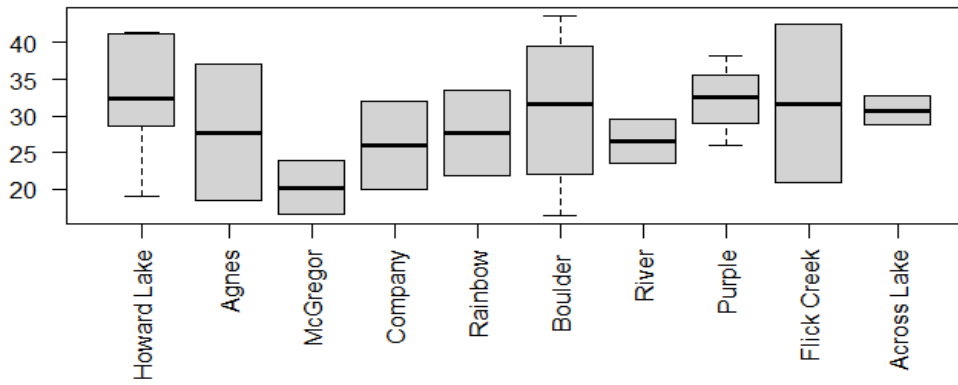


Figure 1-6. Boxplots of the mean composite intervals (CFI) for 10 individual units in Stehekin. Dark line is the median CFI value, and lower and upper edges of boxes are the 1st and 3rd quartiles. Dotted lines (whiskers) extend to minimum and maximum data points. There are no outliers.

1.6.3 Establishment Dates

I did not identify any additional fires through the analysis of establishment dates (Figure 1-7). I found that tree establishment frequently occurred in pulses of six or more trees within 40 years followed by decades of lesser tree establishment, but these pulses were always preceded by a fire. These findings confirm that fires were historically mixed-severity, whereby enough trees were killed by the fires to initiate a pulse of establishment, but not severe enough to be stand-replacing. Most of the trees in the plots established between 1900 and 1940 in response to fires in the early 1900s. I found fewer older trees in the plots despite multiple earlier fires, which again confirms that fires were historically mixed severity, with enough older legacy trees to record fire history despite the replacement of a large proportion of each stand with each subsequent fire.

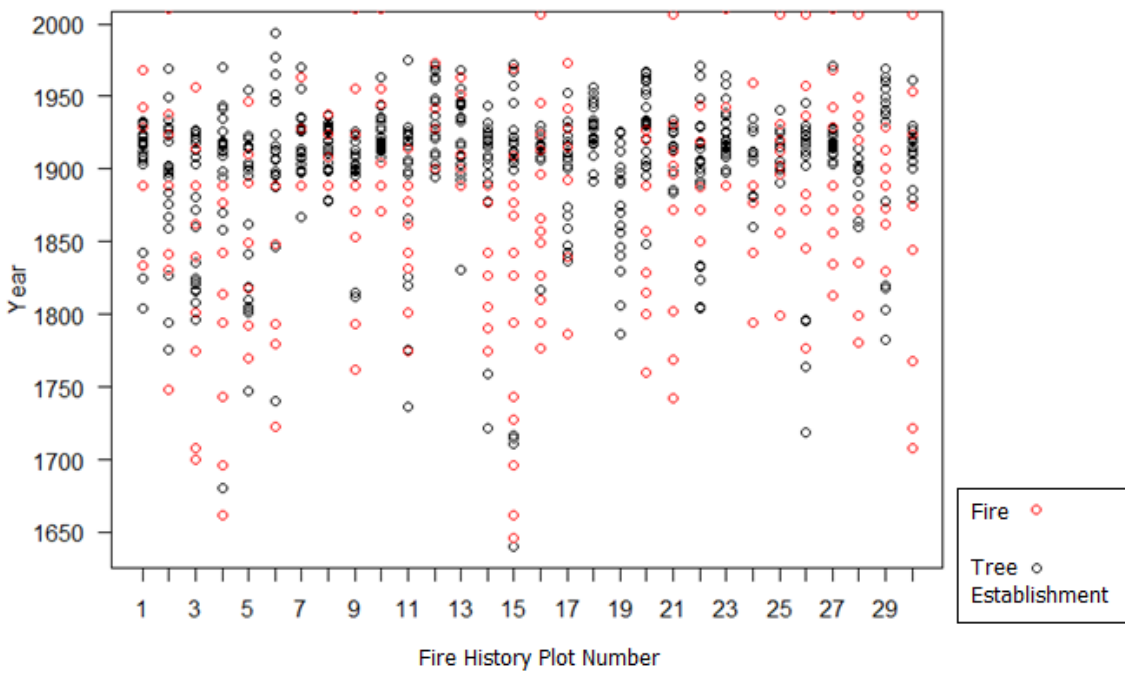


Figure 1-7. Dates of tree establishment in 30 fire history plots, and corresponding fire dates in 28 plots (fire scars not collected in plots 18 and 19). All cases where six or more trees established within 40 years were preceded by a fire, indicating that no high severity fires were missed in the fire scar sampling. See text for explanation.

1.6.4 Effects of Settlement and Fire Suppression

I found a significant difference ($p = 0.047$) in the number of fires that occurred in the first 21 years (1886–1907) of non-indigenous settlement (settlement mean = 1.1 fires) compared to 21 years (1864–1885) before settlement (pre-settlement mean = 0.7 fires) (Table 1-4). Although I did not find a significant decrease in fire frequency during the suppression era (1908 – 1967) vs. pre-suppression (1848 – 1907), I did find a significantly longer fire interval corresponding to mandatory suppression ($p=0.004$). The CFI before suppression (pre-suppression mean = 29.7 years) was almost equivalent to the grand mean CFI for Stehekin, whereas the suppression mean CFI was 50.5 years.

Table 1-4. Analysis of settlement and fire suppression. Summary of t-test results comparing 1) number of fires before (Pre) settlement (1864-1885) and after (Post) settlement (1886 – 1907), and 2) Pre fire suppression (1849 - 1907) and Post fire suppression (1908 – 1967), and 3) interval length Pre and Post fire suppression. * is significant at 95% confidence level, ** is significant at the 99% confidence level.

Settlement (1886)	t-Value	df	p-Value	Pre Mean (SD)	Post Mean (SD)	Mean Difference
1) No. fires +/- 21 years	-2.087	25	0.047 *	0.7 (0.6)	1.1 (0.6)	-0.346
Suppression (1908)	t-Value	df	p-Value	Pre Mean (SD)	Post Mean (SD)	Mean Difference
2) No. fires +/- 59 years	1.138	26	0.266	2.2 (1.0)	1.9 (0.9)	0.296
3) Fire interval length	-3.178	23	0.004 **	29.7 (11.9)	50.5 (28.5)	-20.853

1.6.5 *Historical Fire Severity*

The plots were ranked from lowest to highest fire severity (1 – 24) based on the proportions of fire-scarred to total trees per hectare, the proxy for fire severity. The plot with the highest proportion of scars to trees (25 scarred trees / 225 trees per ha = 0.11) was ranked the lowest fire severity (rank 1), and the plot with the highest proportion (5 scarred trees / 900 trees per ha = 0.01) ranked highest severity (rank 24). The mean proportion of scarred to total trees per hectare was 0.031 (3.1%) with standard deviation of 0.025 (2.5%). The scatterplot of the severity rankings shows a wide variation in the number of fire-scarred trees and tree densities per hectare (Figure 1-8). The units, however, do tend to group by more narrow ranges of severity (Figure 1-9). Notably, the River unit has two plots with equivalent fire severities (0.029 and 0.030), and all 4 plots at Howard Lake have high severity ranks.

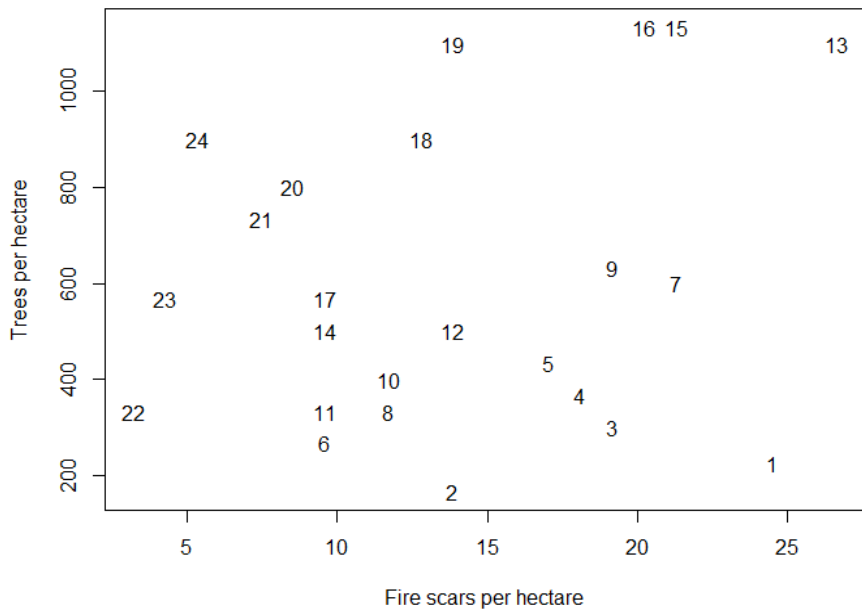


Figure 1-8. Scatterplot of the proxy for fire severity; the proportion of fire-scarred trees to total number of trees per hectare. The proportions (points) are ranked from lowest to highest severity (1 – 24). Lowest severity in the bottom right corner (25 fire scars/hectare in stand with 225 trees/hectare) and highest severity in upper left (5 fire scars/hectare in stand with 900 trees/hectare).

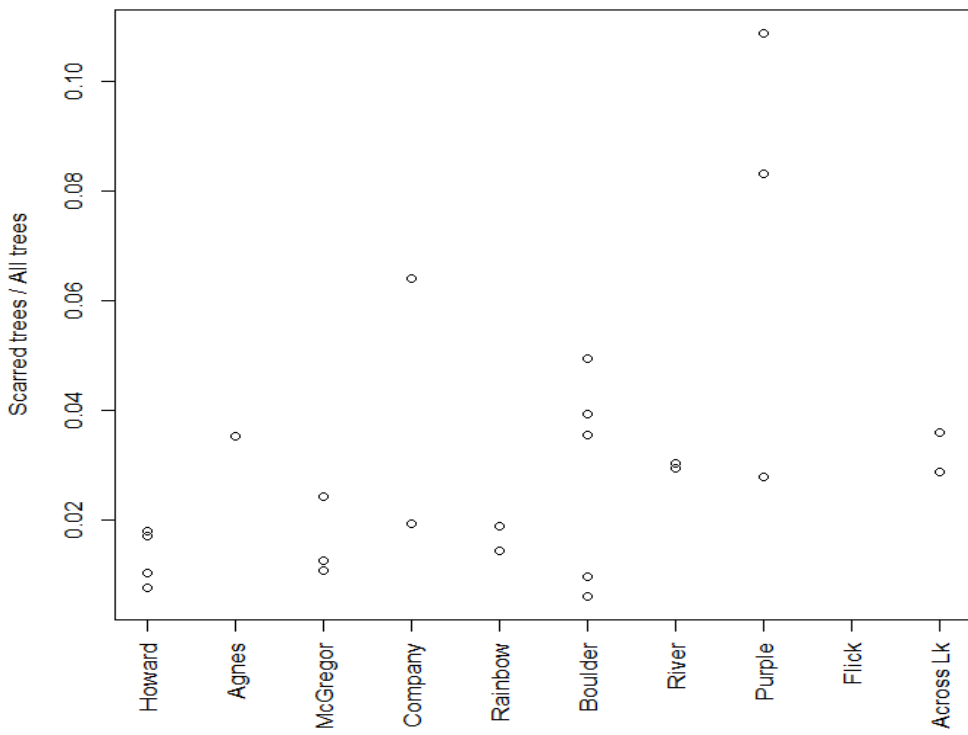


Figure 1-9. Fire severity (proportions of fire-scarred to total trees per hectare) per plot in each unit with fire-scarred trees. Smaller proportions of scarred /total trees represent higher fire severities.

1.6.6 *Fire Frequency Predictors*

The stand characteristics and stand ages of the plots are listed in Table 1-5. I did not identify any significant environmental predictors (aspect, elevation, slope, heat load, or direct incident radiation) of the historical CFI using OLS regression. Bivariate scatterplots of the historical CFI paired with each potential predictor confirmed that there were weak to no statistical relationships between the response and individual predictors.

However, the secondary analysis using ANOVA revealed significant differences in CFIs between plots with/without the presence of ponderosa pine ($p=0.07$, alpha level 0.1) and in interaction between unit, southwest vs. northeast aspects, and ponderosa pine ($p=0.02$) (Table 1-6). I explored these results by plotting CFI by aspect and overlaying the proportions of ponderosa pine and the unit code (Figure 1-10). NE-facing plots were clustered at moderate CFIs (24 to 33 years), whereas SW-facing plots were distributed evenly across the range of CFIs. Ponderosa pine was associated with the longest intervals and absent in all but one of the units (McGregor) with a shorter interval (< 24 CFI). There did not appear to be a direct relationship between the presence of ponderosa pine and plot aspect, but ponderosa pine did tend to vary by unit. Ponderosa pine was present or absent depending upon unit in 5 out of 10 units, and only 2 units had equal numbers of plots with ponderosa pine present and absent. Lastly, plots in the same units shared the same aspect (NE-facing or SW-facing) in all but one unit (Company).

Table 1-5. Summary of structural and environmental characteristics for each unit. Units ordered from north (1) to south (10). Mean tree age derived from cores collected at 20 points along the sampling spiral. Stand characteristics (DBH, PIPO/PSME = proportion of ponderosa pine to Douglas-fir) derived from three 100-m² plots along the spiral. Environmental characteristics for each plot were derived from GIS (shown in table) and sampled locally along the spiral (for reference only).

Unit	Plots	Mean Age	Mean DBH	Trees Per Ha	PIPO /PSME	Mean Slope (%)	Mean Aspect	Mean Elev (m)
1 Howard Lake	5	103	50.2	750	0.32	38.3	SW	707
2 Agnes	2	89	30.3	433	0.00	33.5	SE	588
3 McGregor	3	103	50.0	1000	0.50	39.7	SW	579
4 Company	2	128	49.4	400	0.00	31.0	NE/SW	602
5 Rainbow	3	126	39.9	1017	0.04	48.1	SW	689
6 Boulder	5	98	46.4	527	0.11	47.6	SW	551
7 River	2	126	39.9	517	0.14	40.7	NE	431
8 Purple	4	95	39.0	297	0.04	61.7	SW	698
9 Flick Creek	2	111	41.2	----	----	53.7	SW	481
10 Across Lake	2	94	35.1	300	0.21	64.5	NE	447

Table 1-6. ANOVA of fire frequency predictors shows significant differences in CFI with presence/absence of ponderosa pine (PIPO), and in interaction with location (Unit), SW-facing/NE-facing aspects (SW/NE), and PIPO. • is significant at the 90th confidence level, * is significant at the 95th confidence level.

ANOVA Results: $CFI \approx \text{Unit} * \text{SW/NE Aspect} * \text{Ponderosa Pine}$

Coefficients:	Df	Sum Sq	Mean Sq	F value	Pr (> F)
Unit	1	3.2	3.2	0.066	0.801
SW/NE	1	0.1	0.1	0.001	0.971
PIPO	1	190.6	190.6	3.910	0.068 •
Unit * SW/NE	1	39.3	39.3	0.806	0.385
Unit * PIPO	1	27.4	27.4	0.563	0.466
SW/NE * PIPO	1	44.9	44.9	0.921	0.354
Unit * SW/NE * PIPO	1	316.4	316.4	6.492	0.023 *
Residuals	14	682.4	48.7		$R^2=0.48$

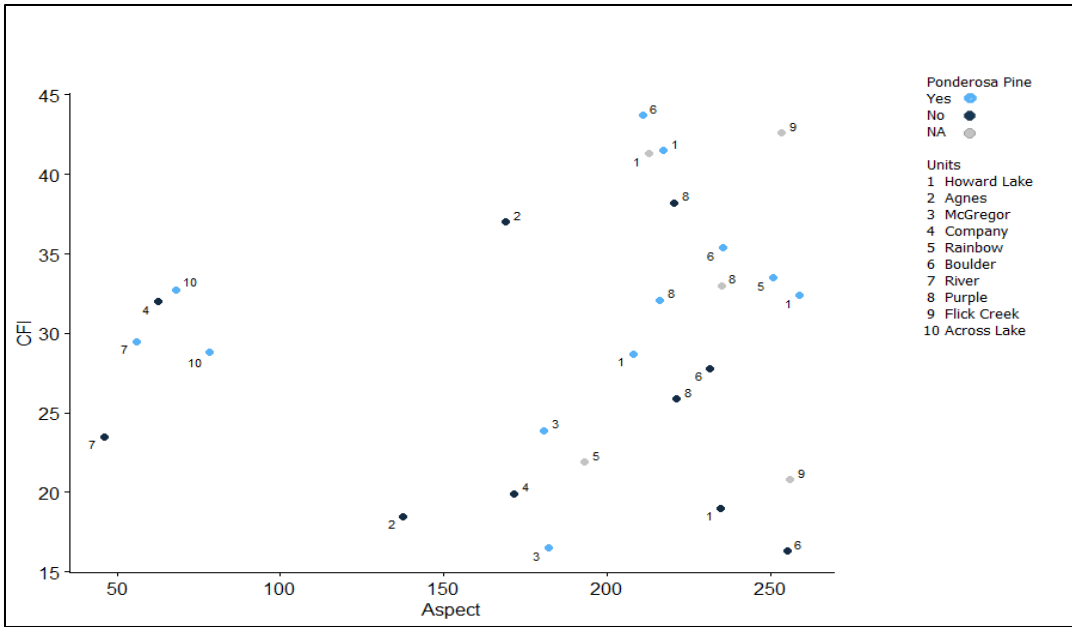


Figure 1-10. Scatterplot of CFI by aspect with unit codes and presence/absence of ponderosa pine indicated at each point.

1.6.7 Fire Severity Predictors

Slope (Log Slope) and the interaction of slope and aspect (Log Slope x Log COS-Aspect) were both identified as significant predictors (Slope: 95th percentile p=0.01; Slope x Aspect: 90th percentile p=0.05) of fire severity in the GLM (Table 1-7). There is an inverse relationship between slope and fire severity such that fire severity decreases as the steepness of the slope increases (Figure 1-11). Slopes ranged from moderate (21.3%) to very steep (65.3%) with the average being moderate (Mean = 43%, SD = 13.5%). Perhaps more intuitive, the regression also revealed that fire severity is lower at cooler (NE-facing) aspects, although the cosine-aspect was not a significant predictor of fire severity except in interaction with slope. The cosine-aspect was more varied and dispersed at higher severities and lesser slopes. The average cosine-aspect on NE-facing cool aspects to one on SW-facing warm aspects.

Table 1-7. GLM of fire severity predictors identifies slope (Log Slope) and the interaction of slope and aspect (COS-Aspect) as significant predictors of fire severity. Fire severity is represented by the proportion of fire-scarred trees per hectare to total trees per hectare. * is significant at 95th percent confidence level, · is significant at the 90th percent confidence level. PRD is proportional reduction in deviance for GLM.

GLM (Quasibinomial): Scars Per Trees \approx Log Slope * Log COS-Aspect

Coefficients:	Estimate	Std. Error	t value	Pr (> t)	
(Intercept)	-3.55	0.125	-28.501	<2e-16	***
Log Slope	0.37	0.132	2.827	0.010	*
Log COS-Aspect	-0.16	0.121	-1.309	0.205	
Log Slope * Log COS-Aspect	-0.21	0.104	-2.050	0.054	.
Null deviance	0.399	on 23 df			
Residual deviance	0.179	on 20 df		PRD	0.552

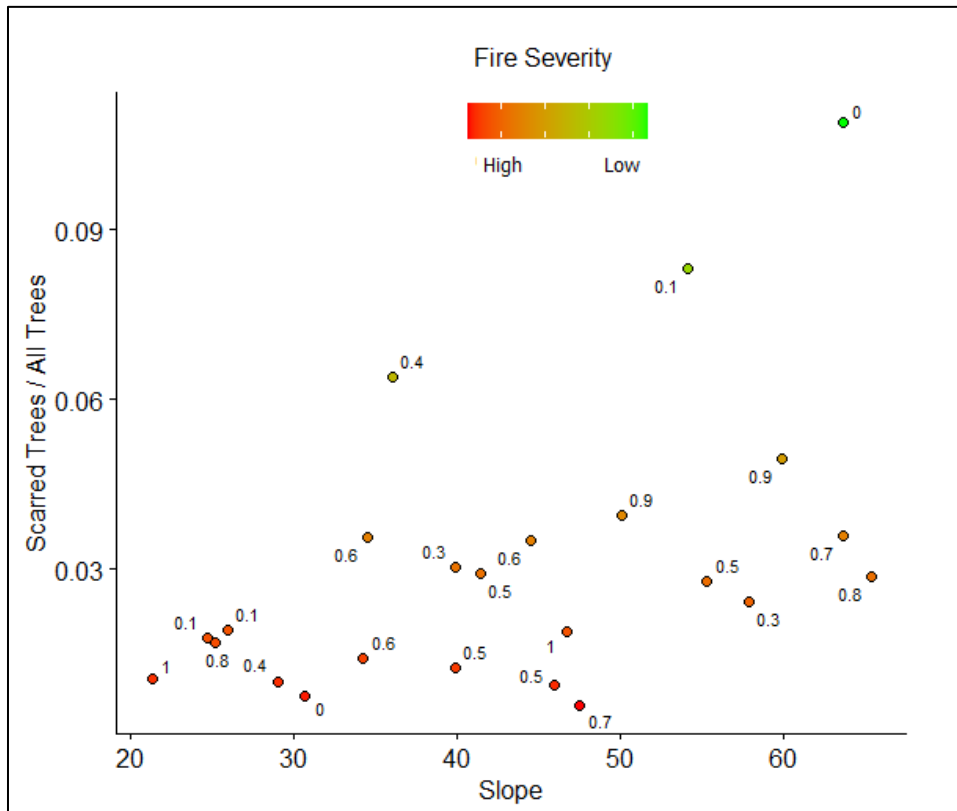


Figure 1-11. Scatterplot of the proxy for fire severity (proportion of scarred trees to total trees per hectare) and mean slope of 24 fire history plots. Low proportions of scarred trees represent higher fire severity. Fire severity decreases as slope increases. Cosine-aspect values for each plot show cooler aspects (lower values) associated with lower fire severity.

1.6.8 Fire Frequency and Severity per Plot

Fire frequency and severity varied across the plots (Figure 1-12). Plots of high severity are distributed across the range of fire frequencies, indicating that there is no relationship between fire frequency and fire severity. Although I found that fire severity differs by unit, I did not find an equivalent relationship between CFI and unit. This is especially evident in the Boulder and Howard Lake units where plots span the range of fire frequency, such that plots with moderate to high fire severities are associated with the shortest and longest fire intervals.

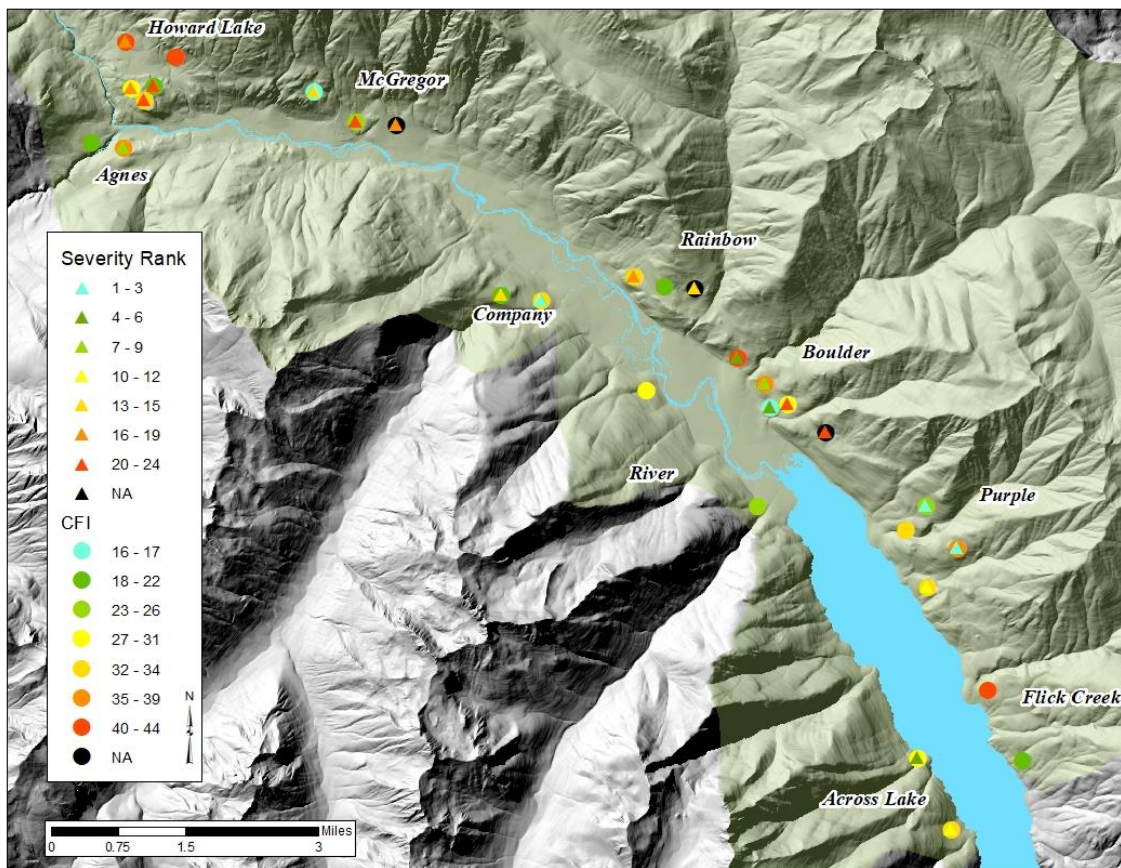


Figure 1-12. Fire severity ranks and mean CFI (years) for 30 fire-history plots in 10 units (in *italics*) in Stehekin, Lake Chelan National Recreation Area. Triangles represent severity rank (1-24) from low to high. Circles represent mean CFI from shortest to longest (16 to 44 years). Solid colored circles have same relative rank for fire severity and CFI. Black indicates data not collected (NA).

1.7 Discussion

My research illustrates the frequent, dominant, and complex nature of fire in the Stehekin valley. The historical mean CFI (31 years, SD=11), grand mean CFI (30 years, SD=8) and narrow range of the unit CFIs (20 to 33 years) verify that fires have been relatively common and persistent throughout the 457-year sampling period (1558–2020). Within that period, I confirmed a brief but significant increase in the number of fires over the settlement era (1886 – 1907), followed by a prolonged fire-free interval during the suppression era (1908 – 1967) that lengthened the mean CFI from 30 years to 51 years ($p=0.004$). Although the frequency of fire has remained relatively high throughout the sampling period, the locations and characteristics of these fires have been highly variable. Throughout the sampling period, and likely well before it, I found a complex interplay of topographic, anthropogenic, and environmental drivers that influenced the frequency, severity, and characteristics of these fires.

The analysis of fire frequency predictors revealed complex interactions between bottom-up controls (species, location, and topography) that have been recognized as important drivers in this complex terrain (Kellogg et al. 2008). The ANOVA revealed significant differences in CFI based on; 1) the interaction of location (unit), SW/NE-facing aspects, and presence of ponderosa pine, and 2) the presence/absence of ponderosa pine (at 0.1 alpha level). I had anticipated finding a positive correlation between the presence of ponderosa pine and lower CFIs, given the well-documented association of ponderosa pine with frequent, low-severity fire regimes of the Pacific Northwest (e.g., Weaver 1959, Pyne 1982, Agee 1993). Instead, my analysis indicated that the presence of ponderosa pine was associated with longer fire intervals (except for in Unit 3, McGregor). Presence of ponderosa pine was also not clearly associated with SW-facing aspects as often described (Everett et al. 2000, Ziegler et al. 2017), and CFI varied across all

aspects.

There are several potential explanations for these counterintuitive results. One possibility is that higher historical densities of ponderosa pine on SW-facing slopes may have been reduced by increased fire intensities in combination with fire suppression. This theory is supported by my analysis of fire severity predictors, in which SW-facing aspects were correlated with higher fire severity than NE-facing aspects. It also agrees with findings that ponderosa pine is more susceptible to mortality with the reintroduction of fire following the prolonged era of fire suppression (Arno et al. 1995, Arno et al. 2000). This hypothesis would explain the significant interaction between ponderosa pine, location, and aspect in the analysis of CFI; assuming ponderosa pine were once prevalent on SW-facing aspects as found elsewhere (e.g., Ziegler et al. 2017), and were killed by higher-severity fires occurring at variable locations following the fire suppression era. However, another explanation, supported by Sherriff and Veblen's (2007) research on the Colorado Front Range, is that ponderosa pine forests may be associated with longer fire return intervals and higher-severity fire effects than previously thought, especially on steeper slopes and at higher elevations. Baker and Ehle (2001), Hessburg et al. (2007), and others have come to similar conclusions.

The analysis of fire severity predictors also confirms the importance of local topography on fire severity as found by Cansler (2011). In the case of my study, the GLM model identified slope and the interaction of slope and cosine-aspect as significant predictors. I was not surprised to find that SW-facing (warm) aspects burned more severely than NE-facing (cool) aspects, similar to the results of studies of mixed-severity fire regimes in the Klamath-Siskyou region of California and Oregon (Beaty and Taylor 2001, Alexander et al. 2006), although in my study cosine-aspect was a significant predictor only in interaction with slope. The influence of slope

on fire severity has been mixed, with steeper slopes associated with high-severity fire effects (e.g., Beaty and Taylor 2001, Holden et al. 2009), high- and low-severity fire effects (Alexander et al. 2006), or only low-severity fire effects in my case as with Collins (et al. 2007). In the case of Stehekin, I suspect that fire severity is lower on steeper slopes because of the fuel conditions and fire behavior. Logs and woody debris roll down the steep and dissected terrain, accumulating in the flatter areas. During fires, burning logs often smolder in the basins with higher fire intensity, and flames make swift runs back up the steeper slopes, moving quickly and burning with lower intensity (*personal observation*).

I found that the interaction of topography, environment, climate, and other factors had a stronger influence on fire frequency and severity than any individual variable did by itself. The variability and complex interactions that I found in fire frequency and fire severity are likely inherent to the mixed-severity fire regime (Halofsky et al. 2011, Hessburg 2007). The fact that all the pulses of tree establishment were preceded by fires in the scar record confirms that fires were of mixed (moderate) severity rather than exclusively high or low severity. Stand-replacing fire would have wiped out the scar record, and low-severity fires would not have precipitated pulses of tree establishment. Instead, trees established after every fire, presumably in variable-sized burn scars where trees were killed, and other areas where fire effects were so mild that the trees were not scarred. This assumption is supported by the proxy for fire severity, in which I found a wide distribution of fire severities across multiple stand densities. It is also verified by the wide range of combinations of fire frequencies and severities found in the units, such that plots that burned with low- or high-frequency fire were associated with all ranges of low- to high-severity fire effects.

The overall theme of fire frequency and severity in the mixed-severity forests of Stehekin

is variability and complexity, providing park managers with challenges and opportunities in fire management, including cause for optimism. Challenges and pitfalls will be associated with predicting the effects of climate change in complex systems where multiple outcomes are possible, emergent properties are difficult to predict, and feedback loops between components obscure the drivers from the responses (Newman et al. 2019). Kennedy et al. (2021) warn about the complications of feedback loops and assumptions that relationships between climate and fire variables will remain stationary over time. However, both research teams suggest that these limitations can be overcome with empirical data collected over the appropriate scale to answer questions regarding climate and fire interactions over short time horizons.

Our optimism should be based on the variability and complexity in mixed-severity regimes which provide forests with resiliency to the potential effects of climate change. For example, the variability of fire frequency and severity in the complex topography of Stehekin provides greater opportunity for tree survival in lightly burned and unburned patches, which increase resiliency to climate change by providing seed sources in postfire stands (Coop et al. 2019). The heterogeneity of fire size and frequency in mixed-severity fire regimes may also provide resiliency through the diversity of species that regenerate in different climate conditions (Hanson et al. 2015).

The challenge and opportunity for managers is to anticipate the potential effects of each wildfire, based on location, terrain, and species, to manage for maximum resilience to climate change. This means allowing more wildland fires to burn in complex topography where the mosaic of fire effects maintains diversity in forest structure, age classes, and fuels to promote ecosystem resilience (Seidl et al. 2014). It also means recognizing when and where the fire-weather outlook and terrain increase the potential for large areas to burn with higher-severity

effects, thus reducing post-fire resilience. In this case, burn techniques used in suppression to minimize fire intensity (e.g., back-burning rather than burning-out with head fire) could be a good strategy to contain the wildfire and limit the size of high-severity patches. Although complexity increases uncertainty in the effects of climate change on mixed-severity fire regimes, it also provides diversity in the ways that ecosystems, and ultimately managers, respond to those changes.

1.8 References

- Agee, J.K. 1993. Fire Ecology of Pacific Northwest Forests. Island Press, Washington, D.C.
- Agee, J.K. 2005. The complex nature of mixed severity fire regimes.in Mixed Severity Fire Regimes: Ecology and Management Symposium Proceedings, Spokane, WA, 17-19 November 2004. Association of Fire Ecology MISCO3. Washington State University, Pullman, WA.
- Agee, J.K., M. Finney, and R. de Gouvenain. 1986. The fire history of Desolation Peak: A portion of the Ross Lake National Recreation Area., National Park Service Cooperative Park Studies Unit, College of Forest Resources, University of Washington, Seattle, WA.
- Alexander, J.D., N.E. Seavy, C.J. Ralph, and B. Hogoboom. 2006. Vegetation and topographical correlates of fire severity from two fires in the Klamath-Siskiyou region of Oregon and California. International Journal of Wildland Fire. 15:237-245.
- Arno, S.F., M.G. Harrington, C.E. Fiedler, and C.E. Carlson. 1995. Restoring fire-dependent ponderosa pine forests in Western Montana. Restoration & Management Notes. 13(1):32-36.
- Arno, S.F., D.J. Parsons, and R.E. Keane. 2000. Mixed-severity fire regimes in the Northern Rocky Mountains: consequences of fire exclusion and options for the future. *In:* D.N. Cole, S.F. McCool, W.T. Borrie, and J. O'Loughlin eds. 2000. Wilderness Science in a Time of Change Conference. Volume 5: Wilderness Ecosystems, threats, and management; 1999, May 23-27; Missoula, MT. Proceedings RMRS-P-15-VOL-5. U.S. Department of Agriculture, Forest Service, Rocky Mountain Research Station, Ogden, Utah, USA.
- Arno, S.F., and K.M. Sneck. 1977. A method for determining fire history in coniferous forests of the mountain west. General Technical Report INT-42, USDA Forest Service, Intermountain Forest and Range Experiment Station, Ogden, Utah.

- Baker, W.L., and D. Ehle. 2001. Uncertainty in surface-fire history: the case of ponderosa pine forests in the western United States. *Canadian Journal of Forestry Research*. 31:1205-1226.
- Beaty, M.R., and A.H. Taylor. 2008. Fire history and the structure and dynamics of a mixed conifer forest landscape in the northern Sierra Nevada, Lake Tahoe Basin, California, USA. *Fire Ecology and Management* 255:707-719.
- Beaty, R.M., and A.H. Taylor. 2001. Spatial and temporal variation of fire regimes in a mixed conifer forest landscape, Southern Cascades, California, USA. *Journal of Biogeography* 28:955-966.
- Brewer, P.W., M.E. Velasquez, E.K. Sutherland, and D.A. Falk. 2016. Fire History Analysis and Exploration System (FHAES) version 2.0.2, [computer software], <https://www.fhaes.org>. DOI:10.5281/zenodo.34142
- Caldbick, J. 2012. Chelan, City of -Thumbnail History. *HistoryLink.org* Essay 10160.
- Cansler, C.A. 2011. Drivers of burn severity in the northern Cascade Range. Master's Thesis. University of Washington, Seattle, Washington, USA.
- Collins, B.M., M. Kelly, J.W. van Wagtendonk, and S.L. Stephens. 2007. Spatial patterns of large natural fires in Sierra Nevada wilderness areas. *Landscape Ecology* 22:545-557.
- Cook, E.R., and L.A. Kairiukstis (eds). 1992. *Methods of Dendrochronology; Applications in the Environmental Sciences*. International Institute for Applied Systems Analysis, Netherlands
- Coop, J.D., T.J. DeLory, W.M. Downing, S.L. Haire, M.A. Krawchuk, C. Miller, M.A. Parisien, and R.B. Walker. 2019. Contributions of fire refugia to resilient ponderosa pine and dry mixed-conifer forest landscapes. *Ecosphere* 10(7):e02809 24 pp.
- Everett, R.L., R. Schellhaas, D. Keenum, D. Spurbeck, and P. Ohlson. 2000. Fire history in the ponderosa pine/Douglas-fir forests on the east slope of the Washington Cascades. *Forest Ecology and Management* 129:207-225.
- Fulé, P.Z., J.E. Crouse, T.A. Heinlein, M.M. Moore, and W.W. Covington. 2003. Mixed-severity fire regime in a high-elevation forest of Grand Canyon, Arizona, USA. *Landscape Ecology* 18:465-486.
- Halofsky, J.E., D.C. Donato, D.E. Hibbs, J.L. Campbell, D.M. Cannon, J.B. Fontaine, J.R. Thompson, R.G. Anthony, B.T. Bormann, L.J. Kayes, B.E. Law, D.L. Peterson, and T.A. Spies. 2011. Mixed-severity fire regimes: lessons and hypotheses from the Klamath-Siskiyou Ecoregion. *Ecosphere* 2(4):1-19.
- Hanson C.T., R.L. Sherriff, R.L. Hutto, D.A. DellaSala, T.T. Veblen and W.L. Baker. 2015. Setting the stage for mixed- and high-severity fire. In D.A. DellaSala and C.T. Hanson (eds.)

- The Ecological Importance of Mixed-Severity Fires: Nature's Phoenix. Elsevier Inc. pp. 3-22.
- Harrell, F.E. 2015. Regression Modeling Strategies: With Applications to Linear Models, Logistics, and Ordinal Regression, and Survival Analysis. Second Edition. Springer International Publishing AG Switzerland. 598 pp.
- Harrod, R.J., B.H. McRae, and W.E. Hartl. 1999. Historical stand reconstruction in ponderosa pine forests to guide silviculture prescriptions. *Forest Ecology and Management* 114:433-446.
- Hessburg, P.F., R.B. Salter, and K.M. James. 2007. Re-examining fire severity relations in pre-management era mixed conifer forests: inferences from landscape patterns of forest structure. *Landscape Ecology* 22:5-24.
- Hessl, A.E., D. McKenzie, and R. Schellhaas. 2004. Drought and Pacific Decadal Oscillation linked to fire occurrence in the inland Pacific Northwest. *Ecological Applications* 14:425-442.
- Heyerdahl, E.K., L.B. Brubaker, and J.K. Agee. 2001. Spatial controls of historical fire regimes, a multiscale example from the interior west, USA. *Ecology* 82:660-678.
- Heyerdahl, E.K., K. Lertzman, and C.M. Wong. 2012. Mixed-severity fire regimes in dry forests of southern interior British Columbia, Canada. *Canadian Journal of Forest Research* 42:88-98.
- Holden, Z.A., P. Morgan, and J.S. Evans. 2009. A predictive model of burn severity based on 20-year satellite-inferred burn severity data in a large southwestern US wilderness area. *Forest Ecology and Management* 258:2399-2406.
- Holmes, R.L. 1983. Computer-assisted quality control in tree-ring dating and measurement. *Tree-Ring Bulletin* 43:69-78.
- Iniguez, J.M., T.W. Swetnam, and S.R. Yool. 2008. Topography affected landscape fire history patterns in southern Arizona, USA. *Forest Ecology and Management*. 256:295-303.
- Johnson, E.A., and S.I. Gutsell. 1994. Fire frequency models, methods and interpretations. *Advances in Ecological Research* 25:239-287.
- Kellogg, L.-K.B., D. McKenzie, D.L. Peterson, and A.E. Hessl. 2008. Spatial models for inferring topographic controls on historical low-severity fire in the eastern Cascade Range of Washington, USA. *Landscape Ecology* 23:227-240.
- Kennedy, M.C., R.R. Bart, C.L. Tague, and J.S. Choate. 2021. Does hot and dry equal more wildfire? Contrasting short-and long-term climate effects on fire in the Sierra Nevada, CA. *Ecosphere* 12(7):e03657.10.1002/ecs2.3657
- Klenner, W., R. Walton, A. Arsenault, and L. Kremsater. 2008. Dry forests in the Southern Interior of British Columbia: Historic disturbances and implications for restoration and management. *Forest Ecology and Management* 256:1711-1722.

- Littell, J.S., Peterson, D.L., and Tjoelker, M. 2008. Douglas-fir growth in mountain ecosystems: Water limits tree growth from stand to region. *Ecological Monographs*, 78(3):349-368.
- McCune, B. and Keon, D. 2002. Equations for potential annual direct incident radiation and heat load. *Journal of Vegetation Science* 13:603-606.
- McKenzie, D., A.E. Hessl, and L.-K.B. Kellogg. 2006. Using neutral models to identify constraints of low-severity fire regimes. *Landscape Ecology* 21:139-152.
- McKenzie, D., and M.C. Kennedy. 2012. Power laws reveal phase transitions in landscape controls of fire regimes. *Nature Communications* doi:10.1038/ncomms1731.
- McKenzie, D. 2020. *Mountains in the Greenhouse: Climate change and the mountains of the Western U.S.A.*, Springer Nature Switzerland AG.
- Newman, E.A., M.C. Kennedy, D.A. Falk, and D. McKenzie. 2019. Scaling and complexity in landscape ecology. *Frontiers in Ecology and Evolution*. 7:293 16 pp.
- Nigh, G.D. 1995. *Compatibility Improvements and Bias Reduction in Height-Age Models*. Province of British Columbia, Ministry of Forests Research Program, Victoria, B.C.
- N.P.S. 2010. North Cascades National Park Service Complex Wildland Fire Management Plan. North Cascades National Park, Sedro Wooley, WA.
- Oliver, C.D., and B. C. Larson. 1981. Final report: Forest resource survey and related consumptive use of firewood in lower Stehekin Valley, North Cascades National Park Complex. College of Forest Resources, University of Washington, Seattle, Washington.
- Perry, D.A., P.F. Hessburg, C.N. Skinner, T.A. Spies, S.L. Stephens, A.H. Taylor, J.F. Franklin, B. McComb, and G. Riegel. 2011. The ecology of mixed severity fire regimes in Washington, Oregon, and Northern California. *Forest Ecology and Management* 262:703-717.
- Poage, N.J., P.J. Weisberg, P.C. Impara, J.C. Tappeiner, and T.S. Sensenig. 2009. Influences of climate, fire, and topography on contemporary age structure patterns of Douglas-fir at 205 old forest sites in western Oregon. *Canadian Journal of Forest Research* 39:1518-1530.
- Pyne, S.J. 1982. *Fire in America: A cultural history of wildland and rural fire*. Princeton, NJ: Princeton University Press. 654 pp.
- Prichard, S.J. 2003. Spatial and temporal dynamics of fire and vegetation change in Thunder Creek watershed, North Cascades National Park, Washington. Ph.D. dissertation. University of Washington, Seattle, WA.
- R Core Team. 2021. R: A Language and environment for statistical computing. R Foundation for Statistical Computing, Vienna, Austria. URL <https://www.R-project.org/>.

- Ramsey, F.L. and Schafer, D.W. 2002. *The Statistical Sleuth: A Course in Methods of Data Analysis*. Second Edition. Duxbury Thomson Learning, Pacific Grove, CA. 742 pp.
- Scheiner, S.M. and J. Gurevitch (eds). 2001. *Design and Analysis of Ecological Experiments*. Second edition. Oxford University Press, Inc., New York, NY. 415 pp.
- Seidl, R., W. Rammer, and T.A. Spies. 2014. Disturbance legacies increase the resilience of forest ecosystem structure, composition, and functioning. *Ecological Applications*. 24(8):2063-2077.
- Sherriff, R.L. and T.T. Veblen. 2007. A spatially-explicit reconstruction of historical fire occurrence in the ponderosa pine zone of the Colorado front range. *Ecosystems*. 10:311-323.
- Stokes, M.A., and T.L. Smiley. 1968. *An Introduction to Tree-Ring Dating*. University of Chicago Press, Chicago, Illinois.
- Stone, C.M. 1983. *Stehokin: Glimpses of the Past*. Long House Printcrafters and Publishers, Friday Harbor, Washington.
- Taylor, A.H., and C.N. Skinner. 2003. Spatial Patterns and Controls on Historical Fire Regimes and Forest Structure in the Klamath Mountains. *Ecological Applications* 13:704-719.
- USDI, B.L.M. 2020. Wildland Fire Management Information. National Interagency Fire Center, Boise, ID. <https://wfmi.nifc.gov/cgi/WfmiHome.cgi>
- Van Wagendonk, J. 2007. The history and evolution of wildland fire use. *Fire Ecology* 3(2):3-17.
- Weaver, H. 1959. Ecological changes in the ponderosa pine forest of the Warm Springs Indian Reservation in Oregon. *Journal of Forestry* 57:15-20.
- Weisberg, P.J. 2004. Importance of non-stand-replacing fire for development of forest structure in the Pacific Northwest, USA. *Forest Science* 50:245-258.
- Wong, C.M. and K.P. Lertzman. 2001. Errors in estimating tree age: implications for studies of stand dynamics. *Canadian Journal of Forest Research* 31:1262-1271.
- Wright, C.S., and J.K. Agee. 2004. Fire and vegetation history in the eastern Cascade Mountains, Washington. *Ecological Applications* 14:443-459.
- Ziegler, J.P., C.M. Hoffman, P.J. Fornwalt, C.H. Sieg, M.A. Battaglia, M.E. Chambers, and J.M. Iniguez. 2017. Tree regeneration spatial patterns in ponderosa pine forests following stand-replacing fire: Influence of topography and neighbors. *Forests* 8:391 doi:10.3390/f8100391 15pp.

Chapter 2. Fuel characteristics of Mount Rainier National Park, Washington, USA:

Mapping with a combination of field, environmental, and LiDAR data¹

2.1 Abstract

I created a fuel map for Mount Rainier National Park to inform models of fire behavior and anticipate wildland fire effects on managed lands. My focus was to maximize accuracy while defining fuel categories that were appropriate to the spatial scales associated with the park. I classified and mapped fuel characteristics (fuelbeds) compatible with the Fuel Characteristic Classification System (FCCS) across Mount Rainier National Park using a combination of empirically derived field data, LiDAR, and climate data. I used the LiDAR and climate data to distinguish high from low surface-fuel loadings and to predict and map their median values from 151 field plots using random forests modeling, with accuracies between 62% and 75%. I also defined and mapped 6 forest structure classes related to fire behavior from LiDAR data. The surface fuels, structure classes, and field data (species and canopy data) were combined and matched to create 29 high-resolution fuelbeds for the Park. I used FCCS to derive fire and fuel potentials, ranked from low to high on an interval scale of 0 to 9, for the fuelbeds. Surface fire behavior potentials (FBP) ranged from 4 to 7 within 51% of the study area, ranking moderately high (score of 7), in contrast to 29% located primarily on the drier east side, ranking moderately low (score of 4). Crown fire potentials (CFP) and available fuel potentials (AFP) were more evenly distributed across the Park. CFP was moderate (38% score of 5), whereas AFP was relatively high throughout the Park, (40% score of 9). I expect that climate change will increase

I wish to acknowledge my collaborators in this work; Van Kane, School of Environmental and Forest Sciences, University of Washington, Seattle, WA, and Catharine Copass, Olympic National Park, 600 E Park Avenue, Port Angeles, WA.

fire size and frequency sooner on the drier east side, but that if the trend towards warmer and drier conditions persists, that fire behavior and effects will eventually be more severe on the west side due to higher FBP and fewer fire-adapted species.

2.2 Introduction

Accurate fine-scale fuel maps can be used for a variety of applications to improve forest management, including quantifying biomass and carbon storage capacity (e.g., Smithwick et al 2009), identifying important wildlife habitat (e.g., North et al. 1999, Roberts et al. 2011, Ucitel et al. 2003), and to inform fire and forest management. Fuel maps are essential for fire research and management to model fuel treatment effectiveness, smoke emissions, and fire spread. The importance of fuel maps in forests with less frequent fire, such as at Mount Rainier National Park (the Park) has increased substantially due to climate change, particularly concerning the increased likelihood of longer fire seasons² and larger areas burned in forest ecosystems (Littell et al. 2009, 2018).

Fuel maps for all federal government lands in the United States have been produced by the Landscape Fire and Resource Management Planning Tools Prototype Project (LANDFIRE) (Rollins and Frame 2006). These maps assigned either the 13 original fire behavior fuel models (Albini 1976, Anderson 1982) or the more recent 40 fuel models developed by Scott and Burgan (2005), using a crosswalk to vegetation layers, and are at 30-m resolution. A similar but independent effort developed a national-scale map assigning “fuelbeds” from the Fuel Characteristic Classification System (FCCS, Prichard et al. 2019), with a different crosswalk from the same vegetation layers used by LANDFIRE (McKenzie et al. 2007). This map was also

² Fire season corresponds to an increased number of days with high fire danger.

at 30-m resolution; later the authors and colleagues aggregated the map to 1-km resolution, to be tractable for air-quality models and others that operate at coarser spatial scales (McKenzie et al. 2012).

These national-scale products are not appropriate at the scale of park operations, despite their relatively fine spatial resolution. On the contrary, their fine resolution (30 m) leads to a false precision, because the fuel characteristics are drawn from vegetation classes that are (typically) at least regional in scale, and therefore, misrepresent the unique ecological character of a local landscape (McKenzie et al. 2007). For example, the FCCS fuelbed “Whitebark pine / Subalpine fir forest” (#61) occurs across the western United States at high elevations (in the national map). Vegetation and fuels in Mount Rainier National Park may differ from those in Glacier National Park, but the national maps assign the same values to surface fuel loadings, canopy cover, and other aspects of the fuelbed. Similar issues arise with other fuelbed assignments across the Park in the national maps, heightened by the diverse topography and microclimates at Mount Rainier.

In this paper, I took steps to increase the local specificity and applicability of fuelbeds and the subsequent map for Mount Rainier National Park. I chose FCCS as the template for the fuel mapping project because of its close links to vegetation and structure, which matched this project’s association with the development of the current vegetation map (Nielsen et al. 2021). I also chose to make the fuelbeds compatible with FCCS because of the three informative indices of fuel and fire potential that FCCS provides for each fuelbed. The three fire-potential ratings, ranked on an interval scale of 0 to 9 (low to high), include: 1) surface fire behavior potential (FBP), 2) crown fire potential (CFP), and 3) available fuel potential (AFP) (Sandberg et al. 2007).

The primary goals of my study were: 1) to map the fuelbeds across Mount Rainier National Park, at high resolution, and 2) to highlight variability in the live and dead fuel loadings, and their associated fire-potential ratings (Sandberg et al. 2007). This will aid resource and fire managers in identifying areas of concern and interest, both currently and into the future, with its potential for warmer, drier, and longer fire seasons due to climate change (Mote et al. 2014).

The effects of climate change on fire regimes in the western United States are becoming clearer, although there is far less certainty with respect to west-side (moist temperate) forests with longer fire rotations such as at Mount Rainier (Littell et al. 2018, Halofsky et al 2020). Although infrequent (400+ years) high-severity fires are the norm throughout Mount Rainier (Hemstrom and Franklin 1982, Agee 1993), the potential for these large fires to occur more frequently has increased, along with the likelihood of a "type change" in the predominant species composition of the forest following stand-replacing fire due to climate change (Stephens et al. 2013). I was particularly interested in assessing fuel loadings on the more mesic east side of the park, where some less predictable mixed-severity fire effects also occur (Siderius and Murray 2005). Knowledge of fine-scale fuel loading and structure is critical for assessing potential fire behavior and prescribing fuel treatments to protect infrastructure while maintaining habitat for species that are poorly adapted to wildfire. For example, old-growth forests dominated by western hemlock (*Tsuga heterophylla* (Raf. Sarg.)) that are habitat for northern spotted owls (*Strix occidentalis caurina*), are critical to protect from the effects of larger stand-replacing fires. Overall, I aimed to identify areas that are more likely to experience increased fire behavior and effects in the Park due to heavy fuel loads, especially in a warmer climate.

Another goal of my study was to determine whether LiDAR technology could

substantially improve the accuracy and resolution of fuel maps. Acquisition of LiDAR data at the park provided me an opportunity to link canopy characteristics to field measurements of both surface and canopy fuels to assess this. LiDAR data have been used to predict canopy characteristics (e.g., canopy bulk density, tree cover, tree height) related to fuel maps (e.g., Riano et al 2003, Anderson et al 2005, Erdody and Moskal 2010, Hermosilla 2014), but only a few studies have used LiDAR to predict surface fuel loads (Mutlu et al 2008, Price and Gordon 2016). Price and Gordon (2016) used LiDAR to map fire hazard in Australian forests with useful but less precise predictions of surface fuels than of fuel cover. Mutlu et al. (2008) used LiDAR-derived canopy conditions to predict surface fuel loadings but modeled the 13 standard fire behavior fuel models (Albini 1976, Anderson 1982) rather than continuous fuel loads.

2.3 Research Questions

- 1)** How accurately can surface fuel characteristics be mapped from remote sensing (LiDAR) and climatology?
- 2)** How are surface and canopy fuels (fuelbeds) distributed across Mount Rainier National Park?
- 3)** How are fire behavior and fuel potentials distributed across Mount Rainier National Park?

2.4 Methods

2.4.1 Summary

I integrated several data sets from across the study area, Mount Rainier National Park.

Figure 2-1 shows the parallel processing of four data sources in multiple steps, to define, map, and interpret fuel characteristics (fuelbeds).

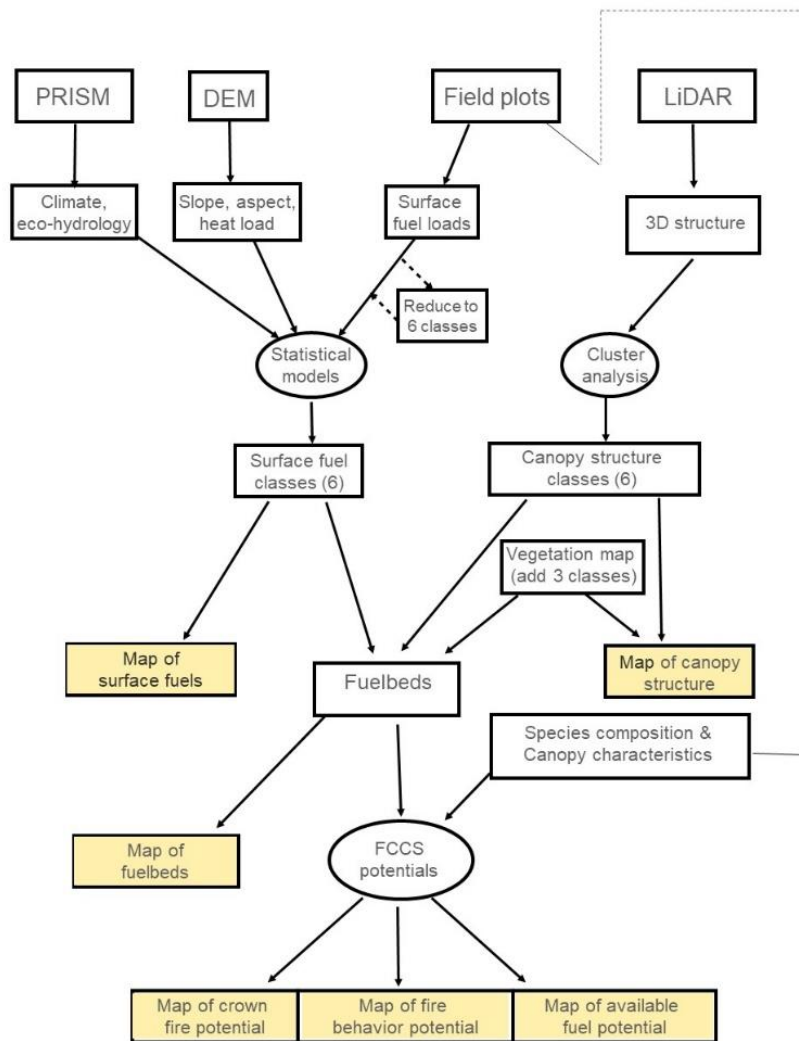


Figure 2-1. Flowchart illustrating the parallel processing of four datasets to build and map 29 fuelbeds and their associated FCCS fire potentials (crown fire, surface fire behavior, and available fuel) for Mount Rainier National Park. Yellow boxes indicate map products.

First, I collected surface and canopy fuels, and potential predictors of different fuel loadings, including 1) climate variables (e.g., actual evapotranspiration, climatic water deficit)

from PRISM data (PRISM Climate Group 2013), 2) topography from digital terrain models (DTMs), 3) surface and canopy fuel characteristics measured on field plots, and 4) canopy metrics from airborne LiDAR data.

Next, I used linear regression and random forests (Ho 1995) modeling, with the surface fuel data from the field as response variables, and topography and climate variables as predictors, to map surface fuel loads across the Park. In a parallel process, I used cluster analysis of the canopy metrics to define and map overstory structure classes across the Park.

I then constructed and mapped fuelbeds by combining the predicted surface fuel loads and the forest structure classes (plus three additional vegetation structure classes). I used species composition and canopy characteristics data from the field to further define the fuelbeds for input into FCCS. I used FCCS to generate fire behavior and fuel potentials, which I used to identify areas with resources at risk across the Park.

2.4.2 *Study Area*

Mount Rainier National Park, in the state of Washington, USA, is a 95,660-hectare national park encompassing Mount Rainier, the highest mountain (4,393 m) within the Cascade Range. Annual precipitation is high, increasing due to orographic effects from about 150 cm at low elevations to over 250 cm in the subalpine zone, the latter mostly in the form of a deep snowpack. Moderately cold winters are typically followed by mild, dry summers. This maritime climate is the reason that west-side, low-elevation forests of Mount Rainier and throughout the Pacific Northwest are the most productive in the western United States (McKenzie 2020).

The study area consists of 70,316 hectares of forest, meadow, and shrubs delineated in the most recent vegetation map of Mount Rainier (Nielsen et al. 2021), to which my project was

related (as a collaborative effort to collect the vegetation and fuels data). Throughout the study area, lower-elevation forests are dominated by western hemlock and Douglas-fir (*Pseudotsuga menziesii* var. *menziesii* (Mirb.) Franco). Moving up in elevation, forests are a mix of Pacific silver fir (*Abies amabilis* (Douglas ex Loudon)) and western hemlock. Mountain hemlock (*Tsuga mertensiana* (Bong.) Carrière)-Pacific silver fir forests are dominant just below subalpine fir (*Abies lasiocarpa* (Hook.) Nutt.) and subalpine fir-whitebark pine (*Pinus albicaulis* (Engelm.)) woodlands. Above tree line (typically 1600 to 2000 m), short-statured shrubs and herbaceous meadows give way to lithomorphic vegetation communities and then permanent snowfields and glaciers.

The dominant fire regime at Mount Rainier is infrequent, large, high-severity fires. The natural fire-return interval for the whole park was calculated at 465 years for the period prior to Euro-American settlement (1200–1850) (Hemstrom and Franklin 1982). Hemstrom and Franklin (1982) also calculated the natural fire rotations for the settlement period (1850–1900) and modern fire suppression era (1900–1978) as 226 and 2583 years respectively. Although fire suppression reduced frequency, the impact of fire suppression on fuel accumulation is negligible, given the long natural fire rotation (Hemstrom and Franklin 1982, McKenzie et al. 2004).

Despite the predominance of high-severity fire in the park, there is evidence of mixed- and low-severity fire as well. Siderius and Murray (2005) recognized a preponderance of mixed-severity fire along the eastern edge of Mount Rainier, presumably due to the drier conditions in this portion of the park. Hemstrom and Franklin (1982) noted that fire was most severe at low to mid elevations and was less severe and more frequent in high-elevation meadows and woodlands. This is supported by the fire record in the Wildland Fire Management Information database (USDI BLM 2020). The fire record also shows that fires were more frequent

throughout the east side than the west side, with 136 of 155 (88%) lightning-caused fires between 1970 and 2019 occurring on the east side of the Park.

2.4.3 *Field Data Collection*

Vegetation composition and fuels data to construct and map FCCS-compatible fuelbeds were collected on 311 plots, of which 262 were ultimately used. The surface fuel loadings from 151 plots (post-processed, accuracy < 1 meter) were used to map surface fuels, and the canopy characteristics and species data from 262 plots (111 with GPS accuracies < 10 meters added to 151 post-processed) were used to develop the fuelbeds (Figure 2-2). The plots that were not used were omitted due to poor location accuracies as determined by GPS in the field or during post-processing, or due to mismatch with the vegetation or structural maps. The majority (212 plots) of data used in the mapping project were collected between 2005 and 2007 in conjunction with the vegetation classification project associated with the most recent vegetation map (Nielsen et al. 2021). Additional canopy density plots were inventoried in 2010 to provide supplemental data on canopy structure to match some of the fuelbed types where GPS accuracy had been low. Sampling locations for all plots were selected subjectively, in proximity to trails, based on canopy homogeneity within prioritized vegetation alliances to inform the vegetation classification project.

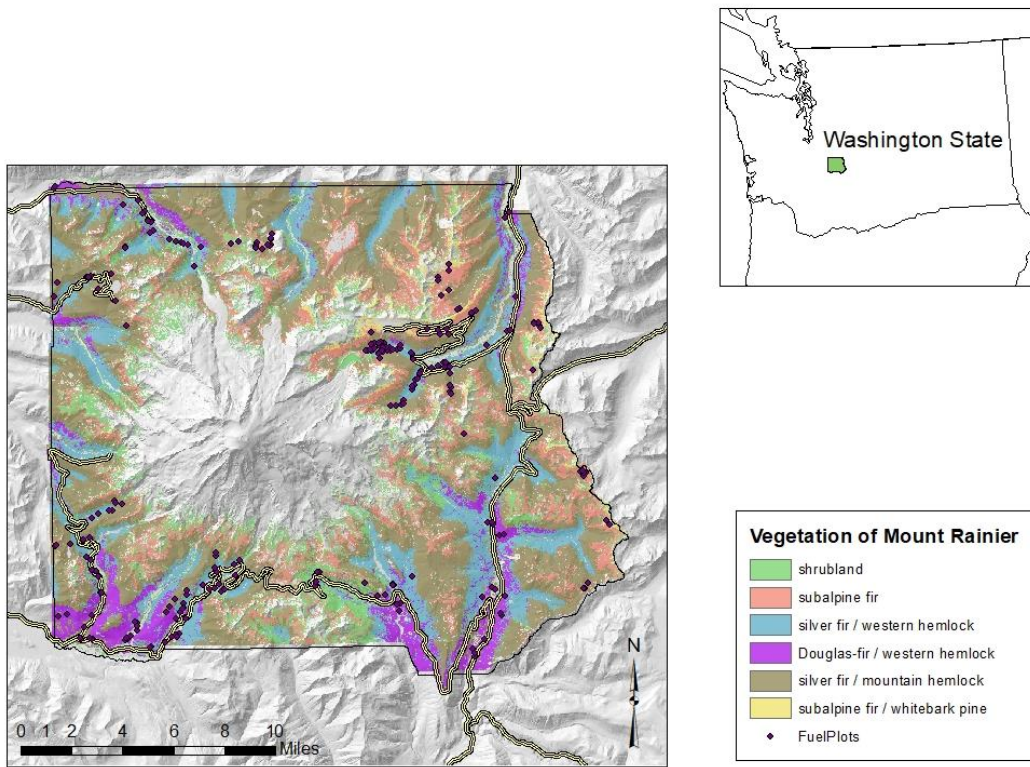


Figure 2-2. Map of study area showing field plot locations by dominant tree species per the vegetation map (Nielsen et al. 2021). 262 fuel plots were used to define canopy characteristics for the final fuelbeds. 151 of 262 fuel plots were used in the surface fuel analysis. Cover for elevations above 2000 m is not shown where rock fields and glaciers centered around the mountain's peak are found.

In each sampling location, a 400-m² circular plot was established. The canopy of each plot was divided into three strata: 1) subcanopy, 2) canopy, and 3) emergent in which a few dominant trees were above the main canopy. The total canopy cover and average height were recorded for each stratum, and species, height, height to live crown, and diameter at breast height (DBH) were recorded for a subsample of up to 5 trees within each stratum. Understory shrub cover and three classes of snags (based on degree of decay) were also recorded. If ladder fuels (continuous fuels within 0.5 m of ground to canopy) were present in 50% or more of the stand, this was noted. These data were collected to provide canopy characteristics and species data for the development of the fuelbeds in FCCS.

Surface fuel data were collected to map surface fuel loading across the park. Two 15-meter “Brown’s transects” (Brown et al. 1982) per plot were used to measure three components of the surface fuels related to fire behavior: 1) litter and duff (ORG, organic), 2) 1-100 hour time-lag classes where; 1 hour = \leq 0.6 cm, 10 hour = 0.6 - 2.5 cm, and 100 hour = 2.5-7.6 cm diameter dead and detached wood (SW, small woody fuel) and 3) 1000 hour time-lag class = >7.6 cm diameter dead and detached wood (LW, large woody fuel). The 1- and 10-hour fuels were tallied for the first 1.8 m, 100-hour fuels were tallied for 3.7 m, and LW were tallied for the whole length (15 m.) of the transect. Organic depths and duff derivations were recorded in five locations along each transect. The litter arrangement (normal, fluffy, or perched) was recorded. Duff derivation was determined for upper layers as either dead moss or litter and for lower layers as humus or muck.

The field data were entered into the National Park Service Fire Effects Assessment Tool (FEAT) Version 2.0 database (an earlier version of the current FEAT and FireMon Integrated (FFI) program (Lutes et al. 2009)) and then exported into Excel spreadsheets for manual calculation of canopy characteristics and surface fuel loadings. The data from the FEAT database are available on the Integrated Resource Management Applications (IRMA) website (<https://irma.nps.gov/DataStore/Reference/Profile/2291576>).

2.4.4 *Climate Metrics*

I based the climate metrics on the PRISM monthly and annual climatological averages (1971 to 2000) mapped at 30 arc-second (~800 m) resolution (Daly et al. 2008, PRISM Climate Group 2013). The PRISM climate modeling project combines data from several sets of weather stations and interpolates annual and monthly precipitation, and monthly mean temperatures

based on reported weather and local elevation. I used the annual precipitation and January and July mean temperatures as independent predictors in my modeling.

I modeled annual actual evapotranspiration (AET) and annual climatic water deficit (hereafter “deficit”) using the PRISM monthly climatological precipitation and temperatures with a modified Thornthwaite water balance model (Thornthwaite 1948; Thornthwaite and Mather 1955). Thornthwaite models calculate available water by considering whether precipitation is likely to be rain or snow, calculating snowpack accumulation and melt (if any), runoff, soil water holding capacity, and potential evapotranspiration (PET) by vegetation. The evolved Thornthwaite model (Hamon 1963, Dingman 2002) has been modified for mountainous terrain by including terms for slope and aspect (Stephenson 1998, Lutz et al. 2010).

2.4.5 *Airborne LiDAR Data and DTMs*

Watershed Sciences, Inc. (Corvallis, OR) collected LiDAR data for the Park plus a 100-m buffer. The company began data collection in September 2007, suspended operations due to early snow fall, and resumed collection from September to October 2008. They used a dual Leica ALS50 Phase II LiDAR system with a scan angle of $\pm 15^\circ$ off nadir. The Leica system recorded up to four discrete returns per LiDAR pulse. Data were acquired at a mean rate of return of 5.7 points per meter. A one-meter resolution DTM was created using the TerraScan v.8.001 and Terra Modeler v7.006 software (Terrasolid, Helsinki, Finland). For forest structure metrics, I subtracted the elevation of the DTM from all LiDAR return elevations to calculate return height above ground. I excluded the small amount of the Park classified as riparian due to the early cold spell during the collection period that resulted in deciduous species being inconsistently in leaf-on or leaf-off condition.

I processed the LiDAR return-point cloud data to generate forest structure and topographic metrics using the U.S. Forest Service Fusion software package, beta version derived from version 3.00 (<http://forsys.cfr.washington.edu/fusion.html>). I aggregated these data to 30-m grid cells. Because many areas in the Park had canopy cover >90%, these areas had too few LiDAR returns <2 m to measure shrub cover across the Park. I therefore calculated LiDAR vegetation metrics only for forest structures ≥ 2 m in height.

2.4.6 *Forest Structure Metrics*

I used the LiDAR data to calculate metrics for canopy height, horizontal and vertical complexity, and cover. I measured canopy heights using return percentiles; for example, the 95th percentile of return heights is the height at which 95 percent of returns ≥ 2 m are below. To capture vertical complexity of the canopy, I calculated the standard deviation and coefficient of variation of the return heights > 2 m. I also used rumple, a simple index of the rugosity of the outer canopy surface (Parker et al. 2004, Ogunjemiyo et al. 2005, Kane et al. 2010b), to measure canopy heterogeneity in both vertical and horizontal dimensions (Kane et al. 2010b), making it a more sensitive measure of the variability of tree clumping among different height strata than just the standard deviation of return height (Kane et al. 2011). Lastly, canopy cover metrics were calculated for four height strata (> 32 m, 16-32 m, 8-16 m, 2-8 m) and for all vegetation > 2 m. These cover measurements are calculated as a proportion: returns within a target stratum divided by all returns in that stratum and below.

2.4.7 *Topographic Variables*

I used the Fusion software to calculate topographic metrics using the vendor-supplied 1-

m DTM (Table 1). Fusion reported elevation at the center point for each 30 m grid cell. I calculated slope, aspect, and curvature at 30-m, 90-m, and 270-m scales. I used an equation by McCune and Keon (2002) to transform aspect to a scale from zero to one, corresponding to northeast (coolest) and southwest (warmest) aspects respectively: $(1-\cos(\theta-45))/2$, where θ = aspect. Curvature, derived from an algorithm by Zevenbergen and Thorne (1987), uses an index from 1 to -1, in which zero indicates a flat surface, and positive and negative values indicate the degree of convexity or concavity, respectively. I used the Fusion software to calculate an integrated solar radiation index (SRI), which uses aspect, slope, and latitude to model the solar radiation on each grid cell during the hour surrounding noon on the equinox (Keating et al. 2007).

Table 2-1. Input variables to classify surface fuel loads and canopy structure classes.

Forest structure metrics (LiDAR)	Abbreviation*	Scales, ranges, or breaks
LiDAR return height percentiles (m)	p95, etc.	95th, 75th, 50th, 25 th
Standard deviation return height (m)	stdev	
Coefficient of variation return height (m)	co-var	
Rumple (rugosity)	rumple	
Canopy cover > 2 m (%)	cvr.gt2	
Canopy cover by height strata (%)	cvr.2to8, etc.	2-8, 8-16, 16-32, >32 m
Topographic Variables (LiDAR-based 1 m DTM)		
Elevation, (m)	elev.30m	30 m
Aspect, (Cosine-transformed)	aspect.30, etc.	30 m, 90 m, 270 m
Slope	slope.30, etc.	30 m, 90 m, 270 m
Slope curvature (concavity or convexness)	curvature.30, etc.	30 m, 90 m, 270 m
Topographic position index (Jenness 2006)	tpi.100, etc.	100 m, 250 m, 500 m, 1000 m, 2000 m
Climate (PRISM)		
Precipitation, annual (mm)	precip	
Actual evapotranspiration, annual (mm)	aet	
Deficit, annual (mm)	deficit	
January temperature, mean (°C)	jan.t	
July temperature, mean (°C)	july.t	
Solar radiation index (relative value)	sri.30, etc.	30 m, 90 m, 270 m

*Example abbreviation given for groups of metrics calculated with different scales, ranges, or breaks.

The topographic position indices (TPI) were calculated based on the algorithm developed by Weiss (2000) and implemented as an ArcMap 10.1 extension (Jenness 2006). The TPI algorithm compares the elevation of each grid cell to the elevation of grid cells in a user-defined circular radius. Values range from -1 to 1, in which negative values indicate a position towards a valley or canyon bottom, values around zero indicate flat areas or mid-slope (which is distinguished by the slope within the cell), and positive values indicate a hill or ridge top. I calculated TPI using neighborhoods of 100 m, 250 m, 500 m, 1000 m, and 2000 m. Areas outside the park and beyond the LiDAR acquisition were included in the neighborhood calculations by using a 10-m U.S. Geological Survey DEM that included the park and surrounding areas. All climatic, forest structure, and topographic variables that I used to predict surface fuel loadings are listed in Table 2-1.

2.4.8 *Defining and Mapping Forest Structure Classes*

Previous work by Kane et al. (2010b) showed that LiDAR variables describing canopy structure co-vary. This allows forest structure classes to be defined, each representing a distinct range of structures corresponding to different developmental stages, disturbance histories, and climate (Kane et al. 2010a, Kane et al. 2011, Kane et al. 2013). I chose three metrics to describe the overall canopy height structure: 95th percentile return height (dominant tree height), 25th percentile return height (canopy base height (Andersen et al. 2005; Erdody and Moskal 2010)), and rumple. To approximate the canopy profile, I used canopy cover measurements for four height strata: 2 to 8 m, 8 to 16 m, 16 to 32 m, and >32 m.

Each of the metrics I chose has a distinctive influence on fire behavior. The cover measurements, indicating stand openness, influence fire behavior potential, whereas canopy height (indirectly, by affecting windspeed), and canopy base height influence crown fire

potential (Schaaf et al. 2007). Although I am unaware of rumple being used in fire behavior or fuel models, I expect that this measure of texture influences fire spread through the canopy profile both vertically and horizontally.

I based the forest-structure class definitions on a random sample of 25,000 grid cells within areas mapped as non-riparian conifer forest. I used hierarchical clustering with Euclidean distances and Ward's linkage method within the `hclust` function of the R statistical package (release 2.6.1) (R Development Core Team 2007) to identify nine statistically distinct forest structure classes.

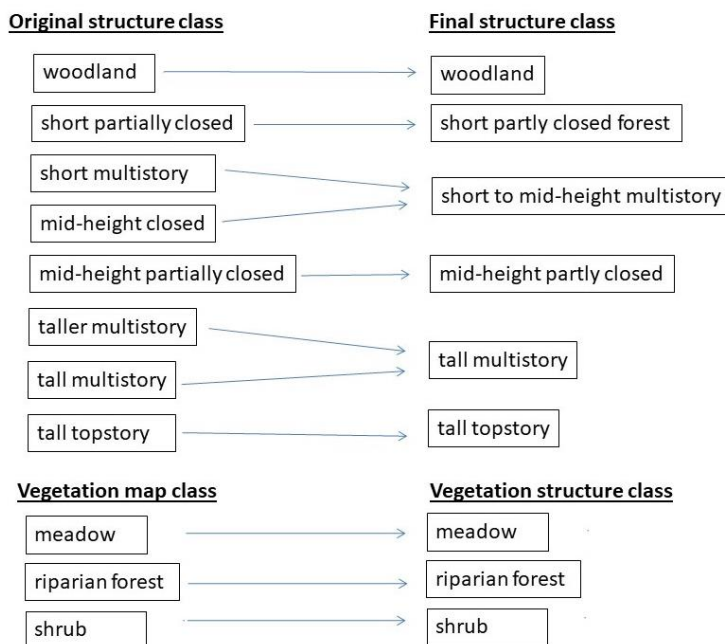


Figure 2-3. Final structural classes: 1) eight structural classes were condensed into six final structural classes, 2) Three vegetation structure classes were added directly from the vegetation map (Nielsen et al. 2021).

I lumped 2 pairs of the 8 forest structure classes into single classes due to common features expected to produce similar fire behavior (e.g., tall multistory was lumped with taller multistory) (Figure 2-3). I added three additional “vegetation structure classes” (meadow, riparian forest, shrub) directly from the vegetation map, for a total of 9 structure classes across the park.

2.4.9 Surface Fuel Modeling and Mapping

I used a sequential approach to predict and map surface fuel loads across the Park using the field data as training data and the LiDAR, topographic, and climate data as predictors. First, I used multiple linear regression and random forests modeling to predict the surface fuel loadings from the field data as continuous response variables. These models had poor fit, so I divided the fuel loadings into high and low classes for each surface fuel class (high/low organic (ORG), high/low small woody fuel (SW), and high/low large woody fuel (LW)) based on their median values (low = 25th percentile and high = 75th percentile values of the full range of each class) and used random forests modeling to predict and map their locations throughout the Park.

Random forests modeling is an extension of non-parametric classification and regression trees (CART) (Breiman et al. 1984), that uses multiple random subsets of data (bagging) and develops a “forest” of regression trees from random draws of the training sample. For each tree, a random portion of the training data is used to develop the model, and the remaining data are used for cross-validation to assess accuracy. The Gini index is used to rank the importance of each predictor by assessing how well it splits the data into homogeneous groups (either all high or all low). The results of all the trees within a model are averaged to report the overall accuracy of the model and to predict values for new data.

Using the plot GPS coordinates, we assigned each field plot to the LiDAR, topographic, and environmental metrics found in the corresponding 30x30 m grid cell. I used the randomForest and partialPlot functions in the random forests package (<http://cran.r-project.org/web/packages/randomForest/index.html>) for the R statistical package (release 2.6.1) to develop and analyze our models.

Because of the stochastic element of random forests, repeated classifications with the

same predictors resulted in differences in classification accuracy of 2% to 10% between runs. For example, in one set of 250 iterations for the high/low ORG classes, the lowest classification error rate was 0.272 and the highest error rate was 0.351. I therefore retained for each model, the one of 250 iterations with the lowest classification error to use for predicting classes across the Park. I then performed leave-one-out cross validations and created 100 models for each plot that was left out to create an average classification accuracy based on 15,100 tests (100×151 plots) per fuel type.

I used the AsciiGridPredict function in the R yaImpute package (Crookston and Finley 2008) (<http://cran.r-project.org/web/packages/yaImpute>) to apply the models and create maps of the 6 surface fuel classes (3 pairs of high/low) across the park. The maps had moderate fine-grain interspersion of classes into areas dominated by other classes. To simplify my maps, I removed the dispersed pixels using the majority filter based on the eight surrounding grid cells in ArcMap 10.1.

2.4.10 Definition and Mapping of Fuelbeds

I built 29 final fuelbeds by overlaying and combining the surface fuel and structure class data layers. All combinations of low and high surface fuel loadings (surface fuel combinations) and forest structure classes were mapped and visually assessed. To reduce complexity in the results and to avoid false precision at the fine scale of the data, infrequent surface fuel combinations (less than 1000 occurrences over the park) were lumped with spatially adjacent surface fuel combinations within the same forest structure classes. For example, an infrequently occurring fuel combination of low ORG, high SW, and low LW in a woodland structure class was lumped with a frequently occurring, adjacent woodland class containing low fuel loadings in

all classes. The consolidated fuelbed was labeled “Woodland with low ORG and low LW”. In other cases, SW and LW fuels were lumped together, and the fuel class became “WF” (all woody fuel).

2.4.11 *Assigning Values to Fuelbeds*

I plotted the continuous surface fuel loadings from the field data to determine the low and high surface-fuel values for each fuel class and found that the distributions of the loadings were approximately bell-shaped. I used the 25th and 75th percentile values of each distribution as the median values for the low and high fuel classes respectively, thereby adjusting for right- or left-skew of the distributions. To assign values for lumped classes, such as for SW in the Woodland with low ORG and LW (example above), I used the median value (50th percentile) for the full range of the fuel class.

The canopy characteristics (species, density, diameter, height, and height-to-live-crown of trees per canopy strata) from 291 field plots were overlaid and matched to the fuelbed map by their location. Twenty-nine field plots were eliminated due to mismatching structures (e.g., designated shrub plots in multistory forest fuelbeds). The canopy characteristics from the final 262 field plots were assigned to the fuelbeds. The field data are summarized by fuelbed in Appendix 1. Canopy characteristics for fuelbeds with little or no corresponding plot data were imputed from adjacent fuelbeds and the vegetation map (Nielsen et al. 2021). The imputed values are indicated in Appendix 1 in italics.

Surface fuel loadings and structural characteristics from the field plots were used to define fuelbeds for the three additional vegetation structure classes. Although Nielsen et al. (2021) differentiated among several different shrub and meadow vegetation types, I combined

them into single shrub and meadow vegetation types, because the field plots did not adequately sample the types identified by Nielsen et al. (2021) for my modeling to differentiate them.

2.4.12 Integration with the Fuel Characteristic Classification System

Each fuelbed represents a unique combination of surface and canopy fuels, vegetation, and structural characteristics, which I designed to be compatible with the FCCS, not only to derive the fire and fuel potentials for Mount Rainier, but also as a repository for the data that I collected on fuel characteristics throughout the Park. Unlike traditional FCCS fuelbeds, in which the vegetation type comprises the foundation to which the ranges of fuel load values are assigned (Riccardi et al 2007), my fuelbeds were constructed from fuel loadings and structure characteristics, and the vegetation types were assigned secondarily.

2.4.13 FCCS Fire Potentials

I entered the fuelbeds as “user-defined” fuelbeds into the Fuel and Fire Tools (FFT) software application (Fire and Environmental Research Applications Team 2020), which integrates FCCS and fire effects modeling programs in order to calculate the FCCS fire potentials for each fuelbed. Each fuelbed has a fire potential based on three indices: 1) surface fire behavior potential (FBP), which is the maximum spread and flame length potential for surface fire, 2) crown fire potential (CFP), defined as the weighted average of the potentials for surface fire to reach the canopy layer and carry through the canopy, and the relative rate of spread, and 3) available fuel potential (AFP), which represents the sum of fuel loadings in all combustion phases (flaming, smoldering, and residual smoldering) that is available to burn (Sandberg et al. 2007).

To make a user-defined fuelbed in FCCS, it is necessary to start with one of the FCCS default fuelbeds in the program and change the values for the fields of interest for which specific data has been collected. I used FCCS fuelbed #238—Pacific silver fir-mountain hemlock forest (Prichard et al. 2011)—as the default fuelbed; values from the FCCS fuelbed were held constant except for the canopy, woody fuels, and litter and duff strata, which were replaced with values from my field data. The following additional changes were made to fuelbeds whose structure class was one of the three additional vegetation structure fuelbeds: 1) species compositions of the shrub and non-woody fuels strata were changed to wetland species for the riparian fuelbed, 2) shrub density and species composition of the shrub stratum were manipulated for the shrubs fuelbed, and 3) the median organic fuel loading of the meadow fuelbed was increased to reflect the substantially higher fuel loading in this type than was found in any of the other fuelbeds. I added a “very high” fuel load class on the data table to represent the higher fuel loading in the meadow fuelbed. Fuel moisture was held constant for all fuelbeds.

2.5 Results

2.5.1 *Structure Classes and Map*

The nine structure classes, comprising six non-riparian forest classes from LiDAR and three additional vegetation structure classes, have distinct combinations of canopy heights, rumple (rugosity), and cover values (Figure 2-4). The median canopy heights (P95) and canopy base heights (P25) of the forest classes increase from lowest heights in the woodland to highest heights in the tall topstory class. The two multistory and one tall topstory classes each have equally high total canopy cover values, but the multistory classes have highest cover below 32 meters, whereas the tall topstory cover is highest in the canopy >32 m strata.

The map of the structure classes illustrates the differences in canopy structure across Mount Rainier National Park (Figure 2-5). Shorter forest structure classes occur at the highest elevations, whereas the tallest forest types are most prevalent at lower elevations. The map also illustrates the influence of climate on the canopy structure classes, as evident in the disproportionate distribution of open woodland on the drier east side of the Park, and tall topstory on the moist west side.

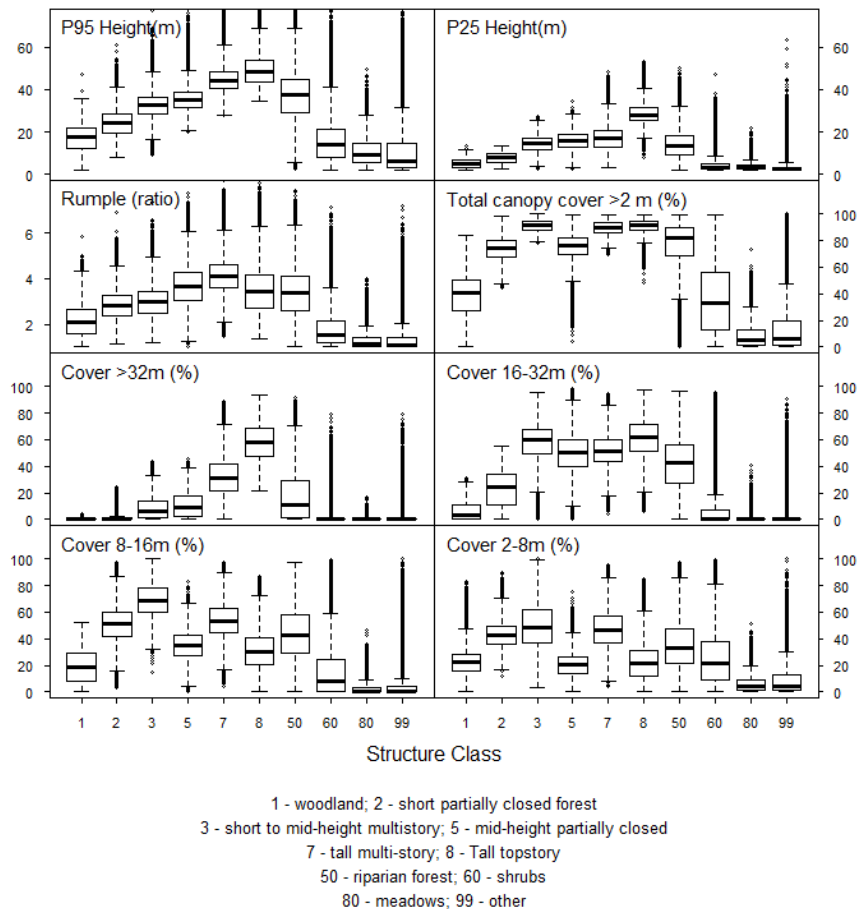


Figure 2-4. Box plots of structural class characteristics. LiDAR-derived height (P95 = dominant tree height, P25 = canopy base height), rumple (rugosity), and canopy cover of the forest structural classes (1–8). Other map-derived types are shown for reference. Total canopy cover >2 m is not used in the classification – shown to compare total cover between classes. Bold lines in box plots show median values; bottom and top of boxes show 25th and 75th percentile values.

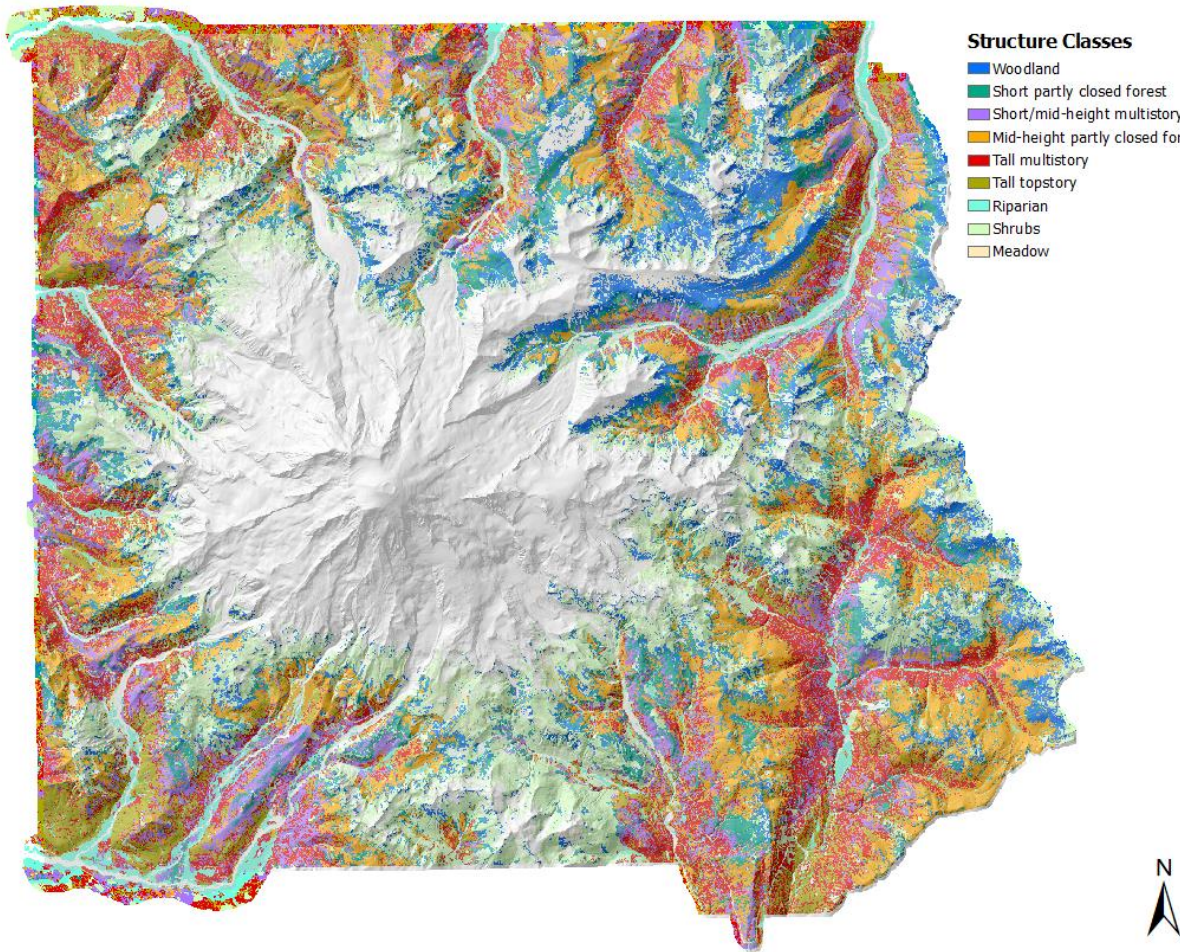


Figure 2-5. Map of nine distinct structure classes distributed across Mount Rainier National Park. Six forest structures are derived from LiDAR and classified by tree height (95th percentile return height), canopy base height (25th percentile return height), and rumple (rugosity) using hierarchical clustering. Three additional vegetation structure classes (riparian, shrubs, and meadow) are from the vegetation map (Nielsen et al. 2020).

2.5.2 *Surface Fuel Models and Map*

Both linear regressions and random forest explained less than 29% of the variation in continuous values for the surface fuels (Table 2-2). The linear regressions performed better than random forest (RF), as shown in the higher R-square values for linear regression compared to the proportion of deviance explained (PDE) for RF. This is especially true in the case of small woody fuels (linear $R^2 = 0.29$, RF PDE = 0.08), although I was aiming for a higher level of

accuracy (> 60%). Classification of the surface fuels into high and low classes above and below the median values per fuel class was more successful. Classification accuracies for the best models selected from 250 iterations ranged from 68.2% for small woody fuels to 78.2% for organic fuels and decreased slightly in all classes with cross validation.

Table 2-2. Results of regressions and classifications for surface fuels (ORG = litter and duff, SW = 1- to 100-hour small woody fuels, LW = 1000-hour large woody fuels) with median values for each fuel type shown. Random forest (RF) and linear regression showed poor ability to predict continuous values for surface fuels (low PDE (proportion deviance explained) and R-squared), whereas classification of surface fuels into high/low classes based on median values with RF was more successful.

Surface fuels classes	Median value kg/m ²	Quantitative models using continuous values		RF High/Low classification accuracy	
		RF PDE	Linear R ²	Original models	Cross- validation
ORG	5.4	0.15	0.24	78.2%	73.8%
SW	0.7	0.08	0.29	68.2%	61.6%
LW	2.7	0.19	0.23	77.5%	74.8%

Significant ($p \leq 0.05$) linear regression predictors

ORG	St. dev. return height, p75 return height, precipitation, aspect 270 m
SW	Canopy cover >2 m, slope 270 m
LW	p75 return height

The predictors of high/low surface fuel classes are listed in order of importance using the Gini index in random forest (Figure 2-6). The most influential predictors for the organic surface fuel classes were related to water balance (precipitation, aet, deficit), temperature, and aspect measured at the 270-m scale. The most influential predictors for small woody fuel classes were related to height of the canopy, overall canopy cover, curvature measured at the 270-m scale, and topographic position measured at the 100-m scale. The most influential predictors for the large woody fuel classes were related to measures of canopy cover, canopy height, and variance in canopy height.

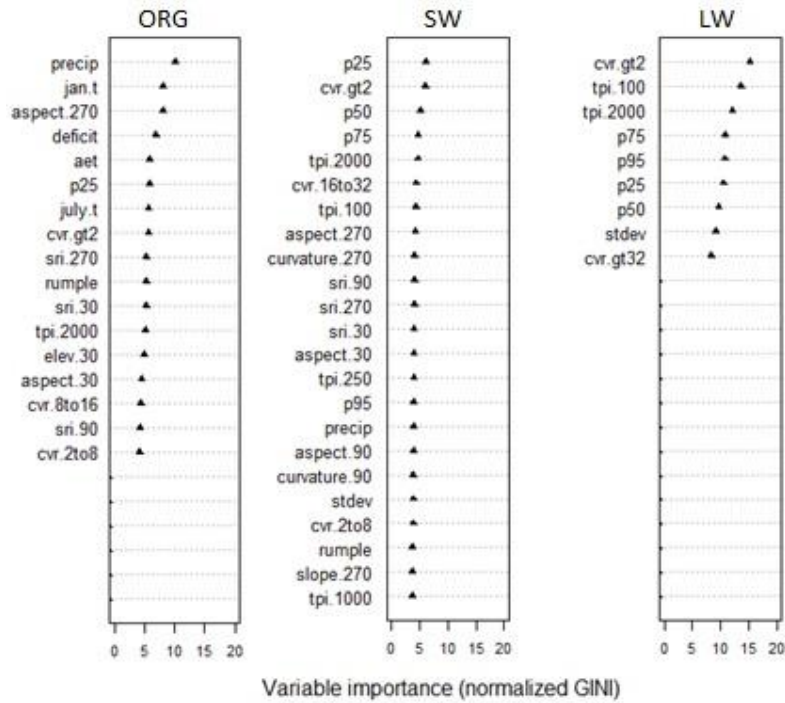


Figure 2-6. Relative importance of predictors to classification of surface fuels into high and low classes (larger value indicates greater importance) using the Gini index in random forest. Order of predictors shown is for the random forest model with the highest correct classification rates selected from 250 models. All predictors (defined in Table 1) were run for each fuel class, but only predictors with values above zero are listed.

The map of the distribution of surface fuel load combinations (Figure 2-7) illustrates differences in the locations of fuel combinations across the Park. I sorted the map colors based on the SW class, which has the highest contrast between fuel loads on the west side (high fuel loads) and east side (low fuel loads). There are also higher ORG fuel loads on the west side, but alpine shrublands with high SW fuel loads on the westside are mainly associated with low ORG fuel combinations. The LW fuel loadings were more evenly distributed across the Park.

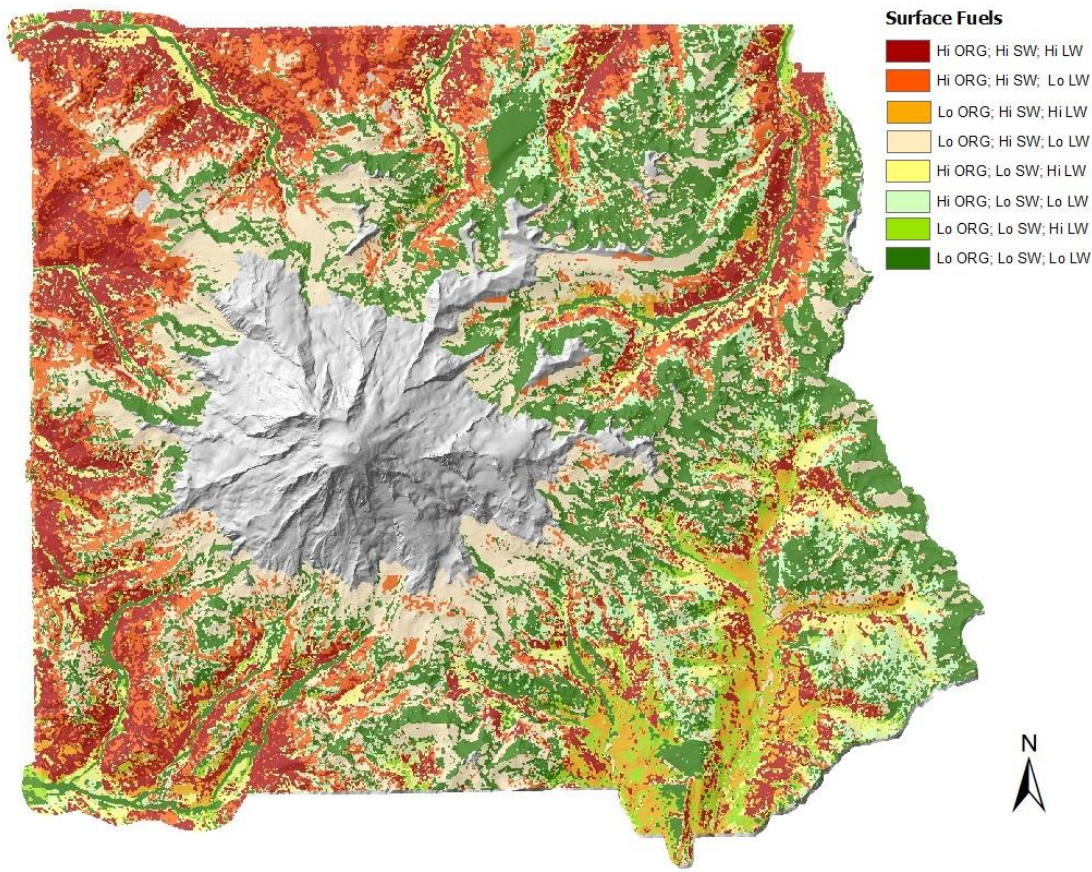


Figure 2-7. Map of surface fuel classes across Mount Rainier National Park showing the distribution of all combinations of high (Hi) and low (Lo) surface fuel classes (ORG = litter and duff, SW = 1- to 100-hour small woody fuel, LW = 1000-hour large woody fuel). Map colors are arranged by the SW class, which contains the most east-west contrast.

2.5.3 Fuelbed Map

The map of the 29 final fuelbeds, which combines the structure and surface fuel maps, illustrates distinct locations for different combinations of canopy structures and fuel loads across the Park (Figure 2-8). For example, fuelbed #11 (woodland with low ORG, low LW) is primarily restricted to high elevations on the northeast corner of the Park and replaced by fuelbeds #22 and #23 (short partly closed forests) elsewhere. Fuelbed #53 (tall multistory with low ORG, low SW) is mainly located in the southeast, whereas fuelbed #62 (tall topstory with high WF) is mainly located in the southwest corner of the Park. The characteristics of each fuelbed and the median values for surface fuels are listed in Tables 2-3 and 2-4, respectively.

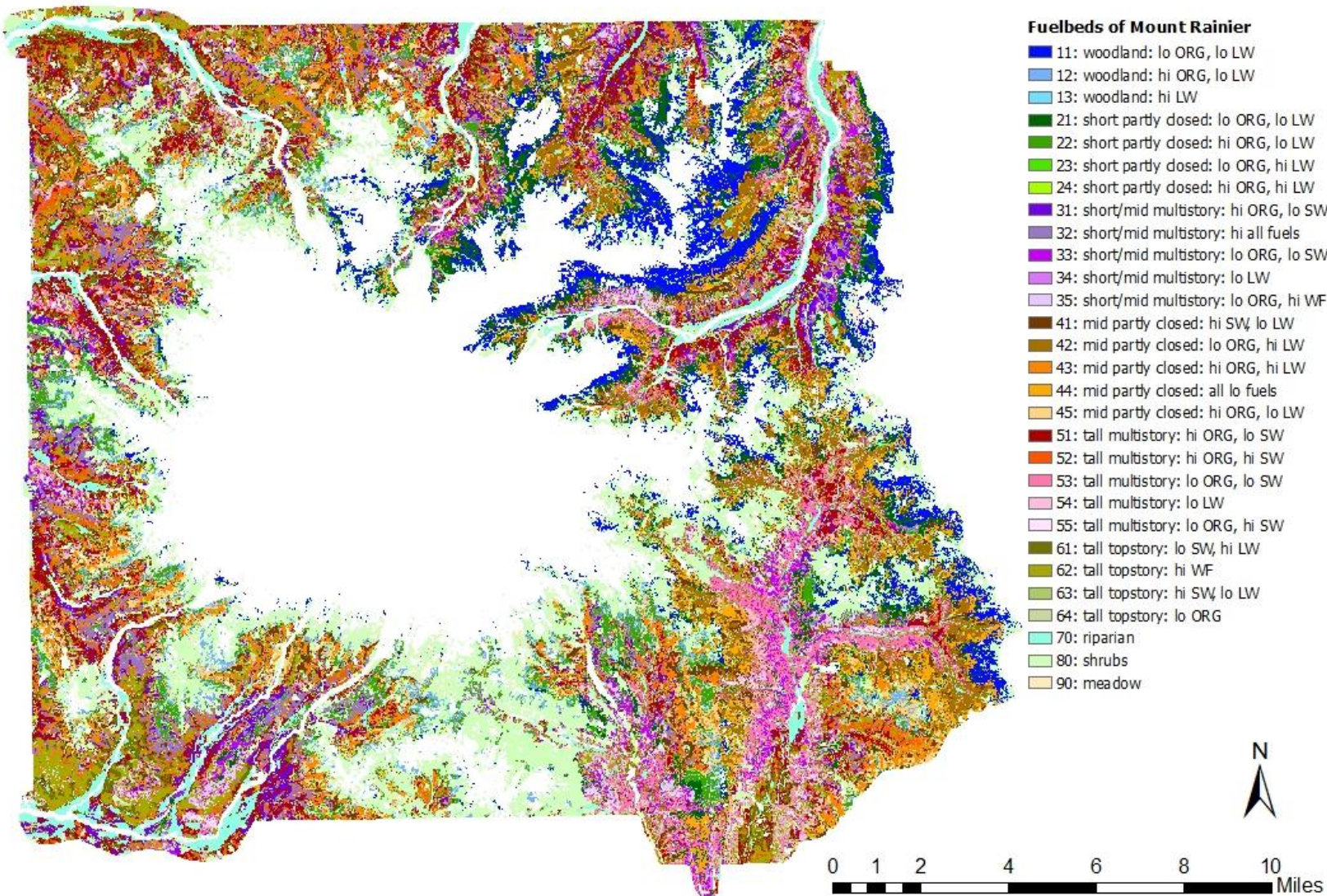


Figure 2-8. Map of fuelbeds for Mount Rainier National Park based on six structural classes developed from LiDAR, three vegetation classes (riparian, shrubs, and meadow) from the vegetation mapping project (Nielsen et al. 2021) and combinations of low (lo) and high (hi) surface fuels (ORG = organic/litter and duff, SW = 1- to 100-hour small woody fuel, LW = 1000-hour large woody fuel).

Table 2-3. Twenty-nine fuelbeds (FB) from structure and surface fuel combinations (ORG = organic/litter and duff, SW = 1 to 100-hour small woody fuel, LW = 1000-hour large woody fuel). Median values for surface fuels; L (low), H (high), VH (very high), and F (full range). FCCS fire behavior potential (FBP), crown fire potential (CFP), and available fuel potential (AFP) indexed from low to high (0-9). Percent of study area (%) and hectares (Ha). 3.1% (2,149 Ha) of study area not sampled.

FB	Structure	ORG	SW	LW	FBP	CFP	AFP	%	Ha
11	Woodland	L	F	L	4	5	6	6.2	4,333
12	Woodland	H	F	L	7	7	7	1.9	1,358
13	Woodland	F	F	H	6	6	9	0.4	298
21	Short partly closed forest	L	F	L	4	5	6	4.2	2,979
22	Short partly closed forest	H	F	L	7	6	6	4.3	2,992
23	Short partly closed forest	L	F	H	4	7	9	0.8	535
24	Short partly closed forest	H	F	H	7	6	9	1.1	797
31	Short to mid-height multistory	H	L	F	7	6	8	3.8	2,668
32	Short to mid-height multistory	H	H	H	7	5	9	2.7	1,926
33	Short to mid-height multistory	L	L	F	4	5	7	2.0	1,375
34	Short to mid-height multistory	F	F	L	6	5	7	2.2	1,522
35	Short to mid-height multistory	L	H	H	4	4	9	1.0	689
41	Mid-height partly closed forest	F	H	L	5	5	7	3.0	2,134
42	Mid-height partly closed forest	L	F	H	4	4	9	4.8	3,380
43	Mid-height partly closed forest	H	F	H	7	5	9	6.0	4,231
44	Mid-height partly closed forest	L	L	L	4	5	7	3.4	2,411
45	Mid-height partly closed forest	H	F	L	7	4	6	2.7	1,874
51	Tall multistory	H	L	F	7	6	9	6.7	4,690
52	Tall multistory	H	H	F	7	6	9	2.2	1,560
53	Tall multistory	L	L	F	4	4	7	3.5	2,459
54	Tall multistory	L	F	F	4	5	9	1.6	1,136
55	Tall multistory	L	H	F	4	2	7	0.7	480
61	Tall topstory	F	L	H	6	5	9	3.1	2,214
62	Tall topstory	F	H	H	5	5	9	3.2	2,240
63	Tall topstory	F	H	L	5	6	9	0.6	430
64	Tall topstory	L	F	F	4	7	9	0.9	628
70	Riparian	F	F	H	6	4	9	4.8	3,354
80	Shrubs	F	L	F	7	0	6	18.4	12,959
90	Meadow	VH	L	L	7	0	5	0.7	527

Table 2-4. Median values for surface fuel classes. Median (minimum, maximum) kg/m² for surface fuel classes (ORG = organic/litter and duff, SW = 1 to 100-hour small woody fuel, LW = 1000-hour large woody fuel).

Surface Fuel Class	Low	High	Very High	Full Range
ORG kg/m ²	2.3 (0, 5.6)	9.8 (5.6, 38.9)	13.6 (8.1, 38.9)	5.6 (0, 38.9)
ORG depth (cm)	8.1 (0, 19.3)	3.3 (1.9, 13.1)	18.6 (4.6, 13.1)	7.6 (0, 1.9)
SW kg/m ²	0.3 (0, 0.7)	1.2 (0.7, 4.3)	NA	0.7 (0, 4.3)
LW kg/m ²	0.3 (0, 2.7)	9.4 (2.7, 56.3)	NA	2.7 (0, 56.3)

2.5.4 Fire Potentials

The FCCS fire potentials ranged from very low (0) to very high (9), with the majority being moderate to high across all structures and fuel loadings (Figure 2-9). Surface fire behavior potentials (FBP) were generally high, with scores ranging from 4 to 7. Unlike the other fuel potential maps, there was a noticeable difference between FBP scores from east to west; with scores of 4 mainly located on the east side, and scores of 7 prominent in the west. Across the Park, 11 fuelbeds (20,403 ha, 29% study area) with low ORG received a moderate FBP score (4), and 11 fuelbeds (35,572 ha, 51% study area) with high (10 fuelbeds) and very high (1 fuelbed) ORG received a high FBP score (7).

Crown fire potential (CFP) varied the most across the fuelbeds, with shrubs and meadows receiving the lowest score (0), fuelbed #55 (tall multistory) receiving a low score (2), and three fuelbeds with a high score (7). The low score for the tall multistory is questionable because there is only one plot associated with this fuelbed, which has an uncharacteristically low canopy density and high height-to-live crown for a multistory canopy. The largest proportion of the study area had a moderate CFP score of 5 over 11 fuelbeds (26,500 ha, 38% study area). The lowest scoring fuelbeds were most prevalent in the south-central portion of the park. Moderate and high crown fire potential scores were fairly evenly distributed across the Park.

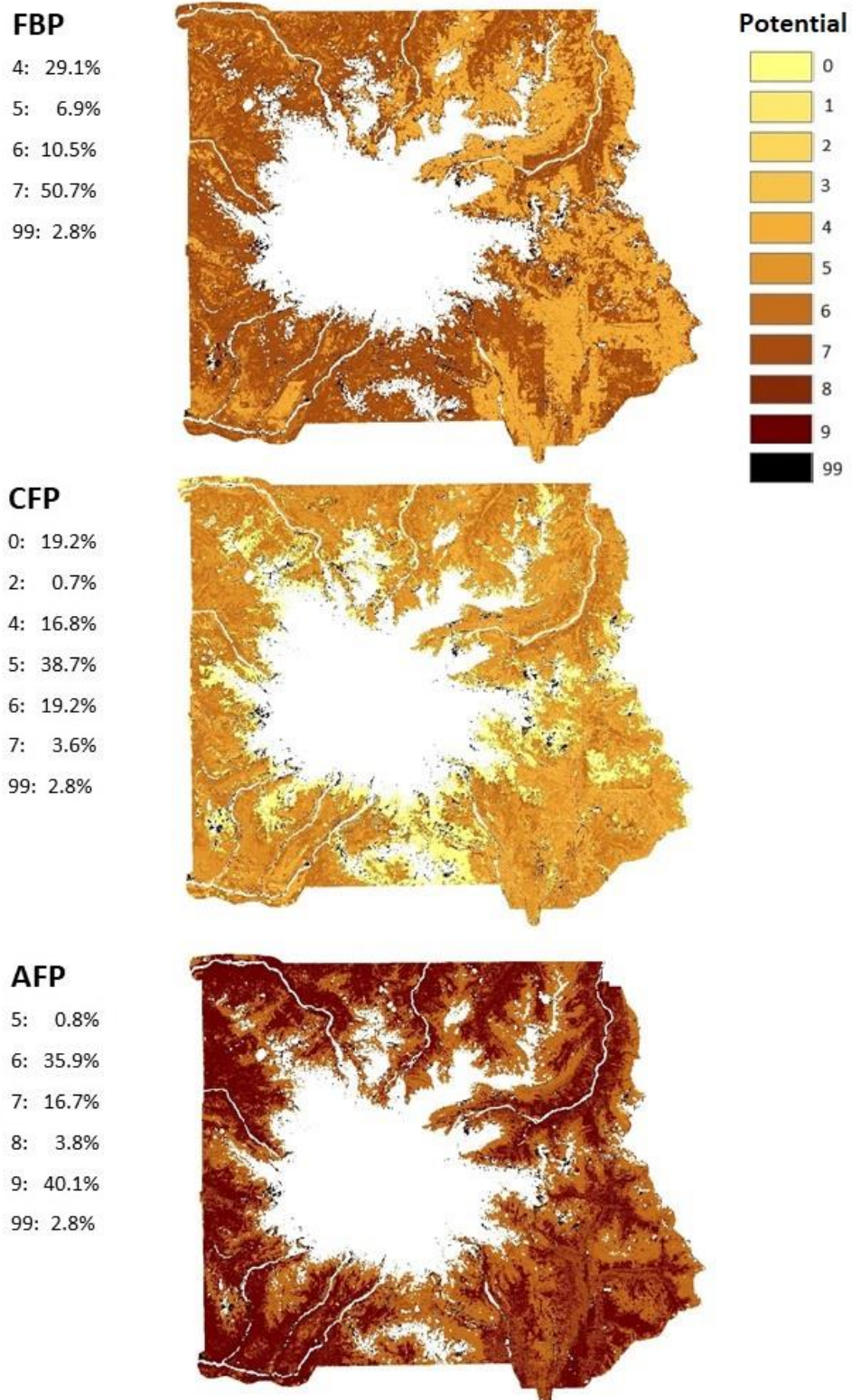


Figure 2-9. Fire and fuel potentials across Mount Rainier National Park. Distributions and relative percentages of surface fire behavior potential (FBP), crown fire potential (CFP), and available fuel potential (AFP) on a scale of 0-9 (low to high), class 99 (other, not evaluated).

Available fuel potential (AFP) scores were relatively high for all fuelbeds, ranging from moderate (score of 5) to very high (score of 9). Over half of the fuelbeds (15 of 29; 31,461 ha, 40% study area) had a score of 9, including all the tall topstory and the majority (3 of 5) of the tall multistory structural classes. The highest AFPs (score of 9) were more prevalent on the west side, but they were well represented throughout the Park.

2.6 Discussion

2.6.1 *Distributions of the Fuelbeds and Fire Potentials*

The fuelbed and fire potential maps illustrate variations and patterns in the distributions of fuel and fire characteristics across Mount Rainier National Park. The most prominent source of variation in the fuel distributions is the influence of the east-west precipitation gradient along the Cascade Crest, creating wetter conditions on the west side of the Park and drier conditions on the east side. These conditions correspond to low frequency high-severity fires in the west giving way to more frequent mixed-severity fire on the eastern slopes of the Park (Hemstrom and Franklin 1982, Agee 1993, Siderius and Murray 2005).

The influence of the east-west gradient was evident in the fuel loadings corresponding to several fuelbeds that were disproportionately located on either side of the Park. Fuelbed #62, which was concentrated on the west side, had high SW and LW fuels, and a very high FBP (score of 9), whereas fuelbed #11, located primarily on the east side, had low ORG, LW, and AFP (score of 6). The surface fuel map also showed higher fuel loads on the west side of the Park, presumably due to less frequent fire (as seen in the fire records (USDI BLM 2020) and higher moisture conditions that support more vegetative biomass (Gholz 1982). The higher fuel loadings in the west were particularly evident in the SW fuel class, and noticeable in the ORG

(litter and duff) class as well. These higher fuel loadings in the SW and ORG classes, which are the primary carriers of surface fires (National Wildfire Coordinating Group 2021), corresponded to higher FBPs on the west side than to the east (scores of 7 vs. 4).

The influence of the east-west gradient was less evident in the distributions of the other fire potentials (CFP and AFP), and most fuelbeds were more evenly distributed throughout the Park. However, I expect that the east-west precipitation gradient still influences fire frequency and severity in these fuelbeds, although this is not evident on the maps because fuel moisture is not accounted for in the fuelbeds and fire potentials (but rather, can be adjusted for in FFT). Higher fuel moistures due to the maritime climate on the west side of the Park likely dampen fuel flammability there.

Beyond the scale of the Park, Littell et al. (2018) warn that climate change will have the largest effect on wildfire area burned in areas where climate, rather than fuels, is the limiting factor. My study confirms that AFP is high throughout Mount Rainier National Park, so the Park is not fuel limited. The fine scale of the fuelbed map allows me to determine more precisely where the largest impacts and changes will occur within the Park. In the short term, I expect that warmer and drier conditions associated with climate change will be more pronounced on the drier east side of the Park, resulting in larger and more frequent fires (Littell et al. 2009, Halofsky 2020). Larger fire growth is particularly associated with having more days in the early and late summers with low vapor pressure deficit (VPD) (Sedano and Randerson 2014, Higuera and Abatzoglou 2020). However, if the trend towards warmer and drier summers continues (Mote et al. 2014), then I expect to have larger stand-replacing fires on the west side eventually due to the greater FBP, higher fuel loadings, and fewer fire-adapted species. Littell et al. (2018) and Kennedy et al. (2021) suggest that this trend could be short-lived because the high AFP and

FBP that increased fire behavior will likely consume these fuels after one or two large fires; then the balance could shift towards more fire on the east again.

2.6.2 *Benefit of LiDAR*

This work highlights the challenges and benefits of merging LiDAR and field data collection to measure and map fuel characteristics. The LiDAR data did not prove to be as useful as I had hoped for mapping surface fuel classes beyond a coarse resolution (high and low classes); however, even this coarse resolution enabled me to compare fuel loadings across the Park and see differences in fire potential at different locations. The LiDAR data provided fine-scale canopy characteristics that I was able to map directly to develop the structural classes and use indirectly to inform the surface fuels map. The combination of the structural classes and the surface fuel combinations provided 29 distinct, local-scale fuelbeds that greatly expand maps and other geospatial information related to fuels and wildland fire at Mount Rainier.

When I began this project, I had expected that surface fuel loads would be related to the forest overstory structure, which was measured in high fidelity with LiDAR data. I was unsuccessful in predicting specific values for surface fuels and had to fall back to predicting high/low fuel classes based on median values by adding climate and topographic variables to structure. Jakubowski et al. (2013) similarly were unsuccessful in predicting surface fuel loads using airborne LiDAR data in Sierra Nevada forests in California, USA. Other researchers have used field data and found that surface fuel loads are not well correlated with the overstory forest structure (Keane et al. 2012, Lydersen et al. 2015), although Hall et al. (2006) and van Wagtendonk and Moore (2010) found stronger relationships.

Kane et al. (2015) found that climate and topography were important predictors of fire

pattern in the Sierra Nevada, which may reflect underlying patterns of fuel deposition related to broad patterns of forest structure. Miller and Urban (1999) modeled interactions between fuels, climate, and elevation, noting that fire spread (which affects fuel distributions) was limited by fuel moisture and more compact needle litter from short-needled species at higher elevations. These relationships among topography, climate, and species clearly influenced the distribution of fuelbeds at Mount Rainier National Park as well (e.g., the smaller volume of SW on the east side of the mountain, especially in the low-statured fuels at high elevation). The fact that this was reflected in the fuelbeds, and their fire potentials, suggests that high/low classes adequately reflected important differences in fire behavior potential.

Although the use of airborne laser scanning (ALS) data has increased the efficiency of mapping canopy characteristics directly in recent years (Mauro et al. 2021), there have been few improvements in mapping surface fuels directly with remotely sensed data (Gale et al. 2021). One exception to this is in the detection of large diameter coarse woody debris (CWD) using a combination of height, pulse-based filters, and linear pattern recognition (Jarron et al. 2021). This innovative technique for detecting CWD could be useful for both improving fuel mapping efforts and detecting wildlife habitat for birds, mammals, amphibians, and reptiles (Bull 2002).

2.6.3 *Management Implications*

The fuelbed and fire potential maps can be used to identify management concerns and restoration opportunities. I use the maps to consider two resource management issues and potential strategies for conservation.

Northern Spotted Owl Habitat:

Fire has been identified as the greatest threat to the 33,185 hectares of contiguous habitat for the threatened and endangered northern spotted owl at Mount Rainier National Park (NPS 2019). This resource concern is validated by the relatively high FBP (ranging from 6 to 9) throughout the Park, and specifically in the tall multistory and tall topstory fuelbeds (7 of 9 fuelbeds with FBP scores of 9) within their preferred habitat (Forsman et al. 1984). If warmer and drier conditions increase with climate change, then these low- to mid-elevation forests, dominated by non-fire adapted species such as western hemlock, are susceptible to large stand-replacing fires (Agee 1993). I examined the fuelbed and fire potential maps to identify concerns and strategies for managing wildfires within several different fuelbeds in preferred spotted owl habitat.

1) Tall multistory fuelbed #53 (low ORG, low SW) clustered on the southeastern slopes of the Park has the lowest combination of fire and fuel potentials (FBP 4, CFP 4, AFP 7) of the tall multistory fuelbeds, other than fuelbed #55, which has CFP of 2, but is more dispersed and has fewer total acres. The moderate FBP of fuelbed #53 may provide an opportunity for managers to backburn towards an oncoming wildfire to prevent fire spread into habitat with higher fire and fuel potentials such as fuelbeds #51 or #52 (tall multistories with high ORG, each scoring 7, 6, and 9 for FHB, CFP and AFP respectively). This action would need to be evaluated with consideration for local onsite fire weather and would be advisable only as a measure to minimize fire size and spread.

2) Tall topstory fuelbed #62 (high SW and LW) is concentrated in the southwest corner of the Park, providing a contiguous fuelbed of preferred spotted owl habitat. It has moderate FBP and CFP scores (5 each), but it has a high AFP (9) that makes it vulnerable to high-intensity

wildfire with warmer and drier conditions. If a wildfire were to occur in this area under current climate, it may be preferable to allow it to burn a smaller footprint of this prime habitat under moister conditions, thus providing a barrier to fire spread in the future.

Whitebark Pine:

Whitebark pine is a fire-dependent species that benefits from frequent low- to moderate-severity fires that maintain canopy openings (Keane et al. 1990, McDowell 2010). Its population is in decline throughout North America due to fire exclusion, insects (especially mountain pine beetle (*Dendroctonus ponderosae*)) and pathogens (white pine blister rust (*Cronartium ribicola*) (Keane and Arno 1993, Tomback et al. 2001)). The impact on whitebark pine from higher intensity fire is complicated (Siderius and Murray 2005). Whitebark pine out-competes other species in recolonizing large, burned areas, because Clark's nutcrackers (*Nucifraga columbiana*), their primary seed dispersers, use openings from stand-replacing fires to cache seeds, and can carry the seeds up to 22 kilometers (Keane et al. 1990, Tomback et al. 2001). However, larger, and more severe fires may eliminate most of the seed source in dwindling populations. In a study of seedling regeneration following two fires in the northern Cascades, areas with the greatest canopy cover of whitebark pine and moderate burn severity had the highest probability of seedling presence (McDowell 2010). McDowell (2010) also found that seedling densities increased with char depth and greater distance into the core burn area, suggesting that moderate severity fires may create opportunities for whitebark pine regeneration.

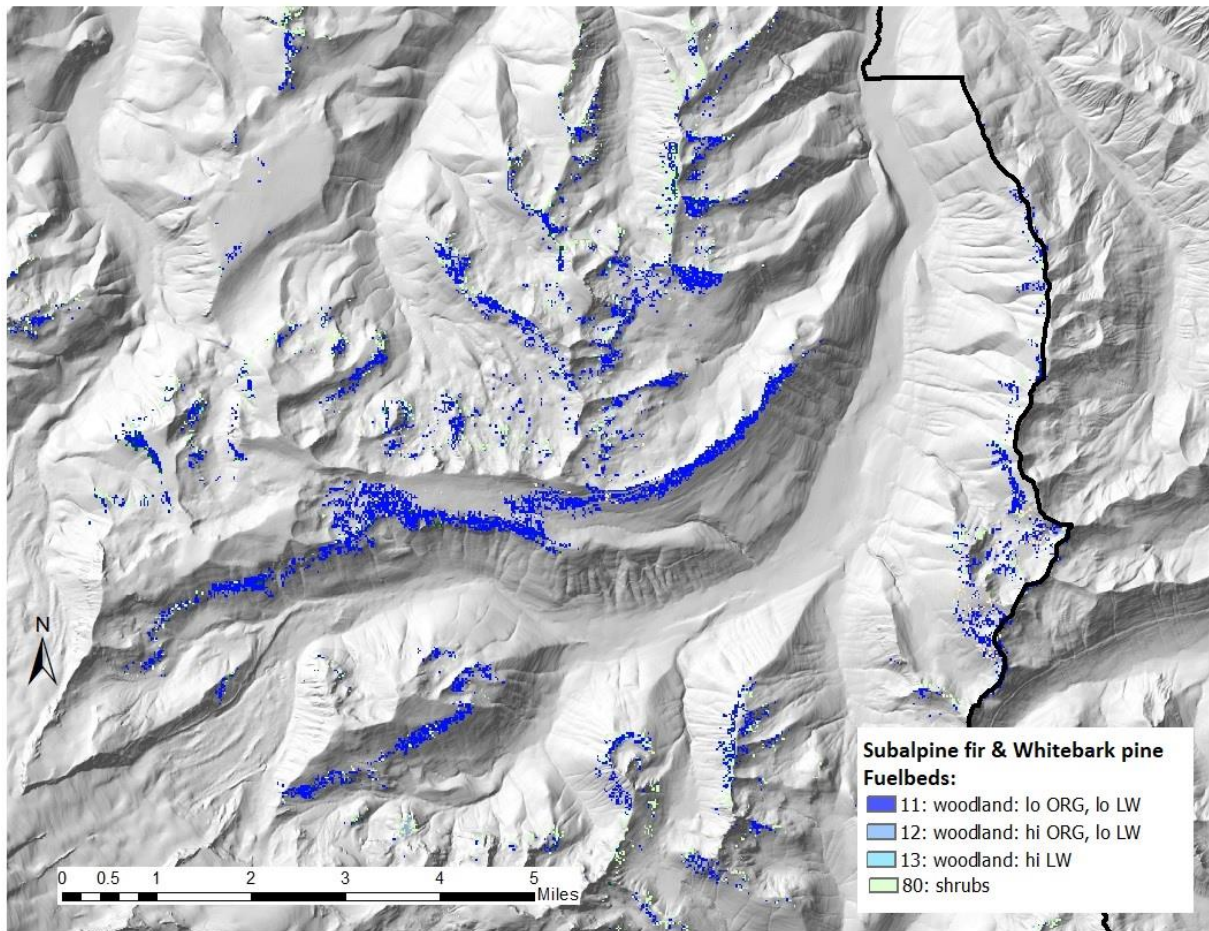


Figure 2-10. Fuelbeds in subalpine fir / whitebark pine vegetation map class (Nielsen et al. 2021) showing that potential whitebark pine habitat is predominantly Fuelbed #11: woodland with low fuel loads.

Woodland fuelbed #11 (low ORG, low LW), located on the northeastern slopes of Mount Rainier, is the predominant fuelbed in potential whitebark pine habitat, as shown by clipping the fuelbed map to the subalpine fir / whitebark pine vegetation mapping class (Figure 2-10). Whitebark pine is likely to tolerate the moderate FBP (4) and CFP (5) in fuelbed #11, but the higher than median AFP (6) could precipitate lethal higher intensity fire in association with warmer and drier conditions (climate change). In the event of a wildfire, or if prescribed burning is an option, it may be helpful to rake fuel accumulations away from the bases of the pines to reduce fire intensity.

2.6.4 Using the Map

I encourage resource and fire managers to utilize the fuelbed and fire potential maps to identify additional areas of interest to the Park, as I suggest for spotted owl habitat protection and whitebark pine restoration. The data from the fuelbeds can also be used as input to fire spread models during wildfire events. The user-defined fuelbeds are stored in the online NPS data store <https://irma.nps.gov/DataStore/> and can be imported into FFT to derive fire behavior statistics using local weather during a fire incident. The median fuel load values from the fuelbeds can also be used in other fire spread models.

Unlike other fuel maps, the fuelbeds for Mount Rainier are based on local data, but some of the values for the fuelbeds are derived from few or no field plots (e.g., 1 plot for fuelbed #55: tall multistory with low ORG, high LW). Fuelbeds with little or no data can be identified by inspecting Appendix 1. Although the map and fire potentials can be used as a means of identifying areas of concern, they cannot replace the need for field reconnaissance. However, they do provide a broad-scale assessment of potential hazards, indicating where field reconnaissance might be most valuable.

2.7 References

- Agee, J.K. 1993. Fire Ecology of Pacific Northwest Forests. Island Press, Washington, D.C.
- Albini, F.A. 1976. Estimating wildfire behavior and effects. Gen. Tech. Rep. INT-30. Ogden, Utah: Department of Agriculture, Forest Service, Intermountain Forest and Range Experiment Station. 92 pp.
- Anderson, H.E. 1982. Aids to determining fuel models for estimating fire behavior. Gen. Tech. Rep. INT-122. Ogden, Utah: Department of Agriculture, Forest Service, Intermountain Forest and Range Experiment Station. 22 pp.
- Andersen, H.E., R.J. McGaughey, and S.E. Reutebuch. 2005. Estimating forest canopy fuel parameters using LIDAR data. Remote Sensing of Environment 94: 441-449.

- Breiman, L., J.H. Friedman, R.A. Olshen, and C.J. Stone. 1984. Classification and regression trees. Chapman and Hall, New York, New York, USA.
- Brown, J.K., R.D. Oberheu, and C.M. Johnston. 1982. Handbook for inventorying surface fuels and biomass in the interior west. General Technical Report INT-GTR-129. Ogden, UT: U.S. Department of Agriculture, Forest Service, Intermountain Forest and Range Experiment Station. 48 pp.
- Bull, E.L. The value of coarse woody debris to vertebrates in the Pacific Northwest. General Technical Report PSW-GTR-181. U.S. Department of Agriculture, Forest Service, Pacific Northwest Research Station.
- Crookston, N.L., and A.O. Finley. 2008. yaImpute: An R package for kNN imputation. *Journal of Statistical Software* 23(10): 1-16.
- Daly, C., M. Halbleib, J.I. Smith, W.P. Gibson, M.K. Doggett, G.H. Taylor, J. Curtis, and P.P. Pasteris. 2008. Physiographically sensitive mapping of climatological temperature and precipitation across the conterminous United States. *International Journal of Climatology*, 28: 2031-2064.
- Dingman, S.L. 2002. Physical Hydrology. Prentice Hall, Upper Saddle River, New Jersey, USA.
- Erdody, T.L., and L.M. Moskal. 2010. Fusion of LiDAR and imagery for estimating forest canopy fuels. *Remote Sensing of Environment* 114: 725-73.
- Fire and Environmental Research Applications Team (FERA). 2020. Fuel and Fire Tools. version 2.0.2003. [computer software], <https://www.fs.usda.gov/pnw/tools/fuel-and-fire-tools-fft>
- Forsman, E.D., E.C. Meslow, and H.M. Wight. 1984. Distribution and biology of the spotted owl in Oregon. *Wildlife Monographs* 87:3-64.
- Gholz H.L. 1982. Environmental limits on aboveground net primary production, leaf area, and biomass in vegetation zones of the Pacific Northwest. *Ecology* 63(2):469-481
- Hall S.A., I.C. Burke, and N.T. Hobbs. 2006. Litter and dead wood dynamics in ponderosa pine forests 541 along a 160-year chronosequence. *Ecological Applications* 16: 2344-2355.
- Halofsky, J.E., D.L. Peterson, and B.J. Harvey. 2020. Changing wildfire, changing forests: the effects of climate change on fire regimes and vegetation in the Pacific Northwest, USA. *Fire Ecology* 16(4):1-26.
- Hamon, W.R. 1963. Computation of direct runoff amounts from storm rainfall. International Association of Scientific Hydrology, Paris, Publication 62-62.
- Hemstrom, M.A., and J.F. Franklin. 1982. Fire and other disturbances of the forests in Mount Rainier National Park. *Quaternary Research* 18(1): 32-51.

- Hermosilla, T., L.A. Ruiz, A.N. Kazakova, N.C. Coops, and L.M. Moskal. 2014. Estimation of forest structure and canopy fuel parameters from small-footprint full-waveform LiDAR data. International Journal of Wildland Fire. 23:224-233.
- Higuera, P.E., and J.T. Abatzoglou. 2020. Record-setting climate enabled the extraordinary 2020 fire season in the western United States. Global Change Biology. DOI:1111/gcb.15388
- Ho, T.K. 1995. Random decision forests. In Proceedings of 3rd international conference on document analysis and recognition. Vol. 1 pp 278-282.
- Jakubowski M.K, Q. Guo, B. Collins, S. Stephens, and M. Kelly. 2013. Predicting surface fuel models and fuel metrics using Lidar and CIR imagery in a dense, mountainous forest. Photogrammetric Engineering and Remote Sensing 79(1): 37-49.
- Jenness, J. 2006. ArcGIS Tools, online www.jennessent.com/arcgis_extensions.htm, Jenness Enterprises, Flagstaff, Arizona, USA.accessed 03/27/2011.
- Kane, V.R., J.D. Bakker, R.J. McGaughey, J.A. Lutz, R.F. Gersonde, and J.F. Franklin. 2010a. Examining conifer canopy structural complexity across forest ages and elevations with LiDAR data. Canadian Journal of Forest Research 40: 774-787.
- Kane, V.R., R.F. Gersonde, J.A. Lutz, R.J. McGaughey, J.D. Bakker, and J.F. Franklin. 2011. Patch dynamics and the development of structural and spatial heterogeneity in Pacific Northwest forests. Canadian Journal of Forest Research 41: 2276-2291.
- Kane, V.R., J.A. Lutz, C.A. Cansler, N.A. Povak, D. Churchill, D.F. Smith, J.T. Kane, and M.P. North. 2015. Water balance and topography predict fire and forest structure patterns. Forest Ecology and Management. 338:1-13.
- Kane, V.R., J.A. Lutz, S.L. Roberts, D.F. Smith, R.J. McGaughey, N.A. Povak, and M.L. Brooks. 2013. Landscape-scale effects of fire severity on mixed-conifer and red fir forest structure in Yosemite National Park. Forest Ecology and Management 287: 17-31.
- Kane, V.R., R.J. McGaughey, J.D. Bakker, R.F. Gersonde, J.A. Lutz, and J.F. Franklin. 2010b. Comparisons between field- and LiDAR-based measures of stand structural complexity. Canadian Journal of Forest Research 40: 761-773.
- Keane RE, K. Gray, and V. Bacciu. 2012. Spatial variability of wildland fuel characteristics in 575 northern Rocky Mountain ecosystems. USDA Forest Service Research Paper RMRS-RP-98, Fort Collins, Colorado, USA.
- Keane, R.E. and S.F. Arno. 1993. Rapid decline of whitebark pine in western Montana: Evidence from 20-year remeasurements. Western Journal of Applied Forestry. 8(2):44-47.
- Keane, R.E., S.F. Arno, J.K. Brown and D.F. Tombach. 1990. Modelling stand dynamics in whitebark pine (*Pinus albicaulis*) forests. Ecological Modelling 51:73-95.
- Keating, K.A., P.J.P. Gogan, J.M. Vore, and L.R. Irby. 2007. A Simple Solar Radiation Index for

Wildlife Habitat Studies. The Journal of Wildlife Management 71: 1344-1348.

Kennedy, M.C., R.R. Bart, C.L. Tague, and J.S. Choate. 2021. Does hot and dry equal more wildfire? Contrasting short- and long-term climate effects on fire in the Sierra Nevada, CA. *Ecosphere* 12(7):1-19.

Littell, J., D. McKenzie, D.L. Peterson, and A.L. Westerling. 2009. Climate and wildfire area burned in western U.S. ecoprovinces, 1916-2003. *Ecological Applications* 19: 1003-1021.

Littell, J.S., D. McKenzie, H.Y. Wan, and S.A. Cushman. 2018. Climate change and future wildfire in the western United States: An ecological approach to nonstationarity. *Earth's Future* 6:1097-1111. <https://doi.org/10.1029/2018EF000878>

Lutes, D.C., N.C. Benson, M. Keifer, J.F. Caratti, A.S. Streetman. 2009. FFI: A software tool for ecological monitoring. *International Journal of Wildland Fire*. 18:310-314.

Lutz, J.A., J.W. VanWagendonk, J.F. Franklin. 2010. Climatic water deficit, tree species ranges, and climate change in Yosemite National Park. *Journal of Biogeography* 37(5):936-950.

Lydersen, J.M., B.M. Collins, E.E. Knapp, G.B. Rollero, and S. Stephens. 2015. Relating fuel loads to overstorey structure and composition in a fire-excluded Sierra Nevada mixed-conifer forest. *International Journal of Wildland Fire*. 24:484-494.

McCune, B. and D. Keon. 2002. Equations for potential annual direct incident radiation and heat load. *Journal of Vegetation Science* 13:603-606.

McDowell, S.A. 2010. Burn severity and whitebark pine (*Pinus albicaulis*) regeneration in the North Cascades. Master's Thesis. Western Washington University.

McKenzie, D. 2020. Mountains in the Greenhouse: Climate change and the mountains of the Western U.S.A., Springer Nature Switzerland AG.

McKenzie, D., C.L. Raymond, L.-K.B. Kellogg, R.A. Norheim, A.G. Andreu, A.C. Bayard, K.E. Kopper, and E. Elman. 2007. Mapping fuels at multiple scales: landscape application of the Fuel Characteristic Classification System. *Canadian Journal Forestry Research* 37:2421-2437.

McKenzie, D., N.H.F. French, and R.D. Ottmar, 2012. National database for calculating fuel available to wildfires. *EOS* 93:57-58.

McKenzie, D., Z. Gedalof, D.L. Peterson and P. Mote. 2004. Climatic change, wildfire, and conservation. *Conservation Biology* 18(4):890-902.

Miller, C., and D.L. Urban. 1999. A model of surface fire, climate and forest pattern in the Sierra Nevada, California. *Ecological Modelling* 114(2): 113–135.

Mote, P., A.K. Snover, S. Capalbo, S.D. Eigenbrode, P. Glick, J. Littell, R. Raymondi, and S. Reeder. 2014: Ch. 21: Northwest. *Climate Change Impacts in the United States: The Third*

- National Climate Assesment, J. M. Milillo, Terese (T.C.) Richmond, and G.W. Yohe, Eds., U.S. Global Change Research Program, 487-513.
- Mutlu, M., S.C. Popescu, C. Stripling, and T. Spencer. 2008. Mapping surface fuel models using lidar and multispectral data fusion for fire behavior. *Remote Sensing of Environment*. 112:274-285.
- N.P.S. 2019. Northern spotted owl monitoring at Mount Rainier National Park. <https://www.nps.gov/articles/northern-spotted-owl-monitoring-at-mount-rainier-national-park.htm>. created 22 Oct 2019, accessed 15 Jan 2021.
- National Wildfire Coordinating Group. 2021. Fire behavior field reference guide, PMS 437. <https://www.nwcg.gov/publications/pms437>. created 2021-07-08, accessed 2022-01-19.
- Nielsen E.M, Copass C, Brunner RL, Wise LK. 2021. Mount Rainier National Park vegetation classification and mapping project report. Natural Resource Report. NPS/NCCN/NRR—2021/2253. National Park Service. Fort Collins, Colorado. <https://doi.org/10.36967/nrr-2286419>
- North, M.P., J.F. Franklin, A.B. Carey, E.D. Forsman, and T. Hamer. 1999. Forest stand structure of the Northern Spotted Owl's foraging habitat. *Forest Science* 45: 520-527.
- Ogunjemiyo, S., G. Parker, and D. Roberts. 2005. Reflections in bumpy terrain: Implications of canopy surface variations for the radiation balance of vegetation. *IEEE Geoscience and Remote Sensing Letters* 2: 90-93.
- Parker, G.G., M.E. Harmon, M.A. Lefsky, J.Q. Chen, R. Van Pelt, S.B. Weis, S.C. Thomas, W.E. Winner, D.C. Shaw and J.F. Franklin. 2004. Three-dimensional structure of an old-growth *Pseudotsuga-tsuga* canopy and its implications for radiation balance, microclimate, and gas exchange. *Ecosystems* 7: 440-453.
- Price, O.F., and C.E. Gordon. 2016. The potential for LiDAR technology to map fire fuel hazard over large areas of Australian forest. *Journal of Environmental Management*. 181:663-673.
- Prichard, S.J., A.G. Andreu, R.D. Ottmar, E. Eberhardt. 2019. Fuel Characteristic Classification System (FCCS) field sampling and fuelbed development guide. Gen. Tech. Rep. PNW-GTR-972. Portland, OR: U.S. Department of Agriculture, Forest Service, Pacific Northwest Research Station. 77 pp.
- Prichard, S.J., C.L. Riccardi, D.V. Sandberg, R.D. Ottmar. 2011. FCCS User's Guide. Version 1.1 pp. 1-121. [CONSUME Users Guide \(fs.fed.us\)](http://fs.fed.us)
- PRISM Climate Group. 2013. Oregon State University, <https://prism.oregonstate.edu>, data created 4 Feb 2014, accessed 16 Dec 2020.
- R Development Core Team. 2007. R: A language and environment for statistical computing. R Foundation for Statistical Computing, Vienna, Austria.

- Reeves, M.C., K.C. Ryan, M.G. Rollins, and T.G. Thompson. 2009. Spatial fuel data products of the LANDFIRE project. International Journal of Wildland Fire 18:250-267.
- Riano, D., E. Meier, B. Allgower, E. Chuvieco, and S.L. Ustin. 2003. Modeling airborne laser scanning data for the spatial generation of critical forest parameters in fire behavior modeling. Remote Sensing of Environment. 86:177-186.
- Riccardi, C.L., R.D. Ottmar, D.V. Sandberg, A. Andreu, E. Elman, K. Kopper, and J. Long. 2007. The fuel bed: a key element of the Fuel Characteristic Classification System. Canadian Journal of Forestry Research 37: 2394-2412.
- Roberts, S.L., J.W. van Wagendonk, A.K. Miles, and D.A. Kelt. 2011. Effects of fire on spotted owl site occupancy in a late-successional forest. Biological Conservation. 144: 610-619.
- Rollins, M.G., and C.K. Frame. 2006. The LANDFIRE Prototype Project: nationally consistent and locally relevant geospatial data for wildland fire management. USDA Forest Service General Technical Report RMRS-GTR-175, Fort Collins, Colorado, USA.
- Sandberg, D.V., C.L. Riccardi, and M.D. Schaaf. 2007. Fire potential rating for wildland fuelbeds using the Fuel Characteristic Classification System. Canadian Journal of Forestry Research 37: 2456-2463.
- Schaaf, M.D., D.V. Sandberg, M.D. Schreuder, and C.L. Riccardi. 2007. A conceptual framework for ranking crown fire potential in wildland fuelbeds. Canadian Journal of Forestry Research 37:2464-2478.
- Scott, J.H., and R.E. Burgan. 2005. Standard fire behavior fuel models: a comprehensive set for use with Rothermel's surface fire spread model. USDA Forest Service General Technical Report RMRS-GTR-153, Fort Collins, Colorado, USA.
- Sedano, F., and J.T. Randerson. 2014. Multi-scale influence of vapor pressure deficit on fire ignition and spread in boreal forest ecosystems. Biogeosciences 11:3739-3755.
- Siderius, J., and M.P. Murray. 2005. Fire knowledge for managing Cascadian Whitebark Pine ecosystems. National Park Service and Crater Lake National Park, Seattle, WA, USA.
- Smithwick, E.A.H., M.G. Ryan, D.M. Kashians, W.H. Romme, D.B. Tinker, and M.G. Turner. 2009. Modeling the effects of fire and climate change on carbon and nitrogen storage in lodgepole pine (*Pinus contorta*) stands. Global Change Biology 15:535-548.
- Stephens, S.L., J.K. Agee, P.Z. Fulé, M.P. North, W.H. Romme, T.W. Swetnam, and M.G. Turner. 2013. Managing forests and fire in changing climates. Science. 342(6154):41-42.
- Stephenson, N.L. 1998. Actual evapotranspiration and deficit: biologically meaningful correlates of vegetation distribution across spatial scales. Journal of Biogeography 25: 855-870.
- Thornthwaite, C.W. 1948. An approach towards a rational classification of climate. Geographical Review 38: 55-102.

- Thornthwaite, C.W., and Mather, J.R. 1955. The water balance. Publications in Climatology 8.
- Tombak, D.F., A.J. Andries, K.S. Carsey, M.L. Powell, and S. Mellmann-Brown. 2001. Delayed seed germination in whitebark pine and regeneration patterns following the Yellowstone fire. *Ecology* 82(9):2587-2600.
- Ucitel, D., D.P. Christian, and J.M. Graham. 2003. Vole use of coarse woody debris and implications for habitat and fuel management. *The Journal of Wildlife Management* 67: 165-72.
- USDI, B.L.M. 2020. Wildland Fire Management Information. National Interagency Fire Center, Boise, ID. <https://wfmi.nifc.gov/cgi/WfmiHome.cgi>
- Van Wagtendonk, J.W., and P.E. Moore. 2010. Fuel deposition rates of montane and subalpine conifers in the central Sierra Nevada, California, USA. *Forest Ecology and Management* 259: 2122–2132.
- Weiss, A.D. 2000. A GIS algorithm for topographic position index. Poster presentation, ESRI Users Conference. San Diego, California, USA. poster online <http://www.jennessent.com/arcview/tpi.htm>
- Zevenbergen, L.W., and C.R. Thorne. 1987. Quantitative analysis of land surface topography. *Earth Surface Processes and Landforms* 12: 47-56.

Chapter 3. Fire-climate interactions: local controls and management implications for moist and dry conifer forests of the Pacific Northwest

3.1 Abstract

I used my research from Chapters 1 and 2 to inform a broader investigation of the influence of bottom-up controls on fire across the forests of the Pacific Northwest, with particular focus on late-successional stands on federal lands. There has been a significant increase in fire activity in the western United States over the past two decades, attributed to climate change, but much of the data that support this attribution is from fires in frequent, low-severity fire regimes. Recent increases in fires with mixed- and high-severity fire regimes of the Pacific Northwest have highlighted the importance of understanding local controls on fire-climate interactions in less frequent fire regimes. I looked at the influence of fuels and topography as bottom-up controls on fire frequency across the continuum of moist, high-severity fire regimes to dry, low-severity fire regimes from the west side of the Olympic Mountains to the east side of the North and Central Cascades. Using this examination of bottom-up controls, I identify and describe a “fuel management continuum” based on retaining fuel moisture in west-side forests through tactical suppression, and limiting fuel loading in dry, east-side forests through well-tested fuels treatment strategies. In mixed-severity forests between these two extremes, there are more opportunities to utilize managed wildfire. Fuel treatments on the west side, outside of the wildland-urban-interface, are ill-advised because they would increase fuel aridity rather than preserve fuel moisture. Although none of the strategies (suppression, managed wildfire, and fuel reduction treatments) are new, the rationale behind when to use them is based on ecologically informed relationships between top-down and bottom-up controls.

3.2 Introduction

Wildfire area burned (WFAB) has increased and will continue to increase throughout the western U.S. due to climate change (McKenzie et al. 2004; Littell et al. 2009, 2018), although the distribution, effects, and implications of this increase depend upon fire-regime characteristics and local controls on fire behavior. Most of the increase in WFAB has been in large fires outside of the maritime Pacific Northwest, although several recent mixed- and high-severity fires in late-successional stands on the west side of the Cascade Range (hereafter “Cascades”) have alerted researchers and managers of the need to project the effects of more frequent fires in higher severity fire regimes and to infer implications for management (e.g., Halofsky et al. 2018a, 2018b; Halofsky et al. 2020; Case et al. 2021; Gaines et al. 2022). An inherently different approach to management from that for low-severity fire regimes may be best. Optimizing the suitability of management in different fire regimes requires understanding the influence of bottom-up controls (e.g., fuels, topography) on fire frequency, severity, and spatial pattern and the interactions between these and top-down controls (e.g., temperature, precipitation) for different fire regimes (Hanan et al. 2021, Kennedy et al. 2021).

In this chapter, I examine the idea of a continuum of aridity as quantified in various metrics (e.g., water-balance deficit) and representing the combined effects of temperature and precipitation on variables, such as fuel moisture, that are directly associated with fire (Stephenson 1998, McKenzie and Littell 2017, Hanan et al. 2021). I use this aridity continuum to inform fire management strategies with respect to fire regimes across the Pacific Northwest.

I focus especially on fire management strategies to protect wilderness character on federally protected lands, given the increased risk to late-successional forests with climate change (Halofsky et al. 2018a). Old-growth forests of the Pacific Northwest have been degraded

extensively due to clear-cut logging and development during the mid- to late-20th century (Reilly and Spies 2015, Gaines et al. 2022) increasing the importance of maintaining late-successional habitat for old-growth dependent species (e.g., northern spotted owl (*Strix occidentalis caurina*), marbled murrelet (*Brachyramphus marmoratus*)) on federally protected lands.

3.3 Fire Regimes of the Pacific Northwest

3.3.1 *Moist and Dry Forests*

Forests and fire regimes of the Pacific Northwest are strongly influenced by the orographic effects of the North Cascade and Olympic Mountains, which create a precipitation gradient from west to east (McKenzie 2020). Mean annual precipitation decreases tenfold from west to east, from over 250 cm on the Olympic Peninsula to less than 25 cm in eastern Washington (Gedalof et al. 2005). Moist forest types (e.g., the extensive “Douglas-fir zone” dominated by Douglas-fir (*Pseudotsuga menziesii* var. *menziesii*), and the later-successional species western hemlock (*Tsuga heterophylla*) and western redcedar (*Thuja plicata*) occur on the west sides of the mountains, and drier forest types (e.g., Douglas-fir / ponderosa pine (*Pinus ponderosa*) mixed conifer forests) are located on the lee sides of the mountains, in the rain shadows. These forests and their fire regimes are commonly referred to as “west side” and “east side” respectively, although they are more accurately described as “moist” and “dry” because both types are found on either side of the Cascade Range, where the split between west and east side is commonly made (Franklin and Johnson 2012). The fire regimes grade from high severity on the moist, west side to low severity on the dry, east side (Figure 3-1).

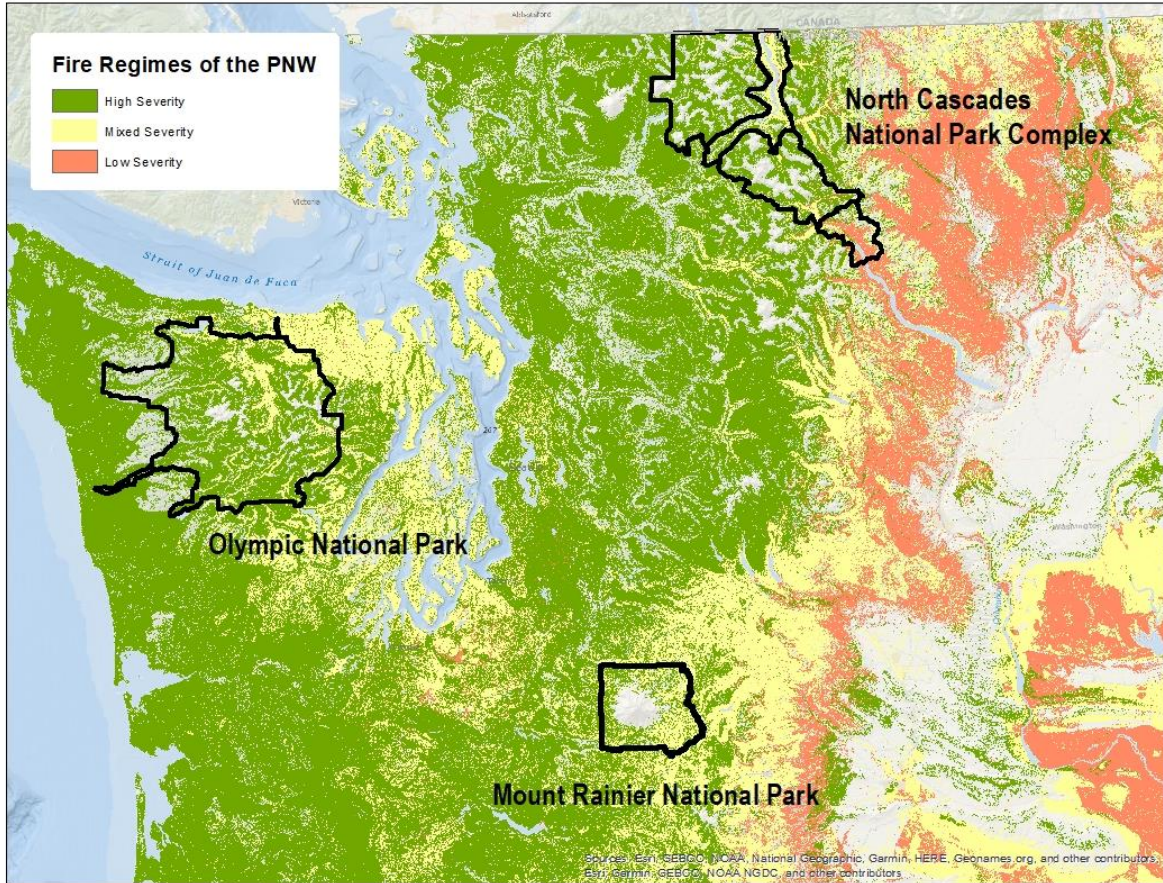


Figure 3-1. Map of fire regimes of the Olympic and Cascade Mountains in the Pacific Northwest with data from LANDFIRE (2022). Low frequency, high-severity fires (green) dominate moist forests on the west side of the Cascades. Mixed-severity fire occurs on east sides of mountains and further inland. High frequency, low-severity fire regimes occur on the eastern slopes of the Cascade Range.

The mild coastal climate on the west side of the Olympic Mountains makes their low-elevation coniferous forests the wettest in the United States, characterized by infrequent, high-severity fires (Franklin and Dyrness 1988), whereas drier forests, which have a mixed-severity fire regime, occur in the rain shadow to the northeast (Henderson et al. 2011, Halofsky et al. 2018a). Farther inland and south, moist coniferous forests with infrequent, large, high-severity fires are common on both sides of Mount Rainier, but subalpine forests and lower-elevation coniferous forests with more frequent, mixed-severity fires occupy the eastern flanks of the mountain (Hemstrom and Franklin 1982, Siderius and Murray 2005). Forests in the North

Cascades follow this same pattern, with moist forests with less frequent, stand-replacing fires in the maritime climate of the western Cascades and increasingly drier forests with more frequent, lower-severity fire to the east. Dry, mixed-conifer forests are on the east side of Ross Lake, still west of the Cascade Crest, but in the rain shadow of high mountains farther west: Mt. Baker (3286 m) and Mt. Shuksan (2783 m) (Agee et al. 1986). Low-elevation mixed-conifer forests on the east side of the Cascade crest, where I conducted the fire history study for Stehekin in Lake Chelan National Recreation Area (Chapter 1), have more frequent and lower mixed-severity fire than at Ross Lake. Even farther east, in the Okanogan highlands, frequent, low-severity fires were common historically (Wright and Agee 2004, Hessl et al. 2004). This area has recently experienced the largest fires in the state of Washington (e.g., 2015 Okanogan Complex, 123,341 ha).

3.3.2 *High-Severity Fire Regimes*

Moist forests in the Pacific Northwest have high-severity fire regimes. In late-successional forests on the west side of the Cascades, fuel loads are typically high due to the predominance of dense, multi-storied stands of mature conifers and long fire-free intervals (e.g., mean fire interval (MFI) of 465 years at Mount Rainier National Park (Hemstrom and Franklin 1982) during which fuels accumulate. These heavy fuels are typically damp and shaded throughout the summer in this maritime climate, and prone to combustion only during extreme and uncommon weather events (high winds and long, hot, and dry periods (Hemstrom and Franklin 1982, Agee and Huff 1987, Franklin and Dyrness 1988, Agee 1993). Therefore, moist forests with high-severity fire regimes are considered “climate limited,” or “flammability limited” (Littell et al. 2009, 2018; McKenzie 2020, chapter 6 therein). When fuel moisture is

low (e.g., drought), and ignition sources (e.g., lightning) are available, then these abundant, continuous fuel loads can affect large, stand-replacing fires (Littell et al. 2009, McKenzie and Littell 2017). The Yacolt fire (1902) in southwestern Washington and the Tillamook fire (1933) in coastal Oregon were high-severity fires that rapidly burned hundreds of thousands of hectares, exemplifying the potential for large fires in moist, west-side forests (Pyne 1982, Gray and Franklin 1997, Franklin and Halpern 2000).

High-severity fires are “stand replacing” because they kill the trees, but in most cases the trees die because they are not fire-adapted species (with exceptions; Douglas-fir is relatively fire resistant), rather than due to the intensity of the fire (Agee 1993). Even low-intensity fire can kill the trees, which then remain standing for years to decades, increasing the potential for multiple reburns, which are historically common in high-severity fire regimes (Agee 1993, Gray and Franklin 1997).

More commonly, fires are very small in moist forests with high-severity fire regimes due to high fuel moisture content. For example, at Mount Rainier National Park, there were 57 fires in 20 years (< 3 fires per year) between 2000 and 2019, with an average fire size of 1 hectare (USDI 2020). Fire size ranged from 0.05 to 23 hectares, with only three fires (5%) greater than 5 hectares (Figure 3-2). However, there have been a few exceptions to this elsewhere in recent years. For example, the 2015 Goodell Fire at North Cascades National Park was 2837 ha, the 2015 Paradise Fire at Olympic National Park was 1141 ha, and the 2018 Cougar Creek fire burned over 16,600 hectares in the Mount Baker-Snoqualmie National Forest near Mount Rainier.

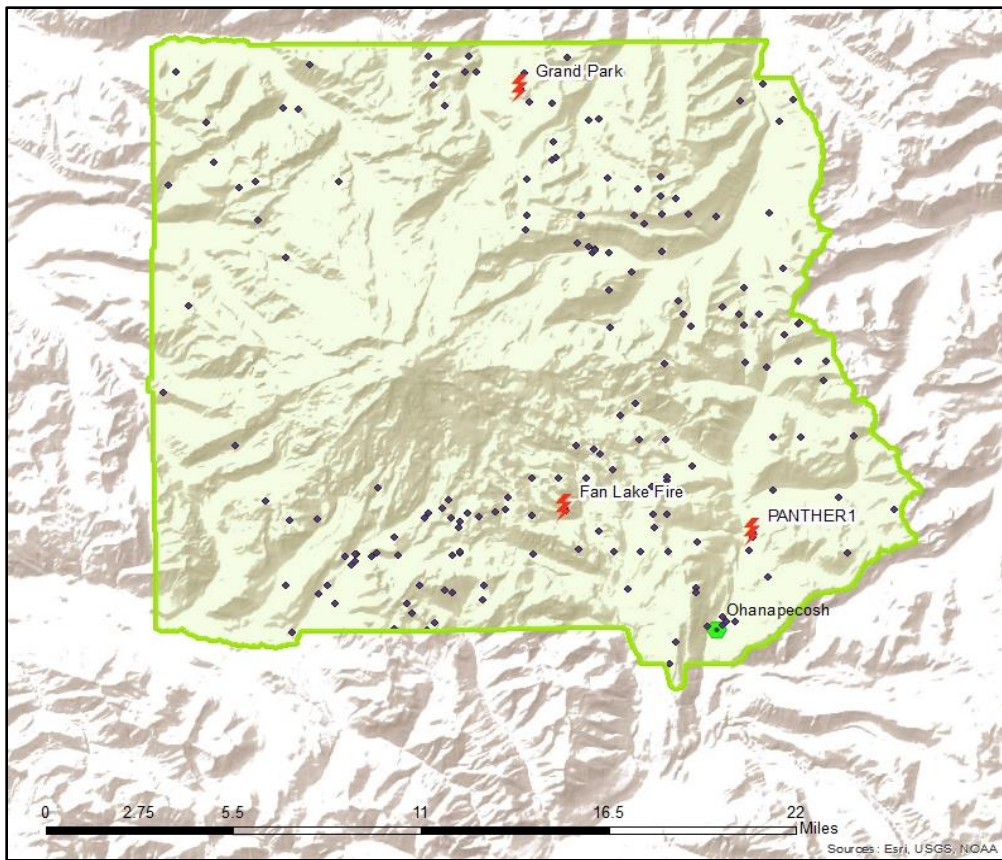


Figure 3-2. Fire frequency across Mount Rainier National Park, 2000–2019. Three fires marked with lightning bolts are over 5 ha: Panther1(2003) = 23 ha, Fan Lake (2018) = 8 ha, Grand Park (2009) = 8 ha. All other fires were <0.5 ha.

3.3.3 Mixed- and Low-Severity Fire Regimes

Forests and fire regimes become increasingly drier in an eastward direction, grading from “high mixed severity” west of the Cascades to “low mixed severity” on the western slopes east of the Cascades. As described earlier, this gradation from higher to lower severity is interrupted by more abrupt transitions from moist, high-severity forests to drier and lower-severity vegetation assemblages on the leeward sides of the mountain peaks. Dry mixed-conifer forests on the western slopes east of the Cascade crest are dominated by a mix of Douglas-fir and ponderosa pine, the ratio of which becomes increasingly more dominated by ponderosa pine to the east. This is the transition from the low mixed-severity regime to the low-severity fire regime where

historically frequent fires consumed mostly surface fuels, thus maintaining open, park-like stands of ponderosa pine in most locations (Weaver 1959, Pyne 1982, Agee 1993).

In mixed-severity regimes, post-fire levels of canopy mortality range from 30 to 80 percent (Agee 1993), with closer to 80% latent mortality in high mixed-severity stands, compared to as low as 20% in low mixed-severity stands. Canopy mortality is, by definition, less than 30% in low-severity fire regimes (Agee 1993). Mean fire intervals (MFIs) also shorten from 250+ years on the west side of North Cascades National Park (Agee et al. 1986, Prichard 2003) to ~30 years in Stehekin, as shown in Chapter 1. MFIs of low-severity fire regimes of the eastern Cascades were as low as 6 years (Everett et al. 2000, Wright and Agee 2004,).

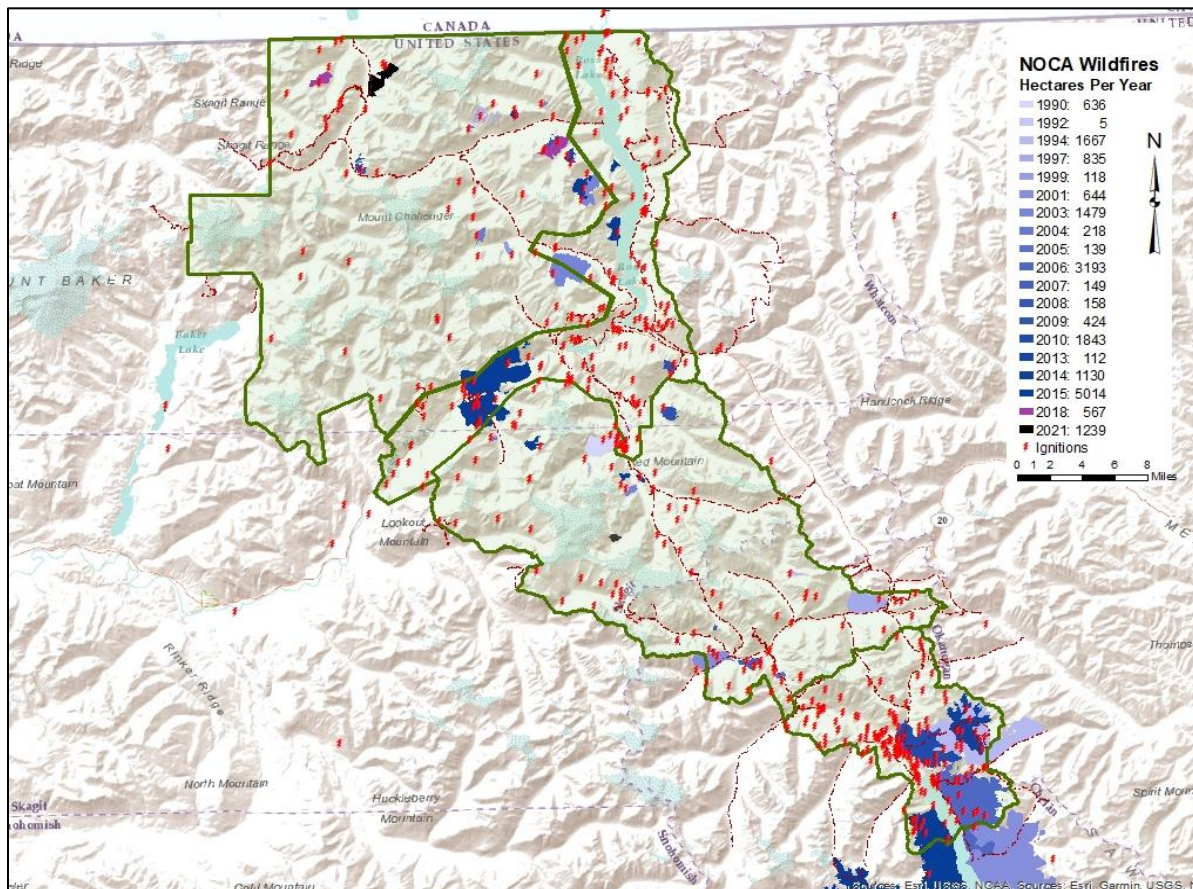


Figure 3-3. 32-year fire history in North Cascades National Park Service Complex (1990–2021). 447 ignitions (red lightning bolts) average 14 fires per year. Fifty fires were larger than 5 hectares.

As with the other fire characteristics, the historical range of fire sizes across mixed- and low-severity fire regimes varied from tens to thousands of hectares, with more frequent large fires occurring in the east. The distribution of fires across North Cascades National Park Service Complex for the past 32 years illustrates this range, with primarily smaller, more severe fires in high mixed-severity forests, and larger, less severe fires on the east side of the Complex (Figure 3-3).

3.4 Top-down and Bottom-up Controls

Climate acts as a broad scale “top-down” control on fires, whereas fuels, topography, and ignition sources are “bottom-up” controls, exerting local and mid-scale effects on fire size and frequency (Heyerdahl et al. 2001, Kellogg et al. 2008, McKenzie et al. 2011). Forest fuels exert bottom-up control by providing potential energy for combustion at fine scales, varying according to their volume, spatial distribution, and vegetation composition (McKenzie et al. 2011).

Topography acts as a direct and indirect control on fire. Directly, topography influences fire behavior (e.g., rate of spread, flame lengths) on slopes, and as a barrier to fire spread (e.g., scree slopes, cliffs) (Dillon et al. 2011). Indirectly, topography acts as a mid-scale (and multi-scale) control because it links the fine-scale variation of fuels to the coarser scale influence of climate, via contrasting microclimates associated with slope and aspect (Kellogg et al. 2008). For example, climate heats and dries fuels differently on south-facing versus north-facing aspects. The degree to which a fire regime is controlled by top-down or bottom-up controls depends on the interplay among the individual controls at different scales (climate, fuels, topography) (McKenzie et al. 2011). For example, topographic complexity acts as a global constraint on fire spread in low-severity fire regimes wherein simpler topography leaves climate “unrestricted” as

a top-down control (McKenzie and Kennedy 2012).

3.4.1 *Top-down Control: Climate in the Pacific Northwest*

Temperatures in the Pacific Northwest have increased by 0.9°C over the past century (1925–2016) (Vose et al 2017) and are expected to increase by 1.7°C to 4.7°C west of the Cascades, and 2.0°C to 5.8°C on the east side of the Cascades, by 2099 (Rogers and Mauger 2021). Changes in precipitation vary from increasing to decreasing depending on location, season and modeling scenario, but models project a decrease in summer precipitation by as much as 30% by 2099 (Walsh et al. 2014).

Climate exerts strong top-down control of fire throughout the western U.S., including the Pacific Northwest, in which it influences WFAB at decadal scales (Hessl et al. 2004) and at finer, annual and interannual scales related to both current and antecedent drought (Gedalof et al. 2005). Atmospheric masses arise from the Pacific Ocean and move eastward where they interact with the mountainous terrain of the Cascades and the Rocky Mountains, getting progressively warmer and drier as they move inland. This general pattern can be interrupted by a high-pressure system (blocking ridge) that diverts moisture from the coast, sometimes creating anomalous easterly “foehn” winds that move warm and dry air from the interior to the coast (Gedalof et al. 2005). These winds are often associated with severe storms that precipitate large, high-severity fires in west-side forests (Agee 1993).

The climate variables that are the strongest predictors of WFAB for moist, west-side forests differ from those of dry, east-side forests. On the west side of the Cascades, WFAB is strongly negatively correlated with growing season (May–September) precipitation in the year of fire, although it is also correlated with antecedent climate: 1-year lagged high winter

precipitation and low winter temperature (increased snowpack), and 2-year lagged high winter precipitation and low summer precipitation (Littell et al. 2009, 2018). WFAB on the east side of the Cascades, estimated in models of the Northern Rocky Mountain ecoprovince, is correlated to summer drought preceded by high winter temperatures (presumably increasing fuel biomass), and by 1-year lagged low precipitation and low temperature (Littell et al. 2009, 2018).

3.4.2 *Bottom-up Controls: Fuels and Topography*

Fuels act as bottom-up controls differently for moist and dry forests (Littell et al. 2018, Hanan et al. 2021). The distribution and abundance of fuels exert strong bottom-up control on fire size and frequency in fuel-limited ecosystems, such as in dry, mixed-conifer forests with frequent, low- and mixed-severity fire regimes on the east side of the Cascades (McKenzie et al. 2006, Kellogg et al. 2008, Littell et al. 2018). Conversely, fuel moisture, rather than fuel loading, acts as the primary bottom-up control on west-side, climate-limited forests that contain high volumes of dead and downed fuels, but where fuel moistures are generally too high for fire to spread (Littell et al. 2009, Littell et al. 2018, Hanan et al. 2021). We observe an “aridity continuum” in climate drivers of fire as fire regimes change from climate-limited to fuel-limited systems (Krawchuk and Moritz 2011, Hanan et al. 2021).

3.4.3 *Bottom-up Control: Fuel Moisture in High-Severity Fire Regimes*

Fuel moisture is a powerful bottom-up control on fire behavior in moist forests of the Pacific Northwest (Littell et al. 2009, 2018; Ren et al. 2022), as illustrated in the map of recent fires across Mount Rainier National Park (Figure 2). All fires are small, presumably due to the high moisture content of the fuels inhibiting fire spread. The disproportionately higher density

of ignitions on the drier east side of Mount Rainier is also related to fuel moisture, in addition to increased convective activity and lightning, because lower fuel moistures provide a more conducive environment for “positive strikes.”

In the process of mapping fuels at Mount Rainier (Chapter 2), I considered how fuel moisture is controlled by topography, elevation, vegetation structure, and fuel type in mountainous terrain. Fuel type (in particular, size classes of dead fuels, or “time-lag” class) is the only direct quantitative link between fuels and climate, whereas there are multiple ways in which the other variables act as intermediary mid-scale controls on fuel moisture. For example, mountains are topographic features that interact with climate, creating a precipitation gradient that influences fuel (vegetation) and soil moisture. Topography also influences vegetation structure by affecting where plants can grow, which in turn exerts influence on fuel type.

The diameter of the fuel exerts a strong influence on fuel moisture. Due to their smaller size, small woody fuels (SW; 0.6 - 7.5 cm) rapidly lose their moisture content when relative humidity is low and VPD is high, becoming active carriers of fire spread. In contrast, large woody fuels (LW; ≥ 7.6 cm) take over 1000 hours (42 days) of consistent weather conditions to gain equilibrium with their environment. Although LW are not the primary carriers of fire, large accumulations of moist fuels can dampen fire spread. Although organic fuels (ORG; litter and duff), are finer than SW, they also may take longer to dry out because they are tightly packed and retain moisture from the soil. This is particularly true of deeper duff layers, which are most affected by soil moisture, whereas upper litter layers are more sensitive to atmospheric moisture (Zhao et al. 2021).

Forest structure is another important control on fuel moisture. Forests with more open structures (less canopy density) dry out more quickly due to higher solar radiation and wind,

whereas shaded fuels from dense multistory canopies hold fuel moisture longer (Agee et al. 2000, Cochrane 2003). It is also probable that shorter forest types will dry out more quickly than taller forests with comparable stand densities because they have less canopy biomass to retain moisture by stabilizing microclimate.

3.4.4 Bottom-up Control: Fuel loading in Low-Severity Fire Regimes

Dry east-side forests with mixed- and low-severity fire regimes are fuel limited rather than climate limited (Littell et al. 2009, 2018; Hanan et al. 2021). The climate on the east side of the Cascades is arid and conducive to lightning and frequent fires that maintain low volumes of surface fuels, making both the distribution and abundance of fuels limiting factors in fire size and frequency (McKenzie et al. 2006). My research (Chapter 1) confirmed the significant lengthening of the mean fire interval in the forests of Stehekin during the fire suppression era. Clearly, the buildup of surface fuels due to fire suppression has altered fire-climate interactions in dry forests in several ways. Fuels are no longer limiting factors on fire frequency or severity in fire-suppressed stands because fuel loadings are uniformly high and continuous, and no longer vary along topographic or aridity gradients.

3.4.5 Bottom-up (but Multi-scale) Control: Topography

Topography controls fire frequency and fire size in dry, east-side forests by constraining and facilitating fire spread and by influencing the distribution of fuels (Kellogg et al. 2008, Dillon et al. 2011, McKenzie and Kennedy 2012). The orientation of topography to prevailing winds can enhance or limit fire spread in various ways. For example, intermediate uphill slopes perpendicular to wind direction can accelerate fire spread, whereas steeper slopes would impede

it. When slopes are parallel to wind direction, longer “fetches” are possible, often increasing fire size when fire spread has no topographic barriers. Spatial distribution and abundance of fuels are controlled by soil moisture that varies with both aspect and slope.

Metrics of topographic complexity can integrate the effects of individual elements such as the orientation with respect to wind. In general, increasing topographic complexity limits climatic controls on fire spread and the ensuing fire sizes (Kennedy and McKenzie 2010, McKenzie and Kennedy 2012). In my fire history research in Stehekin (Chapter 1), although I did not focus on fuel loadings, I was able to infer that topographic complexity was a significant determinant of fire frequency, evidently by limiting fire spread.

3.5 Effects of Climate Change in Moist and Dry Forests

I expect (i.e., global and regional models project) that in the next few decades, maritime influences will buffer the ecosystems of the Pacific Northwest somewhat against the severe effects of a warming climate, in contrast to the American Southwest, for which area burned is expected to increase greatly (McKenzie 2020). Presently, moist west-side ecosystems experience large stand-replacing fires when infrequent, hot, dry weather occurs, suggesting that if there is more hot, dry weather, that there will be more frequent, higher severity fires (Littell 2009, 2018). However, projections of extreme events are much more uncertain than those of global averages. Given that severe west-side fires are associated strongly with those extremes (Gedalof et al. 2005), the following must be considered contingent on the relative importance of extreme weather versus gradual warming and drying.

Greater changes in fire size and severity in moist, west-side forests than on the east side should be expected eventually when fuels in these climate-limited (flammability-limited) forests

become sufficiently dry, more often, to support fire spread. In the meantime, the even hotter and drier conditions on the east side are expected to exacerbate fire size and frequency. This will occur until these forests become more truly fuel limited, in which case we can expect that the lack of fuel (spatial) connectivity and the lower productivity of vegetation will limit fire sizes, and WFAB will decrease (Cansler and McKenzie 2014, McKenzie and Littell 2017, Kennedy et al. 2021).

3.6 Management Implications

The difference among controls on fire frequency for low-, mixed- and high-severity fire regimes suggests adapting fire management, in the face of climate change, with an ecologically informed view of the effects of practices on fire susceptibility, in both the short and long terms. Top-down and bottom-up controls on fire regimes lie on an “aridity continuum” from climate limited (west) to fuels limited (east), corresponding to fuel moisture and fuel loading, respectively. I suggest that there is a corresponding “fuels management continuum” across the fire regimes of the Pacific Northwest (Figure 3-4).

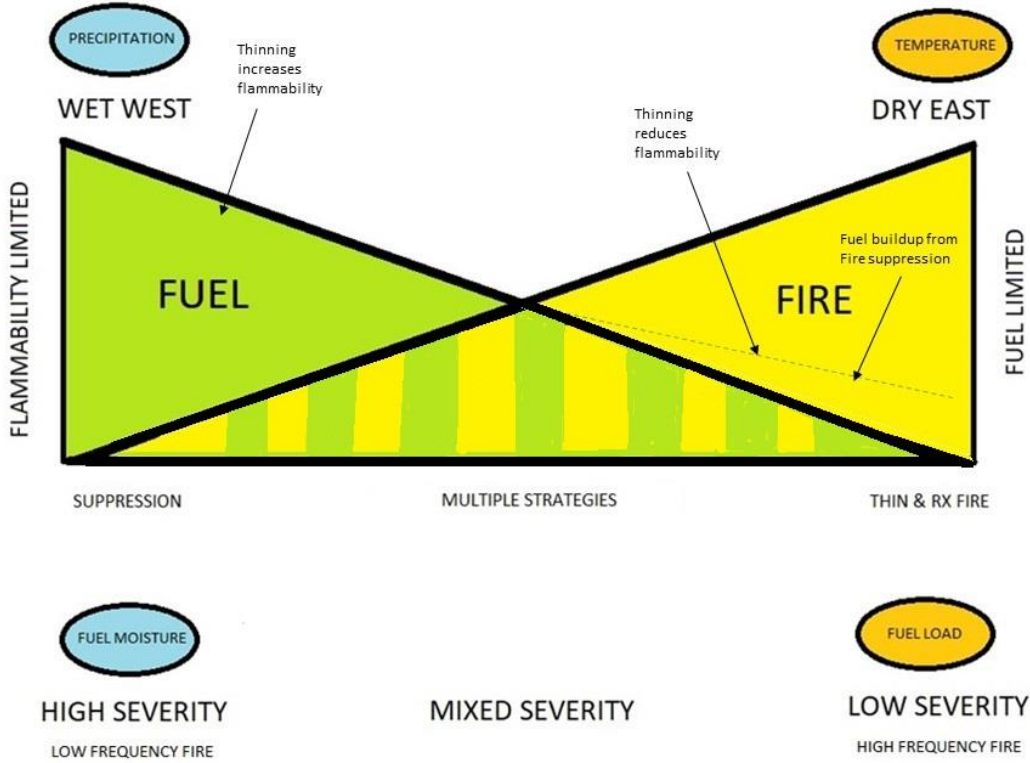


Figure 3-4. Diagram of the fuels management continuum: Moist forests on the west side of the Cascade Range of the Pacific Northwest are flammability limited due to high fuel moisture (bottom-up control) that limits fire spread. Fuel loads are highest in the west (green triangle) and lowest in the east (green and yellow striped triangle), and live and dead fuel moisture content is maintained by multistory shaded canopy fuels that hold moisture. Thinning of fuels on the west side increases flammability through evapotranspiration. In contrast, the east side of the Cascades is fuel limited, maintained by frequent, low-severity fire (yellow and yellow/green triangle = high/low frequency in east/west). Fire suppression led to fuel accumulation (dotted green line). Fuel reduction in the east reduces fire severity in fire-suppressed and climate-altered stands. Multiple strategies to maintain a spectrum of fuel moisture and loading are appropriate in mixed-severity forests that occur between east- and west-side forests.

On the far west (moist) end of the continuum, controlled by fuel moisture, fire size is limited by moist, dense forest and fuel conditions that are rarely conducive to large, high-severity fires, making them “flammability limited” (Littell et al. 2018). On the far east (dry) end, controlled by fuel loading, fire size is limited by sparse fuels where open, park-like stands predominate that were historically maintained by frequent low-severity fires, and hence they are “fuel limited.” Fuel reductions (treatments: thinning, burning, manual and mechanical fuel

reduction) are generally successful in maintaining low surface fuels on the dry, east side. In contrast, strategies to maintain moist, dense forests (e.g., reasoned fire exclusion; Halofsky et al. 2018b) may be appropriate to limit fire size in west-side forests. These contrasting strategies target the different bottom-up controls on fire frequency (fuel loading vs. fuel moisture) for east- and west-side forests and adjust for the other top-down controls: climate, which cannot be easily manipulated, and topography, which is unchanging. Given the extensive literature and general acceptance of fuel treatments for fire management in drier forests (Raymond and Peterson 2005, Prichard et al. 2010), I focus here on a contrasting approach for moist, late-successional forests, which accounts for the different controls and how they are influenced by stand structures. The key issue is maintaining high enough fuel moisture, rather than low enough fuel loading.

The wettest west-side forests (e.g., west side of Olympic National Park and Mount Rainier National Park, far west side in low-elevation Douglas-fir forests at North Cascades National Park) have the longest fire-return intervals between large stand-replacing fires, not only because the weather is not hot and dry enough, or that wind events are rare, but because the wettest forests have the steepest fuel-moisture limitations to overcome. Therefore, management strategies that focus on retaining live and dead fuel moisture content by protecting closed, shaded canopy conditions are critical to minimize ignition potential and fire spread. Thinning in these forests would not only compromise the ecology and habitat of late-successional forests (Agee 1993, Franklin and Johnson 2012, Gaines et al. 2022) but also increase flammability. This suggests that “reasoned fire exclusion” (Halofsky et al. 2018b), the management decision to suppress wildfires where risks outweigh benefits, is the best strategy to minimize fire potential in the wettest, west-side forests. Not only does reasoned fire exclusion forestall the effects of

climate change (Halofsky et al. 2018a), which are uncertain, but it also minimizes fire size, maintaining a greater proportion of intact canopy to retain fuel moisture.

Moist forests with the canopy structures described earlier in the chapter as holding moisture longest (e.g., tall, closed, multistory canopies), retain moisture in the canopy and understory forest, and also retain moisture in the surface fuel and organic horizons. Thus, these canopy structures, when paired with abundant large (1000-hour) woody fuels, which have the greatest moisture holding capacity, will be especially fire resistant. Forests with deep organic horizons will also be less prone to surface fire due to their capacity to hold moisture from the soil as well as from the canopy (Zhao et al. 2021). Hanan et al. (2021) suggest using soil moisture data layers as a tool to interpret where soil moisture content is greatest, and thus where fire spread potential is lowest.

Understanding which areas have the greatest moisture-holding capacity is helpful in weighing the risks and benefits of managing a wildland fire for resource benefit now or suppressing it when it may burn a larger area later at higher severity. Management fires for resource benefit are a good strategy for fires at locations farther east and with moderate fire potentials along the fuels management continuum. Because drier mixed-severity sites are more likely to experience more frequent and larger fires sooner than moist forests farther west, suppression is a less desirable option.

In mixed-severity forests that occur between the two extremes of east and west, representing almost purely fuel-limited versus flammability-limited forests, a broader range of fire management strategies (e.g., managed wildland fires) may apply. For example, within the mixed-severity regime, where fuel loading and fuel moisture are both important factors, smaller wildfires that enhance the mosaic of burned areas will maintain higher structural diversity and

minimize future fire growth. Re-igniting previously suppressed fires is another strategy for increasing burned footprints within the mixed-severity fire regime that could be particularly useful in large wilderness areas (NPS 2010). Fires that started early in the season and were suppressed due to safety concerns or lack of fire personnel to manage them during a busy fire season, can be reignited in late summer or early fall to burn a smaller footprint, the boundaries of which are created by the topography, fuel moisture, and fuel loadings of the site.

Some landscapes may require heterogeneous strategies, depending on not only the importance of fuel moisture versus fuel loading, but also multiple factors such as essential wildlife habitat, vulnerability to severe fire because of topography, or risk to homes or other structures. For example, in the mixed-severity fire regimes of the Stehekin watershed (Chapter 1), which includes forest stands both near the town and in inaccessible wilderness terrain, different management is applied, including wildland fire use in the wilderness away from town, thinning and prescribed burning in fuel-reduction treatment areas adjacent to the community, and immediate suppression within the wildland-urban interface. All these tactics can be informed by an understanding of the contrasting roles of fuel moisture and fuel loading that I have discussed here, and of their relative importance in different microclimates and topography.

3.7 Conclusions

Several researchers have suggested that the fuel treatments that are effective in dry forests are not appropriate for west-side forests in the Northwest (Halofsky et al. 2018b, Gaines et al. 2022). I agree with their reasoning that fuel treatments would create ecosystem changes that have no precedent, and I come to the same solution (reasoned suppression in the moist forests) but via a different conceptual pathway. My recommendations are based on the essential

differences between the drivers of fuel-limited versus flammability-limited systems. We cannot expect west-side forests to be affected by increases in temperature in the same way as low-severity fire regimes in east-side forests, because west- and east-side forests have different drivers and thresholds. We also cannot expect to manage them in the same way across different fire regimes.

3.8 References

- Abatzoglou, J.T., and A.P. Williams. 2016. Impact of anthropogenic climate change on wildfire across western US forests. *Proceedings of the National Academy of Sciences, USA* 113(32):11770-11775.
- Agee, J.K. 1993. *Fire Ecology of Pacific Northwest Forests*. Island Press, Washington, D.C.
- Agee, J.K., B. Bahro, M.A. Finney, P.N. Omi, D.B. Sapsis, C.N. Skinner, J.W. van Wagtendonk, C.P. Weatherspoon. 2000. The use of shaded fuelbreaks in landscape fire management. *Forest Ecology and Management* 127:55-66.
- Agee, J.K., M. Finney, and R. de Gouvenain. 1986. The fire history of Desolation Peak: A portion of the Ross Lake National Recreation Area., National Park Service Cooperative Park Studies Unit, College of Forest Resources, University of Washington, Seattle, WA.
- Agee, J.K. and M.H. Huff. 1987. Fuel succession in a western hemlock / Douglas-fir forest. *Canadian Journal of Forest Research* 17(7):697-704.
- Cansler, C.A., and D. McKenzie. 2014. Climate, fire size, and biophysical setting control fire severity and spatial pattern in the northern Cascade Range, USA. *Ecological Applications* 24:1037-1056.
- Case, M.J., B.G. Johnson, K.J. Bartowitz, and T.W. Hudiburg. 2021. Forests of the future: Climate change impacts and implications for carbon storage in the Pacific Northwest, USA. *Forest Ecology and Management* 482:118886 16 pp.
- Cochrane, M.A. 2003. Fire science for rainforests. *Nature* 421:913-919.
- Dillon, G.K., Z.A. Holden, P. Morgan, M.A. Crimmins, E.K. Heyerdahl, and C.H. Luce. 2011. Both topography and climate affected forest and woodland burn severity in two regions of the western US, 1984 to 2006. *Ecosphere* 2(12):130 33 pp.

Everett, R.L., R. Schellhaas, D. Keenum, D. Spurbeck, and P. Ohlson. 2000. Fire history in the ponderosa pine/Douglas-fir forests on the east slope of the Washington Cascades. *Forest Ecology and Management* 129:207-225.

Franklin, J.F., and C.T. Dyrness. 1988. Natural Vegetation of Oregon and Washington. Oregon State University Press. 452 pp.

Franklin, J.F. and C.B. Halpern. 2000. Pacific northwest forests, in Barbour, *eds.* M.G. and W.D. Billings. North American Terrestrial Vegetation Second Edition. Cambridge University Press. pp. 161-202.

Franklin, J.F. and K.N. Johnson. 2012. A restoration framework for federal forests in the Pacific Northwest. *Journal of Forestry* 110(8):429-439.

Gaines, W.L., P.F. Hessburg, G.H. Aplet, P. Henson, S.J. Prichard, D.J. Churchill, G.M. Jones, D.J. Isaak, and C. Vynne. 2022. Climate change and forest management on federal lands in the Pacific Northwest, USA: Managing for dynamic landscapes. *Forest Ecology and Management* 504:119794 21 pp.

Gedalof, Z., D.L. Peterson, and N.J. Mantua. 2005. Atmospheric, climatic, and ecological controls on extreme wildfire years in the Northwestern United States. *Ecological Applications* 15(1):154-174.

Gedalof, Z. 2011. Climate and spatial patterns of wildfire in North America. In *eds.* McKenzie, D., C. Miller, and D.A. Falk. *The Landscape Ecology of Fire*, Springer, Dordrecht, The Netherlands. pp. 89-116.

Gray, A.N. and J.F. Franklin. 1997. Effects of multiple fires on the structure of southwestern Washington forests. *Northwest Science* 71(3):174-185.

Halofsky, J.E., D.L. Peterson, and B.J. Harvey. 2020. Changing wildfire, changing forests: the effects of climate change on fire regimes and vegetation in the Pacific Northwest, USA. *Fire Ecology* 16(4):1-26.

Halofsky, J.S., D.R. Cronklin, D.C. Donato, J.E. Halofsky, and J.B. Kim. 2018a. Climate change, wildfire, and vegetation shifts in a high-inertia forest landscape: Western Washington, U.S.A. *PLoS ONE* 13(12):e0209490.
<https://doi.org/10.1371/journal.pone.0209490>

Halofsky, J.S., D.C. Donato, J.F. Franklin, J.E. Halofsky, S.L. Peterson, and B.J. Harvey. 2018b. The nature of the beast: examining climate adaptation options in forests with stand-replacing fire regimes. *Ecosphere* 9(3): e02140.10.1002/ecs2.2140.

Hanan, E.J. J. Ren, C.L. Tague, C.A. Kolden, J.T. Abatzoglou, R.R. Bart, M.C. Kennedy, M. Liu, and J.C. Adam. 2021. How climate change and fire exclusion drive wildfire regimes at actionable scales. *Environmental Research Letters* 16. 14 pp.

- Hemstrom, M.A., and J.F. Franklin. 1982. Fire and other disturbances of the forests in Mount Rainier National Park. *Quaternary Research* 18(1): 32-51.
- Henderson, J.A., R.D. Lesher, D.H. Peter, and C.D. Ringo. A landscape model for predicting potential natural vegetation of the Olympic Peninsula USA using boundary equations and newly developed environmental variables. Gen. Tech. Rep. PNW-GTR-841. Portland, OR: U.S. Department of Agriculture, Forest Service, Pacific Northwest Research Station. 35 p.
- Hessl, A.E., D. McKenzie, and R. Schellhaas. 2004. Drought and Pacific Decadal Oscillation linked to fire occurrence in the inland Pacific Northwest. *Ecological Applications* 14:425-442.
- Heyerdahl E.K., L.B. Brubaker, J.K. Agee. 2001. Spatial controls of historical fire regimes: a multiscale example from the interior West, USA. *Ecology* 82:660-678.
- Holsinger, L., S.A. Parks, and C. Miller. 2016. Weather, fuels, and topography impede wildland fire spread in western US landscapes. *Forest Ecology and Management*. 380:59-69.
- Kellogg, L-K.B, D. McKenzie, D.L. Peterson, and A.E. Hessl. 2008. Spatial models for inferring topographic controls on historical low-severity fire in the eastern Cascade Range of Washington, USA. *Landscape Ecology* 23:227-240.
- Kennedy, M.C., R.R. Bart, C.L. Tague, and J.S. Choate. 2021. Does hot and dry equal more wildfire? Contrasting short- and long-term climate effects on fire in the Sierra Nevada, CA. *Ecosphere* 12(7):e03657.10.1002/ec2.3657 19 pp.
- LANDFIRE 2022. Historical fire regime and vegetation departure. Accessed 3/11/2022.
<https://landfire.gov/fireregime.php>
- Krawchuk, M.A. and M.A. Moritz. 2011. Constraints on global fire activity vary across a resource gradient. *Ecology* 92:121-132.
- Littell, J.S., D. McKenzie, D.L. Peterson, and A.L. Westerling. 2009. Climate and wildfire area burned in western U.S. ecoprovinces, 1916-2003. *Ecological Applications* 19(4):1003-1021.
- Littell, J.S., D. McKenzie, H.Y. Wan, and S.A. Cushman. 2018. Climate change and future wildfire in the western United States: An ecological approach to nonstationarity. *Earth's Future* 6:1097-1111. <https://doi.org/10.1029/2018EF000878>
- McKenzie, D. 2020. Mountains in the Greenhouse: Climate change and the mountains of the Western U.S.A. Springer Nature, Switzerland AG.
- McKenzie, D., Z. Gedalof, D.L. Peterson, and P. Mote. 2004. Climatic change, wildfire, and conservation. *Conservation Biology* 18(4):890-902.
- McKenzie, D., A.E. Hessl, and L-K.B. Kellogg. 2006. Using neutral models to identify constraints on low-severity fire regimes. *Landscape Ecology* 21:139-152.

- McKenzie, D. and M.C. Kennedy. 2012. Power laws reveal phase transitions in landscape controls of fire regimes. *Nature Communications* 3:726 doi: 10.1038/ncomms1731.
- McKenzie, D. and J.S. Littell. 2017. Climate change and the eco-hydrology of fire: Will area burned increase in a warming western USA? *Ecological Applications* 27(1):26-36
- McKenzie, D., C. Miller, and D.A. Falk. 2011. Toward a theory of landscape fire. In *eds.* McKenzie, D., C. Miller, and D.A. Falk. *The Landscape Ecology of Fire*. Springer, Dordrecht, The Netherlands. Pp 3-25.
- Mote, P., A.K. Snover, S. Capalbo, S.D. Eigenbrode, P. Glick, J. Littell, R. Raymondi, and S. Reeder. 2014: Ch. 21: Northwest. *Climate Change Impacts in the United States: The Third National Climate Assessment*, J. M. Milillo, Terese (T.C.) Richmond, and G.W. Yohe, Eds., U.S. Global Change Research Program, 487-513.
- National Wildfire Coordinating Group. 2021. Fire behavior field reference guide, PMS 437. <https://www.nwcg.gov/publications/pms437>. created 2021-07-08, accessed 2022-01-19.
- N.P.S. 2010. North Cascades National Park Service Complex Wildland Fire Management Plan. North Cascades National Park, Sedro Wooley, WA.
- Prichard, S.J. 2003. Spatial and temporal dynamics of fire and vegetation change in Thunder Creek watershed, North Cascades National Park, Washington. Ph.D. dissertation. University of Washington, Seattle, WA.
- Prichard, S.J., D.L. Peterson, and K. Jacobson. 2010. Fuel treatments reduce the severity of wildfire effects in dry mixed conifer forest, Washington, USA. *Canadian Journal of Forest Research* 40:1615-1626.
- Prichard, S.J., A.G. Andreu, R.D. Ottmar, E. Eberhardt. 2019. Fuel Characteristic Classification System (FCCS) field sampling and fuelbed development guide. Gen. Tech. Rep. PNW-GTR-972. Portland, OR: U.S. Department of Agriculture, Forest Service, Pacific Northwest Research Station. 77 pp.
- Pyne, S.J. 1982. *Fire in America: A cultural history of wildland and rural fire*. Princeton, NJ: Princeton University Press.
- Raymond, C.L., and D.L. Peterson. 2005. Fuel treatments alter the effects of wildfire in a mixed-evergreen forest, Oregon, USA. *Canadian Journal of Forest Research* 35:2981-2995.
- Reilly, M.J., and T.A. Spies. 2015. Regional variation in stand structure and development in forests of Oregon, Washington, and inland Northern California. *Ecosphere* 6(10):1-27

- Ren, J., E.J. Hanan, J.T. Abatzoglou, C.A. Kolden, C.L. Tague, M.C. Kennedy, M. Liu, and J.C. Adam. 2022. Projecting future fire regimes in a semiarid watershed of the inland northwestern United States: Interactions among climate change, vegetation productivity, and fuel dynamics. *Earth's Future* 10.1029/2021EF002518. 23 pp.
- Rogers, M., and G.S. Mauger. 2021. Pacific Northwest Climate Projection Tool. University of Washington Climate Impacts Group. <https://cig.uw.edu/resources/analysis-tools/pacific-northwest-climate-projection-tool/>
- Sandberg, D.V., C.L. Riccardi, and M.D. Schaaf. 2007. Fire potential rating for wildland fuelbeds using the Fuel Characteristic Classification System. *Canadian Journal of Forest Research* 37:2456-2463.
- Siderius, J., and M.P. Murray. 2005. Fire knowledge for managing Cascadian Whitebark Pine ecosystems. National Park Service and Crater Lake National Park, Seattle, WA, USA. <https://irma.nps.gov/DataStore/DownloadFile/471518>
- Stephenson, N. 1998. Actual evapotranspiration and deficit: biologically meaningful correlates of vegetation distribution across spatial scales. *Journal of Biogeography* 25:855-870.
- Vose, R. S., D. R. Easterling, K. E. Kunkel, A. N. LeGrande, and M. F. Wehner, 2017: Temperature Changes in the United States. Climate Science Special Report: Fourth National Climate Assessment, Volume I. Wuebbles, D. J., D. W. Fahey, K. A. Hibbard, D. J. Dokken, B. C. Stewart, and T. K. Maycock, Eds., U.S. Global Change Research Program, Washington, DC, USA, 185–206. doi:[10.7930/J0N29V45](https://doi.org/10.7930/J0N29V45)
- Walsh, J., D. Wuebbles, K. Hayhoe, J. Kossin, K. Kunkel, G. Stephens, P. Thorne, R. Vose, M. Wehner, J. Willis, D. Anderson, S. Doney, R. Feely, P. Hennon, V. Kharin, T. Knutson, F. Landerer, T. Lenton, J. Kennedy, and R. Somerville, 2014. Chapter 2: Our Changing Climate, eds., J.M. Melillo, T. Richmond, and G.W. Yohe. Climate Change Impacts in the United States: The Third National Climate Assessment. U.S. Global Change Research Program 19-67.
- Weaver, H. 1959. Ecological changes in the ponderosa pine forest of the Warm Springs Indian Reservation in Oregon. *Journal of Forestry* 57:15-20.
- Wright, C.S., and J.K. Agee. 2004. Fire and vegetation history in the eastern Cascade Mountains, Washington. *Ecological Applications* 14:443-459.
- Zhao, L., M. Yebra, A. van Dijk, G.J. Cary, S. Matthews, and G. Sheridan. 2021. The influence of soil moisture on surface and sub-surface litter fuel moisture simulation at five Australian sites. *Agricultural and Forest Meteorology* 298:1-13.

Conclusions

This dissertation is an in-depth analysis of the characteristics associated with mixed- and high-severity fires regimes in the Pacific Northwest (PNW), with an emphasis on proposing strategies for management with respect to climate change. Chapter one provides the quantitative evidence for high-frequency fire in Stehekin, Lake Chelan National Recreation Area, and identifies the bottom-up controls (topography, species, location) influencing a long history of mixed-severity fire. Chapter two provides another detailed analysis; fuel loadings across the moist forests of Mount Rainier, characterized by a low frequency, high-severity fire regime. Chapter three links chapters one and two together as data points along the precipitation gradient from moist, west-side to dry, east-side forests across the PNW, and provides a corresponding fuels management continuum.

This work is a step towards preparing for more frequent and larger fires in the PNW, although there is still much to learn about how complex interactions between climate and fire regimes will manifest. The amount and seasonality of future precipitation in the PNW is still uncertain, as are the vegetation assemblages following more frequent fires in high- and mixed-severity fire regimes. It is critical that researchers and managers focus on collecting empirical data on future fires to increase our understanding of fire effects and post-fire regeneration, calibrate climate-fire models, and ultimately, fine-tune our management response. Most importantly, the results of future research must be conveyed to the managers that steward federal lands across the PNW. Our jobs are not complete until we make the critical link between research and management.

Appendix A: The values in italics are imputed from neighboring fuelbeds and the vegetation map (Nielsen et al. 2021). The fuel models are the 13 standard fire behavior fuel models (Albini 1976, Anderson 1982), included for reference.

Fuel Bed ID	Plot count	Structure	Relative Cover of Trees by Species	Fuel model
11	23	Woodland	50 ABLA, 25 ABAM, 25 TSME	8
12	4	Woodland	66 ABLA, 34 TSHE	2, 5, 8
13	0	Woodland	4 TSHE, 40 ABAM, 34 TSME, 22 ABLA	NA
21	16	Short partly closed forest	31 ABLA, 25 PSME, 19 TSHE, 12 TSME, 7 ABAM, 6 ABPR	8
22	3	Short partly closed forest	33 ABLA, 33 TSHE, 34 ABAM	8
23	2	Short partly closed forest	100 PSME	8
24	1	Short partly closed forest	100 TSME	NA
31	8	Short to mid-height multistory	50 ABLA, 25 TSHE, 13 ABAM, ACRU 12	9
32	5	Short to mid-height multistory	20 ABAM, 60 TSHE, 20 ABLA	8
33	7	Short to mid-height multistory	17 ABAM, 33 TSHE, 33 ABLA, 17 TSME	9
34	8	Short to mid-height multistory	25 PSME, 38 TSHE, 25 ABLA, 12 TSME	8
35	3	Short to mid-height multistory	34 PSME, 33 THPL, 33 ABLA	8
41	8	Mid-height partly closed forest	50 ABAM, 25 PSME, 25 TSME	8
42	14	Mid-height partly closed forest	21 ABLA, 7 PSME, 21 CHNO, 22 TSME, 7 ABAM, 7 PIEN, 15 TSHE	8
43	11	Mid-height partly closed forest	9 ALRU, 9 THPL, 18 CHNO, 18 TSHE, 18 ABAM, 18 PIEN, 10 TSME	7, 8, 9
44	6	Mid-height partly closed forest	33 ABAM, 33 ABLA, 17 ABPR, 17 PSME	8
45	1	Mid-height partly closed forest	100 TSME	6, 8
51	21	Tall multistory	25 TSHE, 12 ABLA, 6 ABPR, 20 ABGR, 25 ABAM, 6 ALRU, 6 TSME	8
52	2	Tall multistory	100 ABPR	9, 10
53	4	Tall multistory	50 TSHE, 50 TSME	6, 10, 11
54	0	Tall multistory	10 TSHE, 69 ABAM, 21 TSME	NA
55	1	Tall multistory	43 PSME, 50 ABAM, 2 TSME, 5 TSHE	10
61	12	Tall topstory	17 PSME, 42 TSHE, 17 THPL, 8 ABAM, 8 PIEN, 8 TSME	8
62	7	Tall topstory	43 PSME, 43 TSME, 14 ABPR	8
63	1	Tall topstory	100 ABAM	8
64	3	Tall topstory	34 ABLA, 33 TSME, 33 TSHE	8
70	40	Riparian	ABLA	2
80	46	Shrubs	NA	5
90	5	Meadow	NA	1

Fuel Bed ID	All Canopy Density			Emergent & Canopy Density			Subcanopy Density			Emergent Canopy Cover			Canopy Canopy Cover			Subcanopy Canopy Cover			Emergent Height (ft)		
	X	Min	Max	X	Min	Max	X	Min	Max	X	Min	Max	X	Min	Max	X	Min	Max	X	Min	Max
11	28	2	65	136	10	304	20	0	91	0	0	0	28	2	55	5	0	15	NA	NA	NA
12	41	2	100	186	20	273	28	0	111	0	0	0	41	2	85	9	0	35	NA	NA	NA
13	31	2	100	146	10	304	21	0	111	0	0	0	31	2	85	5	0	35	NA	NA	NA
21	60	10	100	275	61	769	112	0	455	4	0	30	44	10	75	12	0	35	74	74	74
22	58	40	85	223	50	253	68	0	182	NA	NA	NA	40	30	50	18	0	35	NA	NA	NA
23	95	70	100	23	20	70	34	0	100	NA	NA	NA	63	60	65	33	10	55	NA	NA	NA
24	60	40	80	111	80	130	51	30	70	NA	NA	NA	50	30	70	10	0	20	NA	NA	NA
31	71	40	100	139	20	233	93	10	243	5	0	15	49	40	80	17	0	60	165	136	187
32	99	50	100	270	40	435	304	30	891	9	0	20	74	45	95	22	5	65	128	119	137
33	57	27	100	121	20	192	93	0	192	3	0	15	39	0	80	15	0	25	122	122	122
34	77	35	100	226	132	324	78	0	162	3	0	21	63	35	95	12	0	25	184	184	184
35	50	35	75	111	71	152	7	0	10	NA	NA	NA	48	35	70	2	0	5	NA	NA	NA
41	60	30	100	155	111	182	25	0	51	NA	NA	NA	51	30	75	8	0	25	NA	NA	NA
42	62	20	100	156	111	243	84	0	405	7	0	50	47	20	80	8	0	25	104	104	104
43	71	10	100	168	121	253	51	0	142	2	0	10	60	10	85	9	0	20	134	115	153
44	51	22	75	116	111	121	26	10	51	0	0	0	43	20	60	7	2	15	NA	NA	NA
45	38	1	75	56	0	152	10	0	51	NA	NA	NA	28	0	55	11	1	20	NA	NA	NA
51	82	15	100	86	20	213	113	10	516	4	0	35	53	15	90	25	0	60	173	164	182
52	75	60	90	48	20	213	67	5	100	NA	NA	NA	43	40	45	33	20	45	NA	NA	NA
53	62	40	75	99	20	151	53	35	91	3	0	10	40	35	65	19	10	25	117	117	117
54	77	30	100	82	20	213	94	5	350	3	0	35	49	15	90	24	0	60	154	117	182
55	40	30	50	20	20	151	71	5	200	NA	NA	NA	20	15	25	20	15	25	NA	NA	NA
61	79	30	100	103	30	253	40	0	152	8	0	70	63	40	95	8	0	20	162	162	162
62	90	56	100	105	40	162	16	0	30	4	0	15	75	55	92	11	1	25	187	148	226
63	62	50	80	100	30	170	10	0	30	NA	NA	NA	60	50	80	2	0	10	NA	NA	NA
64	83	45	100	127	121	132	208	61	354	17	0	30	55	35	85	12	10	15	NA	NA	NA
70	65	0	100	123	0	294	111	0	850	2	0	30	51	0	90	12	0	45	167	126	201
80	1	0	9	2	0	40	1	0	30	0	0	0	0	0	9	0	0	5	NA	NA	NA
90	0	0	0	0	0	0	0	0	0	0	0	0	0	0	0	0	0	0	NA	NA	NA

Fuel Bed ID	Canopy Height (ft)			Subcanopy Height (ft)			Emergent Ht. Live Crown (ft)			Canopy Ht. Live Crown (ft)			Subcanopy Ht. Live Crown (ft)			Emergent DBH (in)			Canopy DBH (in)			
	X	Min	Max	X	Min	Max	X	Min	Max	X	Min	Max	X	Min	Max	X	Min	Max	X	Min	Max	
11	57	22	101	27	18	43	NA	NA	NA	10	0	30	4	1	8	NA	NA	NA	15	6	33	
12	73	65	82	32	5	64	NA	NA	NA	14	9	19	4	0	8	NA	NA	NA	17	14	20	
13	60	22	101	27	5	64	NA	NA	NA	10	0	30	4	0	8	NA	NA	NA	15	6	33	
21	62	35	98	30	18	39	35	35	35	17	3	35	13	2	23	33	14	47	13	6	24	
22	61	53	69	25	20	30	NA	NA	NA	23	18	29	6	0	10	NA	NA	NA	13	10	15	
23	91	80	120	26	5	79	NA	NA	NA	10	0	15	6	0	14	NA	NA	NA	17	11	23	
24	96	70	110	33	19	46	NA	NA	NA	23	0	33	11	4	18	NA	NA	NA	17	11	23	
31	88	45	122	31	15	55	57	37	74	38	31	48	14	4	24	47	34	59	16	6	25	
32	97	78	107	34	26	45	55	51	60	67	40	112	22	14	31	46	36	57	18	11	30	
33	88	46	129	28	23	37	49	49	49	41	27	54	15	9	24	44	36	49	17	9	25	
34	80	47	126	28	23	38	100	100	100	36	8	58	13	6	17	52	52	52	15	11	29	
35	118	73	176	19	5	25	NA	NA	NA	30	9	50	10	6	14	NA	NA	NA	35	17	58	
41	95	67	136	35	18	64	NA	NA	NA	35	20	54	13	6	18	NA	NA	NA	20	12	36	
42	87	36	112	33	20	46	26	26	26	41	3	64	16	1	26	43	24	55	18	9	30	
43	93	36	136	36	20	60	54	47	62	42	17	62	16	5	44	46	30	56	19	9	28	
44	91	79	104	37	27	44	NA	NA	NA	22	15	35	12	6	25	NA	NA	NA	19	15	21	
45	96	79	104	33	19	46	NA	NA	NA	23	15	35	11	4	18	NA	NA	NA	25	18	39	
51	119	59	181	47	21	76	83	51	114	50	16	118	19	3	35	46	39	57	25	7	56	
52	177	162	192	49	35	63	NA	NA	NA	59	44	74	13	10	16	NA	NA	NA	49	41	57	
53	93	87	103	34	27	49	63	51	80	45	35	56	22	10	34	48	39	57	24	18	39	
54	121	59	192	46	21	78	76	49	114	51	16	118	20	3	35	46	39	57	28	7	57	
55	128	87	192	78	27	86	NA	NA	NA	80	16	118	33	10	35	NA	NA	NA	76	41	80	
61	139	84	185	61	31	106	83	83	83	74	42	114	23	10	52	45	36	54	26	11	45	
62	114	55	149	45	33	55	56	12	101	74	49	107	30	23	39	60	47	77	24	15	32	
63	129	60	200	45	30	59	NA	NA	NA	58	28	100	7	0	39	NA	NA	NA	31	20	45	
64	147	80	200	26	10	79	NA	NA	NA	19	10	100	8	0	59	50	48	52	20	9	36	
70	99	0	184	35	0	73	69	0	122	36	0	83	13	0	40	45	31	67	20	3	76	
80	NA	NA	NA	0	0	22	NA	NA	NA	NA	NA	NA	NA	0	0	2	NA	0	0	12	3	41
90	NA	NA	NA	NA	NA	NA	NA	NA	NA	NA	NA	NA	NA	0	0	NA	NA	0	0	NA	0	0

Fuel Bed ID	Subcanopy DBH (in)			Organic Fuel Depth (in)			Organic Fuel tons/acre			Small Woody Fuel tons/acre			Large Woody Fuel tons/acre					
	X	Min	Max	X	Min	Max	Med	X	Min	Max	Med	X	Min	Max	Med	X	Min	Max
11	7	5	12	3.2	0	7.2	L	9.5	0	23	F	2.8	0	17	L	1.3	0	10
12	3	2	13	13	7.3	53	H	40	23	158	F	2.8	0	17	L	1.3	0	10
13	7	2	13	7.2	0	53	F	23	0	158	F	2.8	0	17	H	38	10	228
21	5	3	10	3.2	0	7.2	L	9.5	0	23	F	2.8	0	17	L	1.3	0	10
22	4	2	5	13	7.3	53	H	40	23	158	F	2.8	0	17	L	1.3	0	10
23	4	3	5	3.2	0	7.2	L	9.5	0	23	F	2.8	0	17	H	38	10	228
24	6	3	10	13	7.3	53	H	40	23	158	F	2.8	0	17	H	38	10	228
31	5	3	8	13	7.3	53	H	40	23	158	L	1.2	0	2.8	F	11	0	22
32	5	4	8	13	7.3	53	H	40	23	158	H	4.8	2.9	17	H	38	10	228
33	5	3	8	3.2	0	7.2	L	9.5	0	23	L	1.2	0	2.8	F	11	0	22
34	5	4	7	7.2	0	53	F	23	0	158	F	2.8	0	17	L	1.3	0	10
35	5	4	6	3.2	0	7.2	L	9.5	0	23	H	4.8	2.9	17	H	38	10	228
41	7	4	15	7.2	0	53	F	23	0	158	H	4.8	2.9	17	L	1.3	0	10
42	5	3	9	3.2	0	7.2	L	9.5	0	23	F	2.8	0	17	H	38	10	228
43	7	4	12	13	7.3	53	H	40	23	158	F	2.8	0	17	H	38	10	228
44	8	6	11	3.2	0	7.2	L	9.5	0	23	L	1.2	0	2.8	L	1.3	0	10
45	8	7	9	13	7.3	53	H	40	23	158	F	2.8	0	17	L	1.3	0	10
51	8	3	13	13	7.3	53	H	40	23	158	L	1.2	0	2.8	F	11	0	22
52	9	6	12	13	7.3	53	H	40	23	158	H	4.8	2.9	17	F	11	0	22
53	6	4	7	3.2	0	7.2	L	9.5	0	23	L	1.2	0	2.8	F	11	0	22
54	8	3	13	3.2	0	7.2	L	9.5	0	23	H	4.8	2.9	17	F	11	0	22
55	14	6	40	3.2	0	7.2	L	9.5	0	23	H	4.8	2.9	17	H	38	10	228
61	8	2	15	7.2	0	53	F	23	0	158	L	1.2	0	2.8	H	38	10	228
62	6	4	10	7.2	0	53	F	23	0	158	H	4.8	2.9	17	H	38	10	228
63	12	4	19	7.2	0	53	F	23	0	158	H	4.8	2.9	17	L	1.3	0	10
64	4	3	6	3.2	0	7.2	L	9.5	0	23	F	2.8	0	17	F	11	0	22
70	5	2	12	7.2	0	53	F	23	0	158	F	2.8	0	17	H	38	10	228
80	6	3	9	7.2	0	53	F	23	0	158	L	1.2	0	2.8	F	11	0	22
90	NA	0	0	19	13	53	VH	55	33	158	L	1.2	0	2.8	L	1.3	0	10

VITA

Karen Kopper grew up in Connecticut, where she first became enamored with camping, hiking and the outdoors. In 1994, she obtained her undergraduate degree in biology and minor in botany from Humboldt State University, California. Upon graduating she began her long career with the National Park Service (NPS), beginning with two seasons at Wind Cave National Park and one season at Bandelier National Monument as a biological science technician. She joined the private sector for a couple years to work as a freelance botanist and perform wetland delineations, before returning to the NPS as a seasonal botanist at Mount Rainier National Park. In 1999 she obtained a permanent (seasonal) position in fire effects monitoring at North Cascades National Park. Working seasonally enabled her to pursue a master's degree in Ecosystem Science from the University of Washington, College of Forest Resources. Upon her completion in 2003, she was promoted to her current year-round position as Fire Ecologist for North Pacific / Columbia Basin NPS units. She returned to the University of Washington, School of Environmental and Forest Sciences, sponsored by the NPS, to complete this doctorate in fire ecology for the national parks of the Pacific Northwest.

ProQuest Number: 29064365

INFORMATION TO ALL USERS

The quality and completeness of this reproduction is dependent on the quality
and completeness of the copy made available to ProQuest.



Distributed by ProQuest LLC (2022).

Copyright of the Dissertation is held by the Author unless otherwise noted.

This work may be used in accordance with the terms of the Creative Commons license
or other rights statement, as indicated in the copyright statement or in the metadata
associated with this work. Unless otherwise specified in the copyright statement
or the metadata, all rights are reserved by the copyright holder.

This work is protected against unauthorized copying under Title 17,
United States Code and other applicable copyright laws.

Microform Edition where available © ProQuest LLC. No reproduction or digitization
of the Microform Edition is authorized without permission of ProQuest LLC.

ProQuest LLC
789 East Eisenhower Parkway
P.O. Box 1346
Ann Arbor, MI 48106 - 1346 USA